CFD Simulations for Water Evaporation and Airflow Movement in Swimming Baths

Li, Zhigang; Heiselberg, Per Kvols

Publication date:
2005

Document Version
Publisher's PDF, also known as Version of record

AALBORG UNIVERSITY

DEPT. OF BUILDING TECHNOLOGY
AND STRUCTURAL ENGINEERING

CFD Simulations for Water Evaporation and Airflow Movement in Swimming Baths

Zhigang Li (zli@bt.aau.dk)
Per Heiselberg (ph@bt.aau.dk)

Indoor Environmental Engineering

Report for the project “Optimization of Ventilation System in Swimming Bath”, April 2005

ISSN 1395-7953 R0503

Preface

This project report is submitted in accordance with a part of the project work - Development of Electric Conservating Control Strategies and Optimisation of Ventilation Systems and Heat Pumps in Swimming Baths. This part of work is contributed by The Indoor Environmental Engineering Group, Department of Building Technology and Structural Engineering at Aalborg University.

This report presents the results of my work 'CFD simulations for water evaporation and airflow movement in swimming baths' with Professor Per Heiselberg as supervisor.

I wish to express my gratitude to Professor Per Heiselberg and Professor Peter V. Nielsen for their guidance and for giving me the opportunity to fulfil this work.

My thanks also extend to Martin Lykke Jensen (Birch & Krogboe), Ole Juhl Hendriksen (Force), Karl Grau (By & Byg), Rasmus Lund Jensen (Aalborg University) for their hospitality and support. And I also would like to thank all of the colleagues and members of the project group for their valuable assistance during the work.

Zhigang Li

April 2005

Abstract

This report is a part of the project work 'Development of Electric Conservating Control Strategies and Optimisation of Ventilation Systems and heat pumps in Swimming Baths' (Dansk projekttitel: Udvikling af elbesparende reguleringsstrategier og optimering af ventilationsanlæg og varmepumper i svømmehaller).

The aim of my work is to investigate the relation between water evaporation and air movement by CFD simulations, and to determine the mass flow rate of water evaporation for dimensioning the ventilation system in swimming baths, as well as to find out valid evaporation models which can be used to develop a simplified model in BSIM2002. The steady state two-dimensional and three-dimensional CFD simulations are carried out based on water evaporation and moist air flow in the Korsør Svømmehal.

The CFD technology enables engineers to study the fluid dynamics and it is a tool for compressing the design and development cycle. CFD is a sophisticated analysis technique. It predicts not only fluid flow behaviour, but also the heat and mass transfer. CFD calculations are carried out in steady state conditions for the Korsør Svømmehal before renovation. The boundary conditions are collected from the measurement results including air temperature, water temperature, humidity and ventilation flow rate. CFD can give detailed information of air flow and humidity distribution in the swimming hall due to different water evaporation models, and the valid models for swimming baths can be obtained.

The different water evaporation models for swimming baths are compared and used in 2D or 3D CFD simulations in this project. The simulation results show that the two water evaporation models - Shah correlation for unoccupied pool and Shah empirical correlation for occupied pool – are quite good to calculate the water evaporation from baths. Therefore, these two models can be used to determine the mass flow rate of water evaporation and to develop a simplified model in BSIM2002.

Contents

1 Introduction

1.1 Project background

In the coming years a large number of public swimming baths in Denmark need to undergo considerable renovations. Swimming baths have a high consumption of energy for ventilation and water treatment in order to obtain good indoor climate and high water quality.

The data materials from ELO-organization for energy consumption in swimming baths show, that the swimming baths are large energy demand buildings of electric and heating consumption, and that the large differences of energy consumption exist between different swimming baths. The heating and electrical energy consumption is absolutely huge about 2000 and 800 kWh/ (m^2bath year) respectively in Denmark according to “Energiteknik i Svømmehaller”.

At present the swimming baths are controlled by using empirical knowledge, it means, the baths are controlled by hand regulations. Many of these hand regulations are very well-considered, but they are based on existing knowledge and experiences of operation instead of requirement analysis, because there is not valid knowledge about how to obtain the optimized operations from present simulation tools. It is no doubt that the control and regulation strategy is very strong tool to reduce the energy consumption for ventilation and water treatment system. However, it is much difficult to set the optimal regulation conditions because no good model can be used to simulate and compare for different influencing factors.

The control of the ventilation system is very difficult, since it is based on the empirical knowledge instead of the optimal requirement control. Not only should good indoor air quality be considered in swimming baths – primarily from air temperature and humidity, but also the baths, people, building and energy consumption should be considered. Here the water evaporation rate from baths is the essential parameter which influences the indoor climate and energy consumption. It is very important to keep the balance between the air and the water surface, and the water evaporation rate should be reduced as much as possible.

Reliable calculation methods of evaporation from swimming baths is needed for sizing the air conditioning system as well as for energy consumption calculations. No well-verified evaporation model is available at present. Underestimation of evaporation will lead to selection of undersized air conditioning equipment, resulting in excessive humidity that can cause discomfort to the occupant and damage to the building from mold growth and rotting. On the contrary, an overestimation will result in the selection of oversized equipment with high cost, excessive energy consumption and operating problems because of excessive cycling.

Relation between water evaporation, air temperature and air humidity at a still water surface and low air velocity in a swimming bath shows that an acceptable low water evaporation can be obtained when keeping the air temperature 28 °C and water temperature 26°C, which is a starting point for dimensioning the ventilation system and choosing the water temperature. Practical experiences of operation with ventilation show also that the balance between air and water surface is extremely sensitive due to small change in air and water conditions. In addition, the large glass façade also increase the demand for indoor climate and ventilation system when the cold and condensation should be reduced.

When choosing reasonable operating conditions in swimming baths, moisture problems as well as operational expenditure should be controlled. To minimize evaporation rates the pool hall temperature should always be higher than the pool water temperature. The higher the temperature differential between air and water, the lower the evaporation rate from the pool surface. However, in order to maintain a reasonable operating economy, the difference should not be bigger than 2-3°C.

The objective of the ventilation system is to maintain the design temperature and humidity, and to secure good air quality within the pool hall. Air in a swimming pool hall will always have a moisture content higher than that of outside air. It follows therefore that by introducing a calculated amount of fresh air into the pool hall the desired relative humidity can be maintained. This process has the potential to use a great deal of energy so it is essential to recover as much heat as possible from the exhaust air, and to avoid changing air more than is necessary.

The instructions include partly control of the local air temperature over bath, which the air temperature should be 2-3 °C higher than the water temperature in bath, and partly limitation of the air velocity over bath surface. In order to fulfil the instruction’s

requirements, higher regulation accuracy for inlet air temperature, good air mixing with uniform temperature and low air velocity should be demanded. Therefore, the water evaporation rate will be reduced. But, this is a difficult task for ventilation and heating system in swimming baths where the typical room height is about 6-8 meters.

1.2 Aims and method

The objective of the project is to provide incentives for integrating energy efficiency in the planned renovation by developing new energy saving solutions for ventilation and water treatment, and at the same time ensure improvement of indoor climate and water quality.

The research work and development work will be based on measurements in existing swimming baths combined with calculations and analyses for a model swimming bath including indoor climate, working environment, water quality, as well as energy consumption. Furthermore, a complete economical estimation of installations and operation will be made; as such a comprehensive study will often lead to further energy saving measures.

The result of the project will be used to set up a method of fault detection and diagnosis in existing public swimming baths including instructions and solutions for dimensioning of ventilation systems and water treatment facilities. The result will also be used both for new installations and renovations of existing baths.

All of the interesting things give rise to develop an operation tool that can simulate different control strategies for swimming baths with different load. Since there is no existing simulation tool at present, BSIM2002 can carry out these simulations with relative few adjustments. Therefore, BSIM2002, which is a widely used and proved simulation tool, can be further developed with a water evaporation module.

A part of the project work is contributed by Aalborg University, which is to investigate the relation between water evaporation and air movement by CFD simulations, and to determine the mass flow rate of water evaporation for dimensioning the ventilation system in swimming baths, as well as to develop a simplified model in BSIM2002. CFD simulations are carried out according to the Korsør Svømmehal, which are calculated for wintertime, so the solar gain is not

considered and it does not influence the indoor temperature, energy consumption and water evaporation.

1.3 CFD simulation for water evaporation and air movement

The CFD (Computational Fluid Dynamics) technology enables engineers to study the fluid dynamics and it is a tool for compressing the design and development cycle. Using CFD, a computational model can be built to study. When the fluid flow physics is applied to this virtual prototype, the CFD software can simulate how it will perform under real-world conditions and output a prediction of the fluid dynamics. CFD is a sophisticated analysis technique, it predicts not only fluid flow behavior, but also the heat and mass transfer. CFD analysis gives the ability to optimize design early, reducing the need for costly and time-consuming physical testing.

CFD calculations are carried out in steady state conditions for the Korsør Svømmehal before renovation. The boundary conditions are collected from the measurement results including air temperature, water temperature, humidity, ventilation flow rate and so on. The ventilation and water evaporation from baths are mutually coupled, so this case can be used in a CFD calculation model, where both water evaporation and air movement can be dealt with simultaneously. Therefore, the CFD can give detailed different information of air flow and humidity distribution in the room due to different water evaporation models, and a valid model for swimming baths will be obtained.

2 Literature study

2.1 Mechanism of evaporation

In a very succinct description, the heat and mass transfer processes by evaporation from a free water surface take place according to two mechanisms: the heat and mass transfer by the molecular motion (diffusion) and the heat and mass transfer by the gross motion of the fluid over the water surface (advection). Near the water surface, where the fluid velocity is low the advection becomes negligible and the molecular motion or diffusion is predominant being the sole mechanism at the surface-fluid interface. In a very thin layer of air immediately above the water surface, vapor is present which is regarded as being due to the action of molecular diffusion. With forced convection, the evaporation is caused by a combination of advection with diffusion, being the dominant component of the mechanism of heat and mass transfer generally made by the bulk or gross motion of the fluid.

Evaporation from the pool surfaces and the surrounding wet areas is the main contributor to the moisture problem. The quantity of evaporation depends on such factors as pool area, water temperature, air temperature, humidity, air velocity, and the bathing activity. There are many formulae and rules of thumb that profess to calculate evaporation rate.

2.2 References study

A large number papers and equations on evaporation have been written since the late 1800's when the first empirical investigations were published by Dalton, who determined the law of partial pressure [1]. Due to the profusion of equations, mostly empirical, and the inexistence of a consensus, the formulas have been taken from the literature and employed without criteria to several applications around the world. Thus, a large scattering of evaporation rates has been found and the initial results suggested that it might be impossible to determine a generally applicable equation for evaporation.

Of the total heat loss from a free water surface much more than 50% is due solely to evaporation. Therefore, whether an equation severely overestimates or underestimates the actual values, it generates an error of great proportions. As known, accuracy is mandatory for most processes, however, for empirical equations on evaporation this

accuracy has not been too rigorous. On the other hand, the lesser number of theoretical working formulas in relation to empirical ones was expected and this can be attributed to the complexity of the evaporation process [2]. Thus, the literature review is an attempt to find out among the existing well known working formulas, those that more accurately predict actual evaporation rates and can be used in the swimming pool CFD model.

Most of the equations employed so far for the calculation of the evaporation rate from several applications are empirical, which equations result from regression analysis after a large number of experiments in order to get a more general validation. Nevertheless, these equations continue depending or being valid for only particular systems and climates similar to those when the measurements were made. Empirical equations also depend strongly on the differences in analysis techniques. Because of these conditions, practically each empirical equation is needed for each class of climate (humid, windy, sunny, arid, day or night, etc.) existent for each water surface.

Since Dalton [1] started the empirical hydrodynamic approach to the evaporation problem, and stated that evaporation is proportional to the difference in vapor pressure at the surface of the water and in the air and that the velocity of the wind affects this proportionality, numerous researchers started to investigate evaporation based on Dalton's description. Almost all of the general evaporation rate form is:

$$E = \frac{(a + bV)(P_w - P_a)}{h_w} = \frac{h_e (P_w - P_a)}{h_w} \qquad (1)$$

where E is the evaporation rate [kg/m^{2}s]

a, b are the coefficients of empirical equation

V is the wind velocity (velocity of air parallel to water surface) [m/s]

P_w is the saturated water vapor partial pressure at the water temperature [Pa]

P_a is the water vapor partial pressure at the air temperature and humidity [Pa]

h_e is the evaporative heat transfer coefficient [W/m^{2}Pa]

h_w is the latent heat of vaporization of water [J/kg]

$(P_w\text{-}P_a)$ is the vapor pressure difference between air saturated at pool surface temperature and the room air [Pa]

a subscript, at room temperature and humidity

w subscript, saturated at water surface temperature

Note: In this project report, all the units are SI (International System of Units) units.

2.2.1 Unoccupied pools

Carrier correlation:

In 1918, Willis H. Carrier published the following empirical formula which is the most widely used correlation by far [3]:

$$E = \frac{(0.0888 + 0.0783V)(P_w - P_a)}{h_w} \qquad (2)$$

This formula was based on tests performed on an unoccupied pool, along which air was blown. No tests were done without forced air flow. It has been widely used for calculating evaporation from pools without forced air flow by imputing *V=0* in the formula. The 1999 ASHRAE Handbook [4] recommends this equation for occupied public swimming pools with normal activity, partially wet deck, and some allowance for splashing.

Smith et al. correlation:

Smith et al. [5] estimated the rate of evaporation through an energy balance on the water in the pool. Essentially, evaporation was attributed entirely to the difference between the total energy supplied to the water and the sensible heat gained by water. Evaporation from the wet deck and from the wet bodies of the swimmers were not considered. They stated that during their tests, a number of activities occurred at the same time, including swimming, diving, and aquatic exercise. This is usually the case in public pools and this may be regarded as normal activity.

They conducted tests on occupied and unoccupied swimming pools and gave empirical formulas. They recommended that results of the Carrier correlation should be multiplied by 0.73.

$$E = \frac{0.73(0.0888 + 0.0783V)(P_w - P_a)}{h_w} \qquad (3)$$

Various empirical correlations:

Based on their own data, many authors have published equations of the following form [6] [7] [8] [9] [10] [11]:

$$E = g\left(P_w - P_a\right)^n \qquad (4)$$

where *?* is a constant, and *n* varies from 1 to 1.2.

Shah correlation:
Shah [6] developed a formula based on the analogy between heat and mass transfer:

$$E = \frac{1}{3600} C r_w \left(r_a - r_w\right)^{\frac{1}{3}} \left(W_w - W_a\right) \qquad (5)$$

where C is a constant defined as

$$C = 35, \quad for \quad \left(r_a - r_w\right) \succ 0.02$$
$$C = 40, \quad for \quad \left(r_a - r_w\right) \prec 0.02$$

if $\left(r_a - r_w\right)$ is negative, its absolute value is used

? is the density of air [kg/m^3]

W is the specific humidity of air [kg of moisture/kg of air]

According to above equations, evaporation increases as the pool area increases, in other words as the area of contact between water and air increases. According to Eq. (5), evaporation increases with increasing W_w and decreasing $?_w$, these occur as water temperature increases. Thus, these formulas indicate that evaporation will increase with increasing water temperature.

Shah evaluated these correlations based on undisturbed water pool test data. The Shah correlation agreed with almost all of the data and had a mean deviation of 21%. The Carrier and Smith et al. correlations overpredicted the data by an average of 132% and 76% respectively.

Hyldgård correlation:
Hyldgård [12] measured the water evaporation and heat balance in models and full-scale swimming baths. The evaporation rate graphs were obtained and can be used to control and design swimming baths. Unfortunately the evaporation equation has not

been obtained. He gave the valuable parameter settings for public baths for good indoor comfort and energy consumption saving, which is used in Denmark at present:

Water temperature t_w = 26 °C,

Air temperature t_a = 29 °C,

Air relative humidity f_a = 60%,

Inlet air temperature t_i = 31 °C - 32 °C

2.2.2 Occupied pools

It is well known that rate of evaporation from disturbed water surfaces is higher than that from undisturbed surfaces; for example, Doering [13] compared occupied and unoccupied swimming pools and showed those differences.

The rate of evaporation from occupied pools is higher than that from unoccupied ones for a variety of reasons, most notably the increase in contact area between air and water. Contributing are the wet bodies of occupants and the wetting of the deck. Occupants cause waves, ripples, and mist, the extent of which in creases with the number of occupants and their activity level; thus, diving and polo cause more of an increase in air-water contact area than normal swimming. A normal activity pool may be considered one that has mostly inactive or normally swimming occupants and small amount of diving.

Shah phenomenological correlation:

Shah [8] defined the pool utilization factor F_u:

$$F_u = \frac{A_{\max}}{\frac{A_{pool}}{N}} \qquad (6)$$

where N is the number of occupants

A_{max} is the pool area per person at maximum occupancy [m^2/person]

A_{pool} is the surface area of pool [m^2]

Then, Shah derived the new correlation:

$$E = E_o(3.3F_u + 1) \quad for \quad F_u \prec 0.1 \qquad (7)$$

$$E = E_o(1.3F_u + 1.2) \quad for \quad 0.1 \le F_u \le 1$$

$$E = 2.5 \qquad for \qquad F_u \succ 1$$

where E is the rate of evaporation at actual occupancy [kg/m^{2}s]

E_0 is the rate of evaporation from unoccupied pool [kg/m^{2}s]

Shah empirical correlation:

Based on test data for normal activity pools, Shah [8] published the following formula:

$$E = \frac{1}{3600}\left(0.113 - 0.0000175\frac{A}{N} + 0.000059(P_w - P_a)\right) A/N < 45 \qquad (8)$$

It is applicable when A/N is less than 45.

Shah analytical correlation:

If A/N is greater than 45, then:

$$E = E_0\left(14.85\frac{N}{A} + 1\right) \qquad (9)$$

If A/N is between 4.5 and 45, then:

$$E = E_0\left(5.85\frac{N}{A} + 1.2\right)$$

If A/N is less than 4.5, then:

$$E = 2.5E_0$$

The value of E_0 is calculated by the formula for unoccupied pools. Generally, it is the same as the Shah phenomenological correlation.

Biasin and Krumme correlation:

Biasin and Krumme [15] have given figures from German standards according to which A_{max} is almost constant at 4.5 m^2 per person for ordinary swimming pools, and gave the following correlation of their data:

$$E = \frac{1}{3600}\left[0.118 + \frac{0.01995(P_w - P_a)F_u}{133.3}\right] \qquad for \qquad 0.1 \le F_u \le 0.7 \qquad (10)$$

Another expression of Biasin and Krumme formula is:

$$E = \frac{1}{3600}\left[0.118 + \frac{0.01995(P_w - P_a)e}{133.3}\right]$$

Where e is the empirical factor as:

e = 0.5 for public pools

e = 0.4 for hotel pools

e = 0.3 for private pools

During night the formula is:

$$E = \frac{1}{3600}\left[-0.059 + \frac{0.0105(P_w - P_a)}{133.3}\right]$$

ASHRAE Handbook method:

The ASHRAE Applications Handbook [16] recommends that evaporations calculated with the Carrier formula be multiplied by the factors in Table 2.1. Thus, the Carrier formula is recommended unchanged for occupied public pools with normal activity.

Type of pool	Multiplying factor
Residential	0.5
Condominium	0.65
Therapy	0.65
Hotel	0.8
Public school	1.0
Whirlpool, spa	1.0
Wavepool, water slide	1.5 (minimum)

Table 2.1: Multiplying factors for Carrier correlation, according the ASHRAE Applications Handbook.

Smith et al. Correlation [5]:

$$E = E_0\left(4.27\frac{N}{A} + 1.04\right) \qquad (11)$$

Shah compared the correlations for occupied public pools with data from his measurements. The ASHRAE Handbook method correlated all data for higher

occupancies (*A/N* is less than 10.8), with a mean deviation of ±30%. At lower occupancies, it greatly overpredicted. The Shah empirical correlation predicted almost all data within ±15%. The Shah analytical correlation had a mean deviation of ±26% for all data and predicted data for *A/N* of less than 9 within ±30%. The Smith et al. correlation is found to be unsatisfactory for all values of occupancy.

VDI 2089 Correlation:

The German calculation formula VDI-2089 [17] states the required data for the design of indoor swimming pools, and the evaporation rate is calculated as follows:

$$E = \frac{1}{3.6\times10^{8}} e \times (P_w - P_a) \qquad (12)$$

Where P_w is the saturated water vapor partial pressure at the water temperature

P_a is the water vapor partial pressure at the air temperature and humidity

e is the empirical as:

e = 0.5 for covered pool surfaces

e = 5 for calm surface

e = 15 for private swimming pool, not very occupied

e = 20 for public swimming pool, normal activity

e = 28 for leisure pool

e = 35 for wave pool

References:

[1] Dalton J. Experimental essays on the constitution of mixed gases; on the force of steam or vapor from water and other liquids in different temperatures, both in a Torricellian vacuum and in air; on evaporation and on the expansion of gases by heat. Mem. Manchester Liter. And Phil. Soc. 5-11, 535-602, 1802

[2] Ernani Sartori. A critical Review on Equations Employed for the Calculation of the Evaporation Rate from Free Water Surfaces. Solar Energy Vol. 68, N0. 1, pp. 77-89, 2000

[3] W. H. Carrier. The temperature of evaporation, ASHVE Trans. 24 25-50, 1918

[4] ASHRAE Handbook HVAC Applications, ASHRAE, Attlanta, GA, 1999

[5] C. C. Smith, G. O. G. Lof, R. W. Jones, Rates of evaporation from swimming pools in active use, ASHRAE Trans. 104 (1A) 514-523, 1999
[6] Shah, M. M. Rate of evaporation from undisturbed water pools to swimmbad. Electrowaerme Internationaal 32 (A3), A115-A129, 2002
[7] Boelter L. M. K., H. S. Gordon, J. R. Griffin. Free Evaporation into Air of Water from a Free Horizontal Quiet Surface. Industrial & Engineering Chemistry 38(6) 596-600, 1946
[8] Shah, M. M. Prediction of evaporation from occupied indoor swimming pools. Energy and Buildings, 35, 707-713, 2003
[9] Himus G. W. and J. W. Hinchley. The Effect of a Current of Air on the Rate of Evaporation of Water Below the Boiling Point. Chemistry and Industry August 22, 840-845, 1924
[10] Leven K. C. Betrag zur Frage der Wasserverdunstung. Wärme-und Kältetechnik 44(11), 161-167, 1969
[11] Tang T. D., M. T. Pauken, S. M. Jeter, and S. I. Abdel-khalik. On the Use of Monolayers to Reduce Evaporation from Stationary Water Pools. Journal of Heat Transfer 115(1), 209-214, 1993
[12] C. E. Hyldgård. Water Evaporation in Swimming Baths. Roomvent 90, 1990
[13] Doering. Zur Auslegung von Luftungsanlagen für Hallenschwimmbäder. HLH 30(6): 211-216.
[14] Box T. A Practical Treatise on Heat. 1876
[15] K. Biasin, W. Krumme. Die Wasserverdunstung in einem Innenschwimmbad, Electrowaerme International 32 (A3) A115-A129, 1974
[16] ASHRAE Handbook HVAC Applications, ASHRAE, Attlanta, 2003
[17] VDI 2089, Blatt 3, Technische Gebäudeausrüstung von Schwimmbädern – Freibäder, 2000

3 Comparison for different evaporation models

3.1 The thermodynamic properties of moist air

3.1.1 Moist air

The composition of atmospheric air is variable, particularly with regard to amounts of water vapour. The working substance in air conditioning problems is called moist air, which is defined as a binary mixture of dry air and water vapour. Moist air may contain variable amounts of water vapour from zero (dry air) to that of saturated moist air. Goff [1] has defined saturation of moist air as that condition where moist air may coexist in neutral equilibrium with associated condensed water, presenting a flat surface to it.

The humidity ratio, W, is defined as the mass of water vapour per unit mass of dry air in a moist air mixture [2]:

$$W = \frac{m_v}{m_a}$$

Where W is the humidity ratio

m_v is the mass of water vapour in the moist air mixture [kg]

m_a is the mass of dry air in the moist air mixture [kg]

Therefore, the mass fraction of the water vapour, $?_v$, can be calculated as:

$$x_v = \frac{m_v}{m_a + m_v} = \frac{W}{1+W}$$

3.1.2 Relative humidity

Two measures of humidity relative to saturation conditions are commonly used. Degree of saturation is defined by the relation:

$$m = \frac{W}{W_s}$$

Where μ is the humidity ratio

W_s is the humidity ratio at saturation for the same temperature and pressure as those of the actual state

Relative humidity f is defined by the relation:

$$j = \frac{x}{x_s} = \frac{1 + \frac{0.622}{W_s}}{1 + \frac{0.622}{W}}$$

Where f is the relative humidity

x is the mole fraction of the water vapour in the moist air mixture

x_s is the mole fraction of the water vapour at saturation for the same temperature and pressure as those of the actual state

3.1.3 Partial pressure

A useful expression for the humidity ratio can be derived by the partial pressure of water vapour and the total pressure of the mixture:

$$W = 0.622 \frac{P_w}{P_a} = 0.622 \frac{P_w}{P - P_w}$$

Where P_w is the partial pressure of water vapour [Pa]

P_a is the partial pressure of dry air [Pa]

P is the total pressure of the mixture [Pa]

The perfect-gas approximation for the relative humidity can be obtained:

$$j = \frac{P_w}{P_s}$$

Where P_s is the partial pressure of water vapour at saturation for the same temperature and pressure as those of the actual state [Pa]

Ps can be calculated by the following equation [3]:

$$\ln\left(\frac{P_s}{P_c}\right)=\left(\frac{T_c}{T}-1\right)\times\sum_{i=1}^{8}F_i\left[a\left(T-T_p\right)\right]^{i-1}$$

Where P_c is the pressure of water tripe point, P_c = 22.089MPa

T_c is the absolute temperature of water tripe point, T_c = 647.286 K

Constant: F_1 = -7.4192420

$F_2 = 2.9721000\times10^{-1}$

$F_3 = -1.1552860\times10^{-1}$

$F_4 = 8.6856350\times10^{-3}$

$F_5 = 1.0940980\times10^{-3}$

$F_6 = -4.3999300\times10^{-3}$

$F_7 = 2.5206580\times10^{-3}$

$F_8 = -5.2186840\times10^{-4}$

a = 0.01

T_p = 338.15 K

3.1.4 Density

The density of moist air may be calculated by:

$$r=\frac{101325}{461.5\times\left(273.15+t\right)\times\left(0.622+W\right)}$$

Where *?* is the density of moist air [kg/m^3]

t is the temperature of moist air [ºC]

3.2 Comparison for different evaporation models

3.2.1 Comparison conditions

The different water evaporation models should be compared in the same conditions. For good indoor air quality and energy saving, the water temperature generally keeps at 26 degree; the relative humidity should keep 60%. Here the models are compared in the conditions of air temperature from 23 ºC to 29 ºC and the horizontal air velocity is 0.1m/s. The relation between water evaporation, air temperature and air humidity at a still water surface and low air velocity in a swimming bath shows that an acceptable low water evaporation can be obtained when keeping the air temperature 28 °C and water temperature 26°C, which is a start point for dimensioning the ventilation system and choosing the water temperature. Practical experiences of operation with

ventilation show also that the balance between air and water surface is extremely sensitive due to small change in air and water conditions. Table 3.1 shows the comparison conditions for water evaporation calculations.

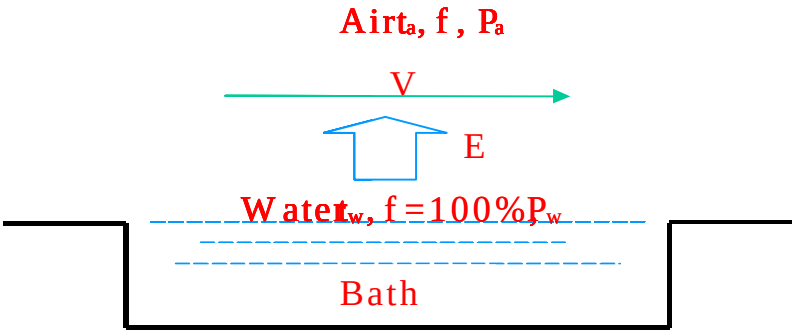

Fig. 3.1 Schematic of water evaporation in a bath.

T_w	T_{air}	? $T=T_{air}-T_w$	f	Pws	hw	Vx	Pas
Water Temperature	Indoor air Temperature	Temperature difference	indoor air relative humidity	Partial pressure of saturated water at T_w	Latent heat coefficient	horizontal air velocity	Partial pressure of saturated water at T_{air}
[°C]	[°C]	[°C]		[Pa]	[J/kg]	[m/s]	[Pa]
26	23	-3	0.6	3363	2548550	0.1	2810
26	24	-2	0.6	3363	2548550	0.1	2985
26	25	-1	0.6	3363	2548550	0.1	3169
26	26	0	0.6	3363	2548550	0.1	3363
26	27	1	0.6	3363	2548550	0.1	3567
26	28	2	0.6	3363	2548550	0.1	3782
26	29	3	0.6	3363	2548550	0.1	4008

Pa	? P=Pws-Pa	?a	?w	? ?=?a-?w	Ww	Wa
Partial pressure of saturated water at T_{air} and f		Moist air density	Moist air density	Density difference	Specific humidity of air at T_w and saturation	Specific humidity of air at T_{air} and f
[Pa]	[Pa]	[kg/m3]	[kg/m3]	[kg/m3]	[kg/kg]	[kg/kg]
1686.0	1677	1.1730	1.1406	0.0324	0.021448	0.01001
1791.0	1572	1.1668	1.1410	0.0258	0.021448	0.01124
1901.4	1461.6	1.1616	1.1410	0.0205	0.021448	0.01197
2017.8	1345.2	1.1564	1.1410	0.0153	0.021448	0.01269
2140.2	1222.8	1.1510	1.1410	0.0100	0.021448	0.01350
2269.2	1093.8	1.1458	1.1410	0.0047	0.021448	0.01431
2404.8	958.2	1.1403	1.1410	0.0007	0.021448	0.01521

Table 3.1: shows the comparison conditions for water evaporation calculations.

The swimming baths can be divided into two types, unoccupied pools and occupied pools. These widely used evaporation models for swimming baths will be compared as follows.

3.2.2 Unoccupied pools

Table 2.2 shows the evaporation models for unoccupied swimming baths, which are named as Carrier, Smith, Hyldgård, Shah, VDI2089, Biasin & Krumme models respectively. Carrier formula now is used as the evaporation rate formula in occupied pools in American standard ASHREA, because the measurements results were obtained from still water surface, and the evaporation rate will be over predicted very much. Smith thought the evaporation rate should be multiplied a factor 0.73 to carrier formula in order to reduce the water evaporation rate. Hyldgård described the evaporation rate according his measurements, but unfortunately no empirical formula was obtained; the evaporation rate value can be obtained from figures in his literature. Shah described the evaporation rate by means of moist air density and absolute humidity. Germany standard VDI describes the evaporation rate by means of factors according to different using style in swimming pools. Table 3.3 shows the water evaporation rate calculations for these different models. Figure 3.2 and Figure 3.3

show the water evaporation rate comparisons for different models in two different units – kg/m^{2}s and g/m^{2}h.

Evaporation model	Formula
Carrier (1918)	$E = \frac{(0.0888 + 0.0783V)(P_w - P_a)}{h_w}$
Smith (1999)	$E = \frac{0.73(0.0888 + 0.0783V)(P_w - P_a)}{h_w}$
Hyldgård (1990)	See his literature, no formula
Shah (2002)	$E = \frac{1}{3600} C r_w (r_a - r_w)^{\frac{1}{3}} (W_w - W_a)$
VDI2089 (2000)	$E = \frac{1}{3.6 \times 10^8} \times 5 \times (P_w - P_a)$
Biasin & Krumme (1974)	$E = \frac{1}{3600}\left[-0.059 + \frac{0.0105(P_w - P_a)}{133.3}\right]$

Table 3.2: The different evaporation models for unoccupied pools.

T_w	T_{air}	E	E	E	E	E	E
Water Temperature	Indoor air Temperature	**Carrier** evaporation rate	**Smith** evaporation rate	**Hyldgård** evaporation rate	**Shah** evaporation rate	**VDI2089** evaporation rate	**Biasin&Krumme** evaporation rate
[°C]	[°C]	[kg/m^{2}s]	[kg/m^{2}s]	[kg/m^{2}s]	[kg/m^{2}s]	[kg/m^{2}s]	[kg/m^{2}s]
26	23	6.358E-05	4.642E-05		4.045E-05	2.329E-05	2.030E-05
26	24	5.960E-05	4.351E-05		3.345E-05	2.183E-05	1.801E-05
26	25	5.542E-05	4.045E-05		2.880E-05	2.030E-05	1.559E-05
26	26	5.100E-05	3.723E-05		2.757E-05	1.868E-05	1.304E-05
26	27	4.636E-05	3.385E-05	1.361E-05	2.170E-05	1.698E-05	1.037E-05
26	28	4.147E-05	3.027E-05	4.444E-06	1.518E-05	1.519E-05	7.544E-06
26	29	3.633E-05	2.652E-05	3.056E-06	6.967E-06	1.331E-05	4.577E-06

Table 3.3: The water evaporation rate calculations for different models.

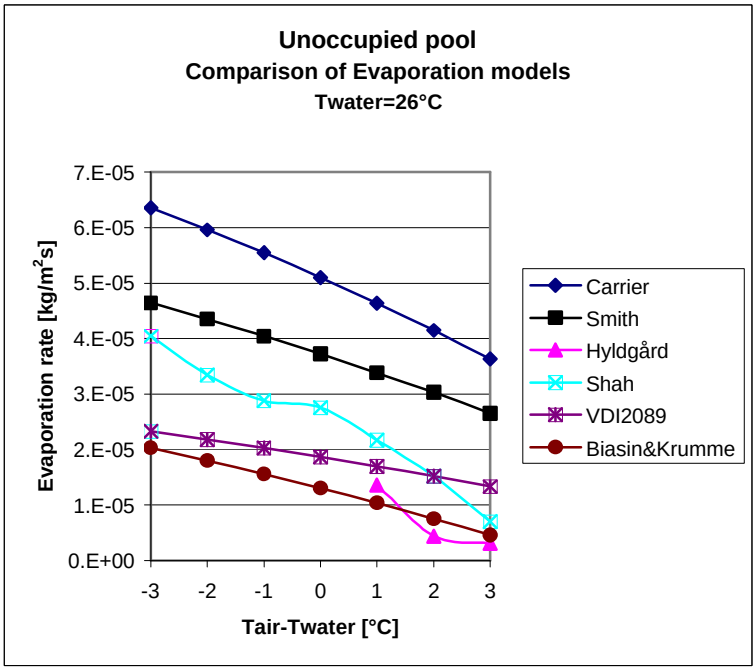

Figure 3.2: The water evaporation rate comparison for different models.

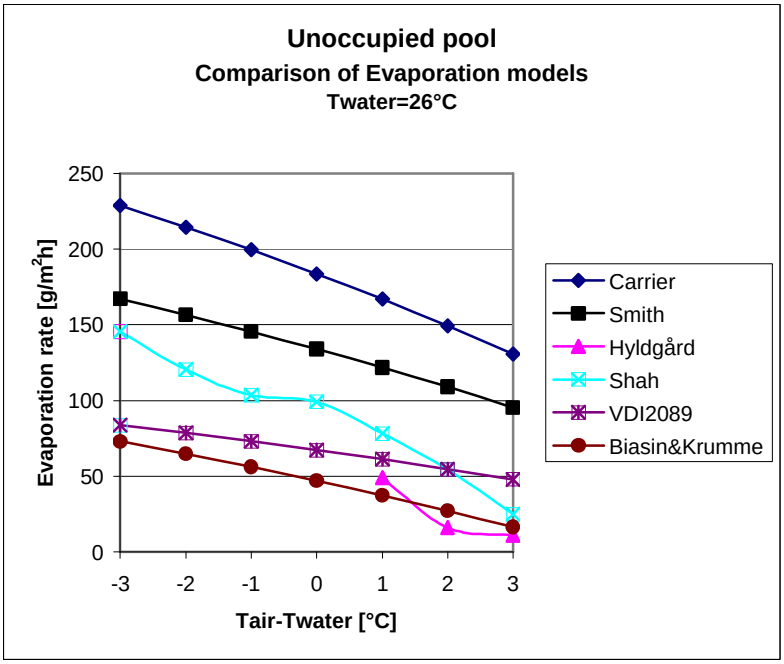

Figure 3.3: The water evaporation rate comparison for different models.

For the unoccupied pool, it is clear to see that the different evaporation models will give rise to quite different evaporation rates. Carrier formula is quite high and now is

used as the occupied pools model in American standard. Smith formula decreases the evaporation rate by multiplying a factor. VDI2089 is similar with Shah formula in this temperature range. Hyldgårs formula is quite low because the air velocity used 0.1m/s is quite low in his formula. Shah stated that the shah correlation is quite good agreement with almost all of the measured data of swimming baths.

It also can be found out from this figure that the higher of the temperature differential between air and water will give rise to the lower of the evaporation rate from the pool surface. So, in order to minimize evaporation rates the air temperature should always be higher than the water temperature. However, in order to maintain a reasonable operating economy, the difference should not be bigger than 2-3°C.

For unoccupied indoor swimming pools, Shah correlation is a reliable method of calculating water evaporation rate. Because it has been verified for a wide range of air-water temperatures, humidities, and pool sizes and is firmly rooted in theory, it also can be used with confidence for other pool types. So the Shah correlation formula is recommended for all types of indoor water pools with undisturbed surfaces and unforced airflow over those surfaces.

3.2.3 Occupied pools

Table 3.4 shows the evaporation models for occupied and normal activities swimming baths. Actually the ASHRAE formula is same as carrier formula. In this formula, the air velocity in horizontal direction also be taken into account and the velocity will influence the evaporation rate little higher. Smith, Shah empirical, Shah analytical and Biasin & Krumme formulas take into account the influence of occupants' number. And VDI2089 uses a factor 20 to express the occupied and normal activities baths.

Table 3.5 shows the water evaporation rate calculations for these different models in occupied pools. Figure 3.4 and Figure 3.5 show the water evaporation rate comparisons for different models in two different units – kg/m^2s and g/m^2h.

Evaporation model	Formula
ASHRAE (2003)	$E = \frac{(0.0888 + 0.0783V)(P_w - P_a)}{h_w}$
Smith (1999)	$E = E_0\left(4.27\frac{N}{A} + 1.04\right)$
Shah empirical (2003)	$E = \frac{1}{3600}\left(0.113 - 0.0000175\frac{A}{N} + 0.000059(P_w - P_a)\right)$ A/N<45
Shah analytical (2003)	$E = E_0\left(14.85\frac{N}{A} + 1\right)$ A/N > 45; $E = E_0\left(5.85\frac{N}{A} + 1.2\right)$ 45> A/N > 4.5 $E = 2.5E_0$ A/N < 4.5
VDI2089 (2000)	$E = \frac{1}{3.6\times10^8}\times 20\times(P_w - P_a)$
Biasin&Krumme (1974)	$E = \frac{1}{3600}\left[0.118 + \frac{0.01995(P_w - P_a)F_u}{133.3}\right]$ *for* $0.1 \le F_u \le 0.7$

Table 3.4. The evaporation model for occupied pools.

T_w	T_{air}	E	E	E	E	E	E
Water Temperature	Indoor air Temperature	**ASHRAE** evaporation rate	**Smith** evaporation rate	**Shah empirical** rate	**Shah analytical** rate	**VDI2089** evaporation rate	**Biasin&Krumme** evaporation rate
[°C]	[°C]	[kg/m^{2}s]	[kg/m^{2}s]	[kg/m^{2}s]	[kg/m^{2}s]	[kg/m^{2}s]	[kg/m^{2}s]
26	23	6.358E-05	5.934E-05	5.882E-05	7.220E-05	9.317E-05	6.415E-05
26	24	5.960E-05	4.907E-05	5.710E-05	5.971E-05	8.733E-05	6.219E-05
26	25	5.542E-05	4.225E-05	5.529E-05	5.140E-05	8.120E-05	6.012E-05
26	26	5.100E-05	4.044E-05	5.339E-05	4.921E-05	7.473E-05	5.794E-05
26	27	4.636E-05	3.184E-05	5.138E-05	3.874E-05	6.793E-05	5.565E-05
26	28	4.147E-05	2.227E-05	4.927E-05	2.709E-05	6.077E-05	5.324E-05
26	29	3.633E-05	1.022E-05	4.704E-05	1.244E-05	5.323E-05	5.070E-05

Table 3.5: The water evaporation rate calculations for different models.

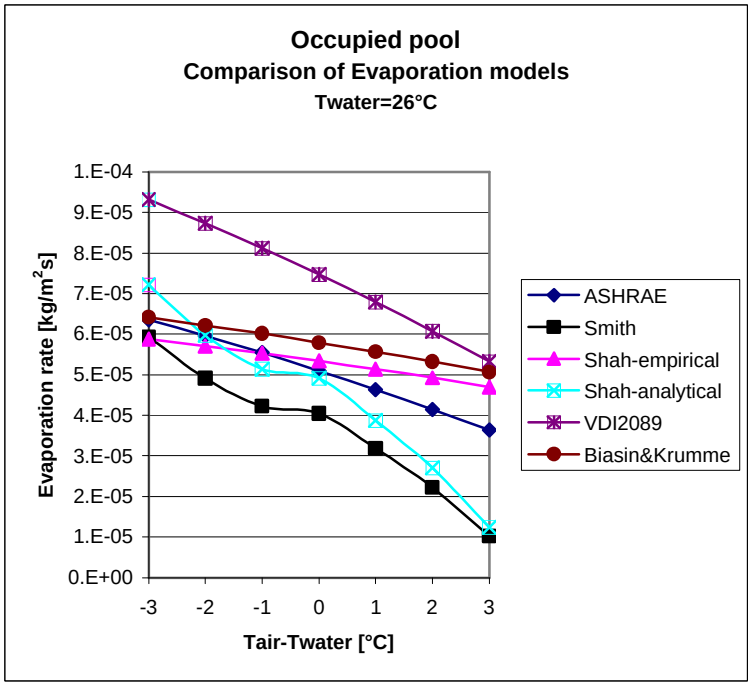

Figure 3.4: The water evaporation rate comparison for different models.

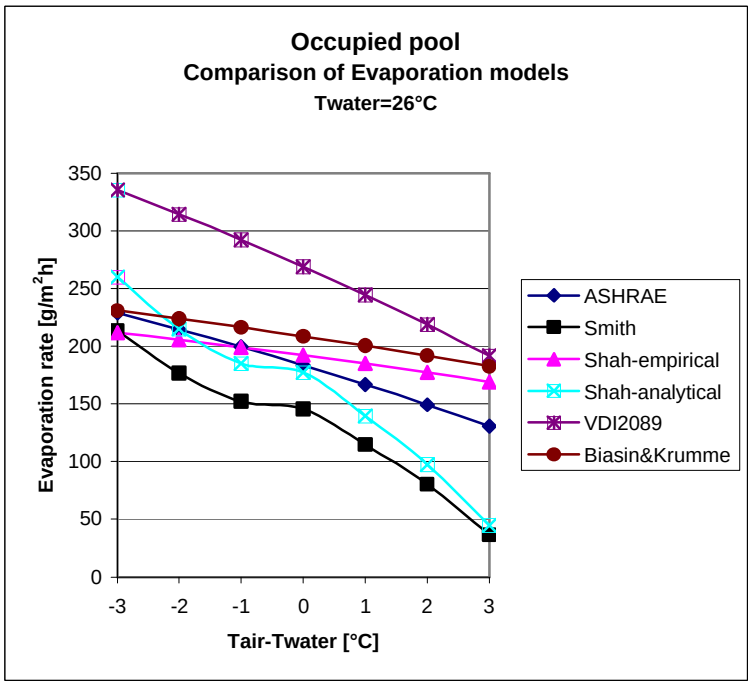

Figure 3.5: The water evaporation rate comparison for different models.

The rate of evaporation from occupied pools is higher than that from unoccupied ones for a variety of reasons, most notably the increase in contact area between air and

water. The increasing evaporation rate is from the wet bodies and the activities of occupants and the wet deck. ASHRAE correlation can be used for higher occupancies. Biasin & Krumme and Shah empirical formula are very similar each other. VDI2089 is quite higher and Smith formula is quite lower. Shah recommended that for occupied swimming pools with normal activity, shah empirical formula would be better. For occupied swimming pools with normal activity, Shah empirical correlation fits best with available data in his literature.

Figure 3.6 shows the water evaporation rate comparison of Shah empirical correlation for different occupant's number. It shows very little differences of water evaporation rate.

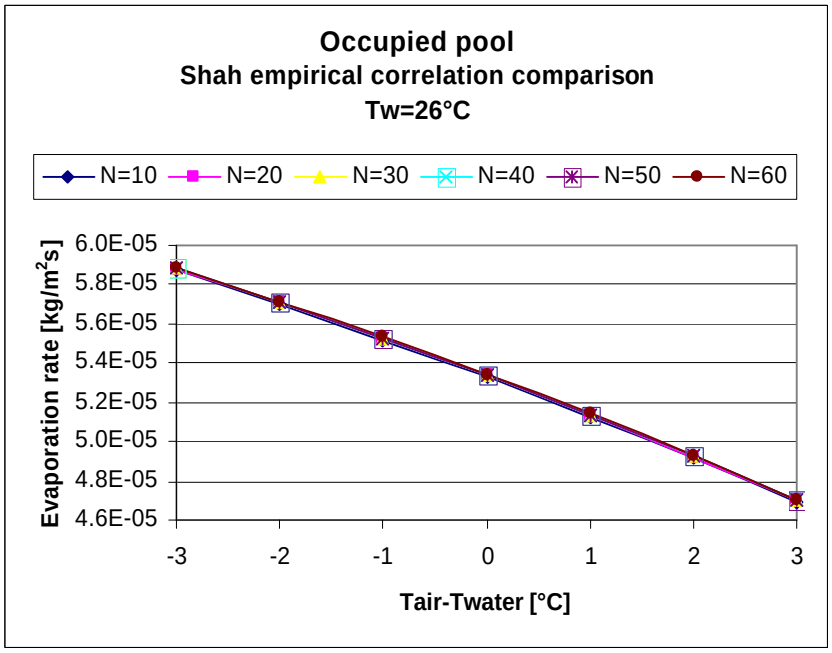

Figure 3.6: The water evaporation rate comparison of Shah empirical correlation for different occupant's number.

References:

[1] J. A. Goff and S. Gratch. Standardization of Thermodynamic Properties of Moist Air. Trans. ASHVE, 55, 463-464, 1949

[2] T. H. Kuehn et al. Thermal Environmental Engineering. 179-182,1998, ISBN 0-13-917220-3
[3] W. C. Reynolds. Thermodynamic Properties in SI: Graphs, Tables, and Computational Equations for 40 Substances. Department of Mechanical Engineering, Stanford University, 1979

4 CFD Modelling

4.1 Introduction

CFD (Computational Fluid Dynamics) has been used in the field of building services design for at least the last decade and it is a technology that has come to be accepted by a significant number of engineering consultants and building end users. CFD modelling is being promoted as a tool for predicting ventilation rates and air flow patterns as part of the building design process. The potential benefits of this form of modelling are that designs can be optimised to make the most efficient use of ventilation, and so to increase air quality and decrease energy use.

CFD is a very strong tool for engineer to compress the design and development cycle. From the results of CFD simulations, the detailed air flow field in swimming hall can be obtained in this project. Therefore, the relation between water evaporation and air movement can be investigated, and the water evaporation rate for dimensioning the ventilation system in swimming baths can be determined. So, an operation tool for control strategies and a water evaporation module for BSIM2002 can be developed.

The CFD analysis of steady state moist air flow in this report is simulated by the commercial software - FLUENT 6.1.18, which is the trademark of FLUENT Inc. FLUENT uses Computational Fluid Dynamics techniques to predict the airflow, heat transfer and species transport within rooms or buildings. The complex effects of air viscosity, buoyancy and turbulence are properly represented so that a detailed and accurate picture of the air distribution, water vapour transport and the consequent heat-transfer process can be obtained.

4.2 Governing equation

The computational procedure, adopted for the evaluation of such two-dimensional and three-dimensional turbulence flow, is based on the solution of the governing equations for the dependent variables, which are three velocity components, pressure, temperature.

Continuity equation

$$\frac{\partial r}{\partial t}+\frac{\partial}{\partial x_i}\left(rU_i\right)=0$$

Where r is density of the fluid [kg/m^3]

t is time [s]

U_i is mean velocity component corresponding to the i direction [m/s]

x_i is coordinate direction i [m]

Momentum equations (Navier-Stokes equations)

$$\frac{\partial}{\partial t}(rU_i) + rU_j\frac{\partial U_i}{\partial x_j} = -\frac{\partial P}{\partial x_i} + \frac{\partial}{\partial x_j}\left(m\frac{\partial U_i}{\partial x_j} - r\overline{u_i'u_j'}\right) + rg_i$$

Where P is pressure [Pa]

m is laminar dynamic viscosity [kg/ms]

u_i' is fluctuating velocity component in the i direction [m/s]

g_i is gravitational acceleration in the i direction [m/s^2]

Energy equation

$$\frac{\partial}{\partial t}(rT) + rU_j\frac{\partial T}{\partial x_j} = \frac{\partial}{\partial x_j}\left(g\frac{\partial T}{\partial x_j} - r\overline{u_j'T'}\right) + S_T$$

Where T is time-mean temperature of the fluid [°C]

g is diffusion coefficient

T' is fluctuation temperature [°C]

S_T is source term [W/m^3]

4.3 CFD model

The project refers to the study of moist airflow, heat and mass transfer and water vapour mixing with the moist air and transport inside the Korsør swimming pool. Airflow is considered to be turbulent and steady state, and the turbulent flow is described by the widely used standard *k-e* turbulence model.

Standard *k-e* model

$$\frac{D}{Dt}(rk) = \frac{\partial}{\partial x_j}\left[\left(m + \frac{m_t}{s_k}\right)\frac{\partial k}{\partial x_j}\right] + G_k - re$$

$$\frac{D}{Dt}(re) = \frac{\partial}{\partial x_j}\left[\left(m + \frac{m_t}{s_e}\right)\frac{\partial e}{\partial x_j}\right] + C_{e1}\frac{e}{k}G_k - rC_{e2}re$$

Where k is turbulent kinetic energy [J/kg]

e is rate of dissipation of turbulent kinetic energy [J/kg s]

m_t is turbulent viscosity [kg/ms]

G_k is buoyancy term

Constant: Ce_1 =1.44, Ce_2 =1.92, s_k =1.0, s_e =1.3

Species transport model

FLUENT can model the mixing and transport of species by solving conservation equations describing convection and diffusion for each component species. In this project, water vapour can be considered specie distributed inside the swimming pool.

In order to solve conservation equations for species, Fluent predicts the local mass fraction of each species, Y_i, through the solution of a convection-diffusion equation for the *i*th species. This conservation equation takes the following general form:

$$\frac{\partial}{\partial t}(rY_i) + \nabla \cdot (rvY_i) = -\nabla \cdot J_i + S_i$$

Where S_i is the rate of creation by addition from the dispersed phase plus any user-defined sources.

An equation of this form will be solved for *N-1* species where *N* is the total number of fluid phase species present in the system. Since the mass fraction of the species must sum to unity, the *N*th mass fraction is determined as one minus the sum of the *N-1* solved mass fractions. To minimize numerical error, the *N*th species should be selected as that species with the overall largest mass fraction. Therefore, there are two species in the CFD model – water vapour and air. Water vapour should be the first specie and the air should be the second specie. Then FLUENT can calculate mass diffusion in turbulent flows and species transport in the energy equation.

4.4 Water vapour source

When an unsaturated air flows against a wet surface in a swimming pool, some water will evaporate. The air-water interface is very thin and the interface may be considered to be in saturation condition. So this very thin boundary layer can be defined as a mass source term to describe the water vapor mass flow rate. The thickness of the boundary layer is assumed to be 5mm, and the temperature of the boundary layer is same as the water temperature. Figure 4.1 shows the Schematic of the water evaporation source term.

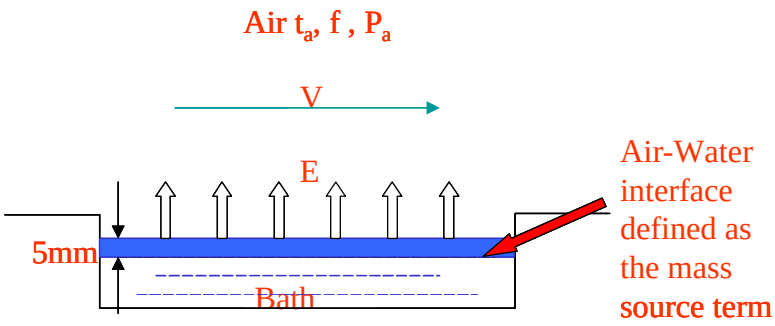

Figure 4.1: Schematic of the water evaporation source term.

4.5 Korsør Svømmehal

The CFD simulations are carried out for the moist air flow and water evaporation in the Korsør Svømmehal, which pictures are shown as follows.

Figure 4.2: The outside view of the Korsør Svømmehal.

Figure 4.3: The outside view of the Korsør Svømmehal.

Figure 4.4: The inside view of the Korsør Svømmehal.

Figure 4.5: The inside view of the Korsør Svømmehal.

5 2D CFD simulations

5.1 Introduction

Even though two dimensional CFD simulations can not obtain very accurate results, the CFD modelling always start from 2D modelling, because 2D modelling is preparation for 3D modelling. In another words, 2D modelling is used to get information of air flow field, and to test the water evaporation models and to test the feasibility of the CFD model.

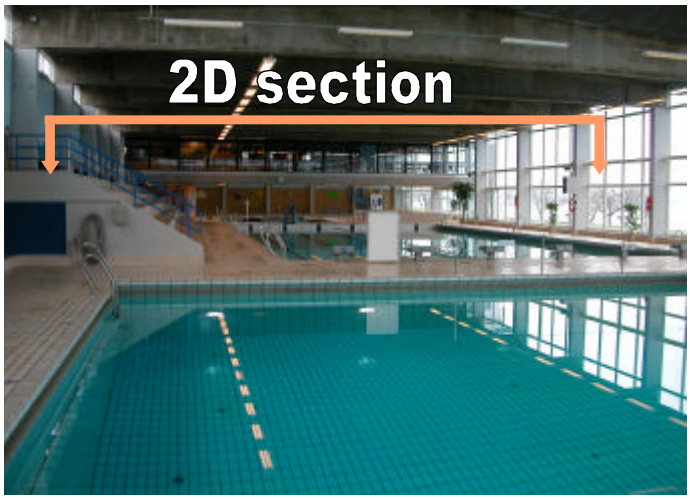

Figure 5.1: 2D modelling section for CFD simulations of Korsør Svømmehal.

Figure 5.1 shows the inside of korsør svømmehal and the 2D modeling section. The inlet air from ventilation system at the right side flows over the swimming bath and then exhaust from outlet at the left side. So this section expresses the characteristic of air flow and can be considered to be two dimensional section for CFD modelling.

5.2 Two-dimensional model

The geometry of the 2D section of the Korsør Svømmehal and the boundary conditions are appropriately represented in the CFD model.

5.2.1 Geometry

The main dimensions of the geometry are determined based on the drawings of ventilation system and building structure of the Korsør Svømmehal. The slope roof is simplified to be flat roof.

Building Height [m]	7.5
Building Length [m]	22.5
Bath Length [m]	12.5
Distance between floor and water surface	0.3
Inlet Width[m]	0.07
Outlet Width [m]	0.063

Table 5.1: Main dimensions of the 2D geometry in CFD modelling.

5.2.2 Boundary conditions

1. Thermal boundary conditions

The thermal boundary conditions are simplified as the constant temperature according to the first measurement data shown in Figure 5.2.

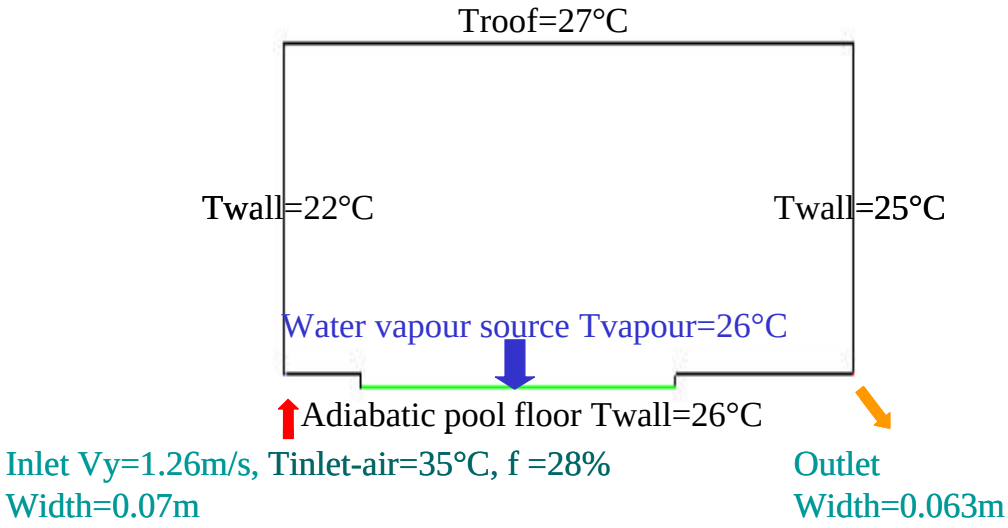

Figure 5.2: Boundary conditions of the 2D model.

2. The supply moist air

The inlet fixed airflow rate of the ventilation system is set to be 20,000 m^3/h = 5.56 m^3/s based on the experiment results. Because the length of the real building is 63 m, the inlet air velocity is set to be 1.26 m/s. And the temperature of the supply airflow is 35°C, the relative humidity of the supply airflow is 28%. Therefore, the mass fraction of water vapour in the inlet moist air is calculated to be 0.00979.

5.2.3 Grid

The domain is discretized to a non-uniform grid made of 8500 grids totally. The refined grids are used over the water surface and the water vapour source area.

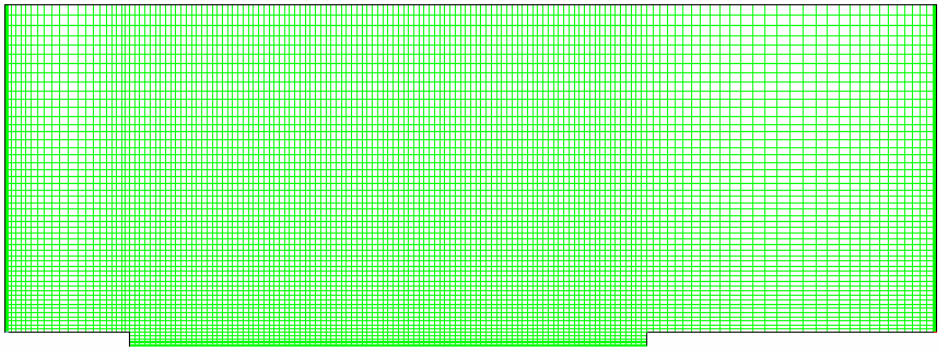

Figure 5.3: The grids of 2D modelling.

5.2.4 Convergence

The converged solutions are obtained by the second order accuracy and the convergence criterion is set to be 10^{-4}.

5.2.5 Simulation cases

Table 5.2 shows the four CFD simulation cases where the evaporation rate calculations are based on T_w = 26°C, T_{air} = 28°C and f = 60%.

Model	Pool type	Evaporation rate of water vapour source [kg/m^{3}s]
	No evaporation in pool	0
Shah	Unoccupied pool	0.003036
Shah empirical	Occupied pool	0.009853
ASHRAE	Occupied pool	0.008294

Table 5.2: Simulation cases in 2D simulations.

5.3 2D simulation results

The characteristics of moist air flow in the swimming hall can be understood by post-processing of the simulation results.

5.3.1 Results of unoccupied Shah correlation case

Figure 5.4 shows the velocity vectors distribution. The inlet moist air from inlet ventilation grill flows upward then flows to the opposite wall and backwards. The air velocity is little higher close to outlet. Figure 5.5 shows the air velocity in horizontal direction which influences the evaporation rate for Hyldgårds and Carrier models; in the area close to the water surface the air X velocity is higher than 0.1m/s. So it is easily to understand that the Hyldgårds and Carrier models will underpredict the water evaporation rate.

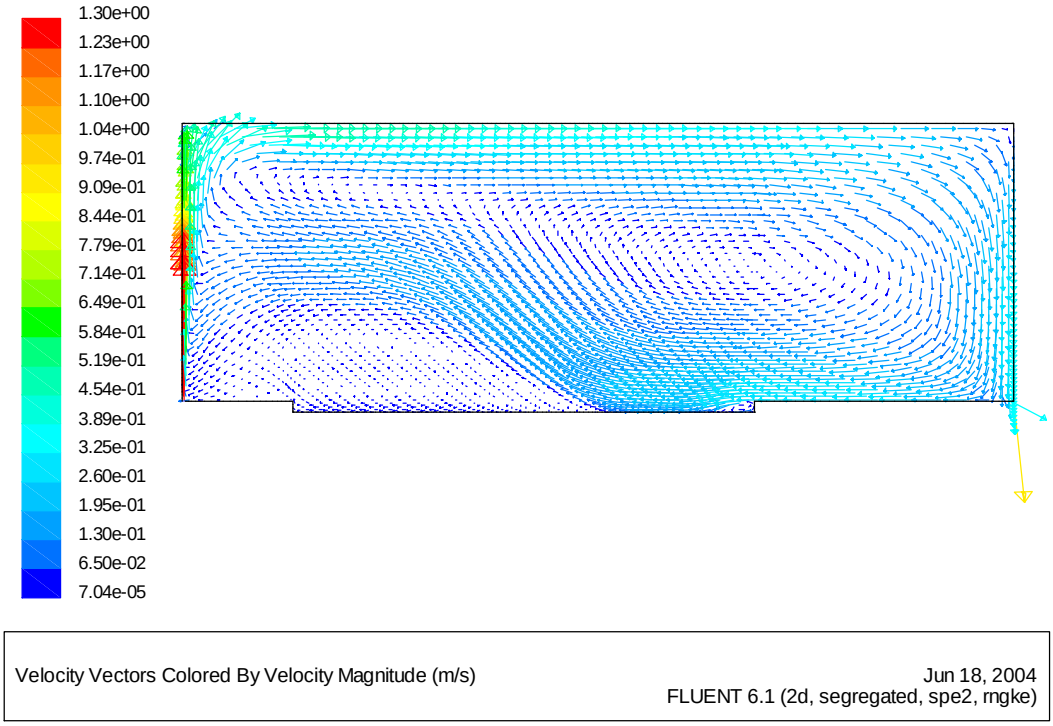

Figure 5.4: The velocity vectors of unoccupied Shah correlation case.

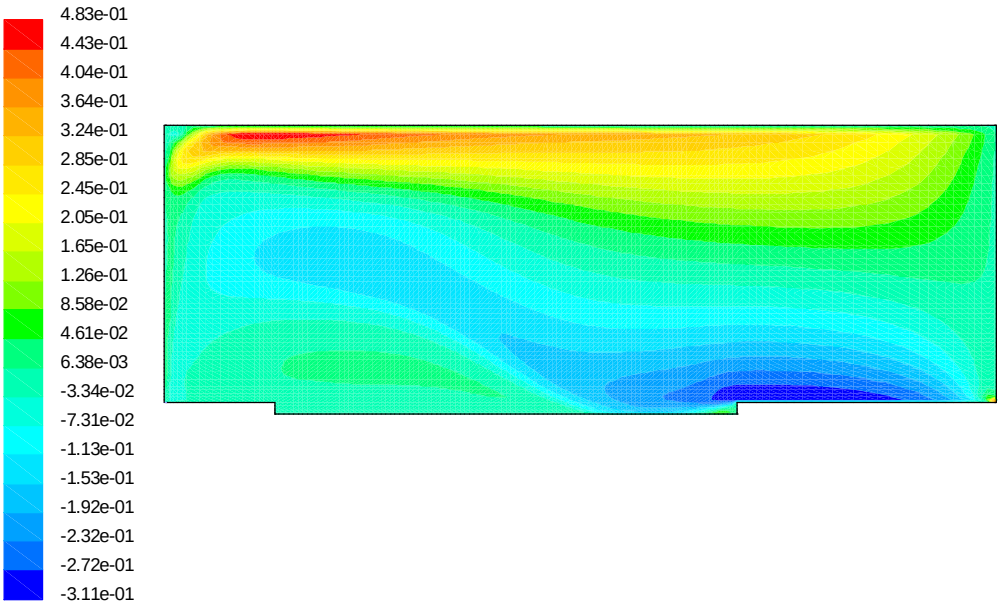

Figure 5.5: The X velocity contours of unoccupied Shah correlation case.

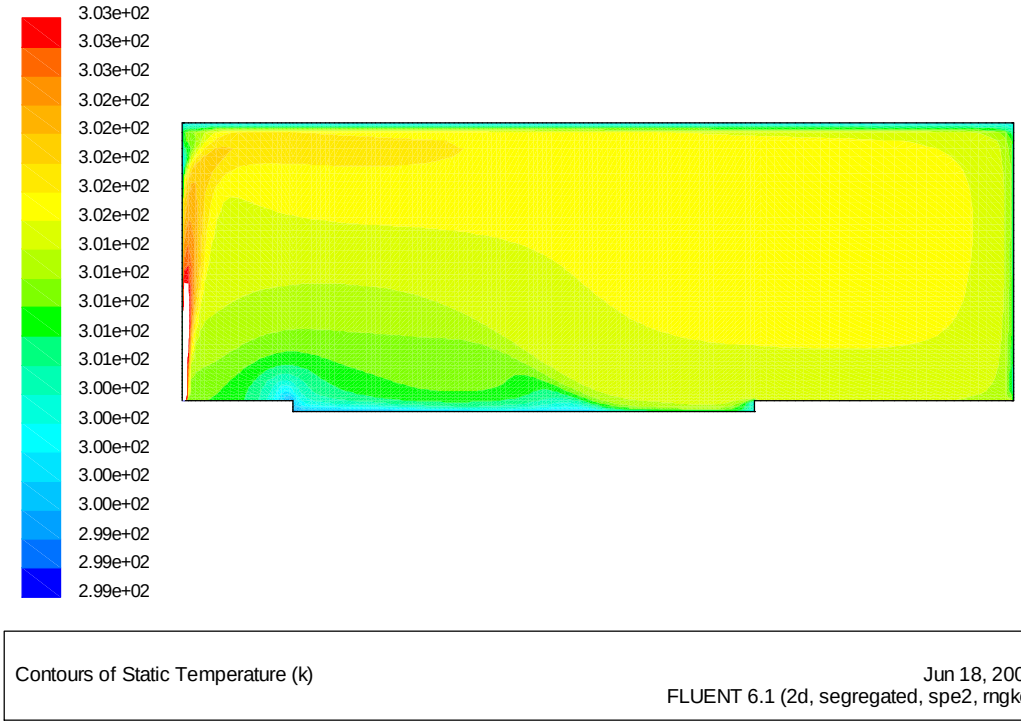

Figure 5.6: The temperature contours of unoccupied Shah correlation case.

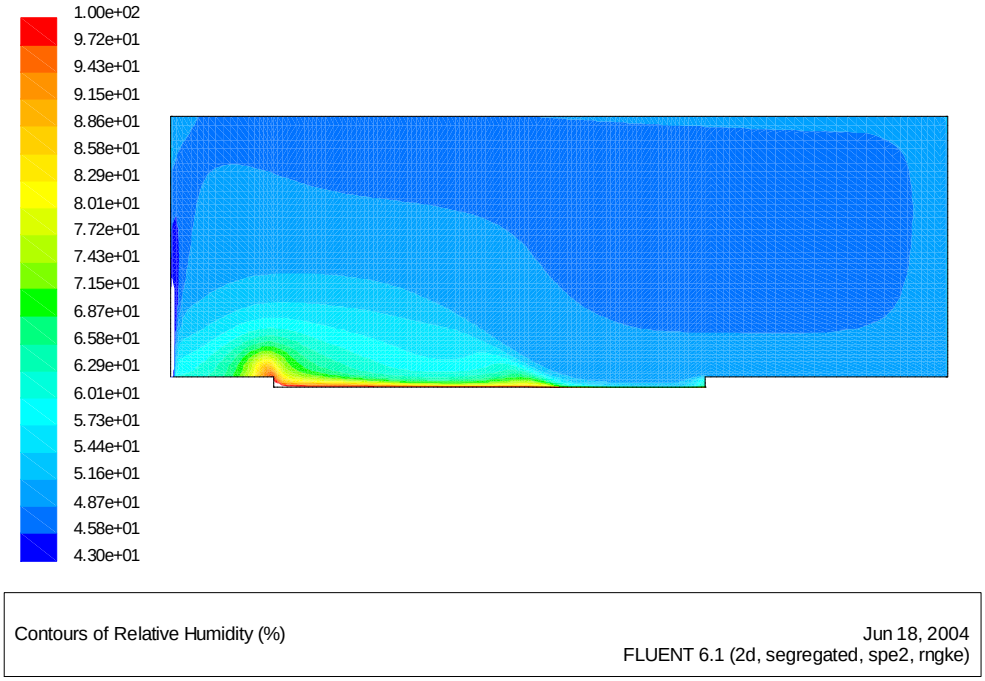

Figure 5.7: The relative humidity contours of unoccupied Shah correlation case.

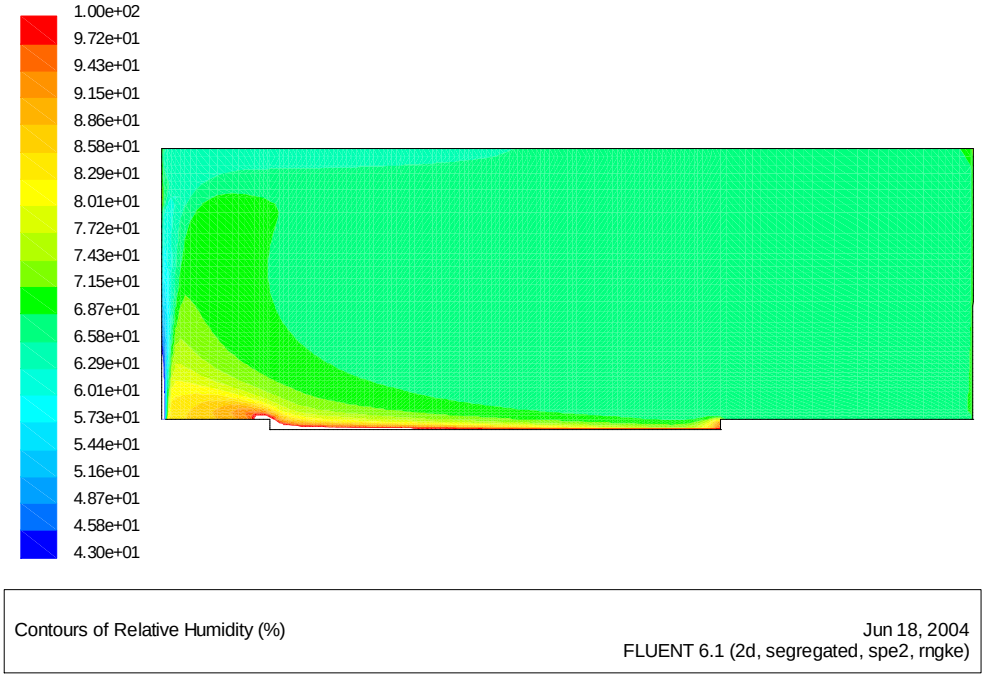

Figure 5.8: The relative humidity contours of occupied Shah empirical correlation case.

5.3.2 2D simulation result comparisons

To compare the relative humidity distribution for two different models, the unoccupied Shah correlation and the occupied Shah empirical correlation are shown in Figure 5.7 and Figure 5.8. The higher evaporation rate of the occupied Shah empirical correlation will give rise to the higher relative humidity.

The different parameters distributions on the middle line (X=9.25m) in the swimming pool for different models will be compared as follows. Different models will give different velocity distributions but the range of the velocities is almost same, shown in Figure 5.9. Similarly, the X-velocity distributions on this middle line are shown in Figure 5.10.

The temperature distribution on the middle line in Figure 5.11 shows that the temperature will decrease because of the water vapour in lower temperature. The temperature difference between them is about 0.5 degree along the line. The evaporation rate will influence the relative humidity very much shown in Figure 5.12. Higher evaporation rate will give rise to higher relative humidity. Over a certain height inside the swimming pool the relative humidity changes very small for every evaporation model.

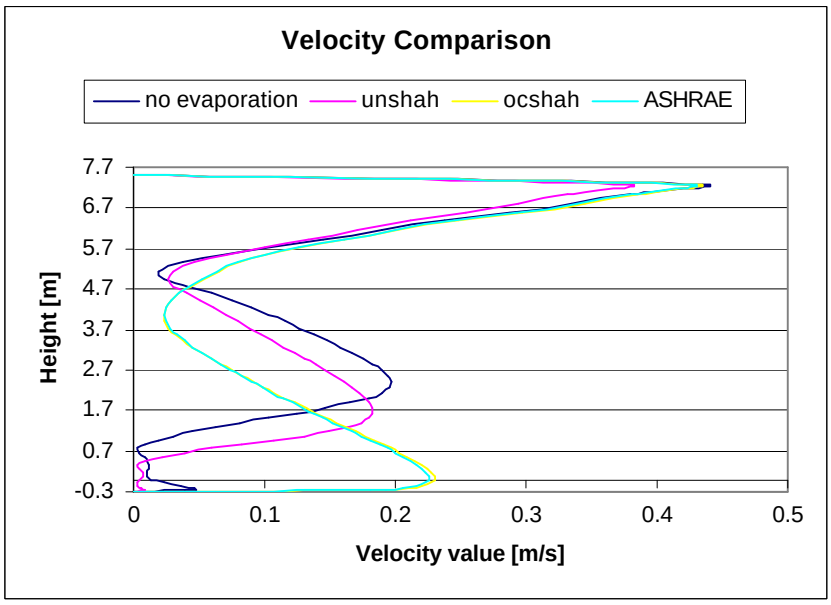

Figure 5.9: The comparison of velocity value distribution at X=9.25m for different evaporation models.

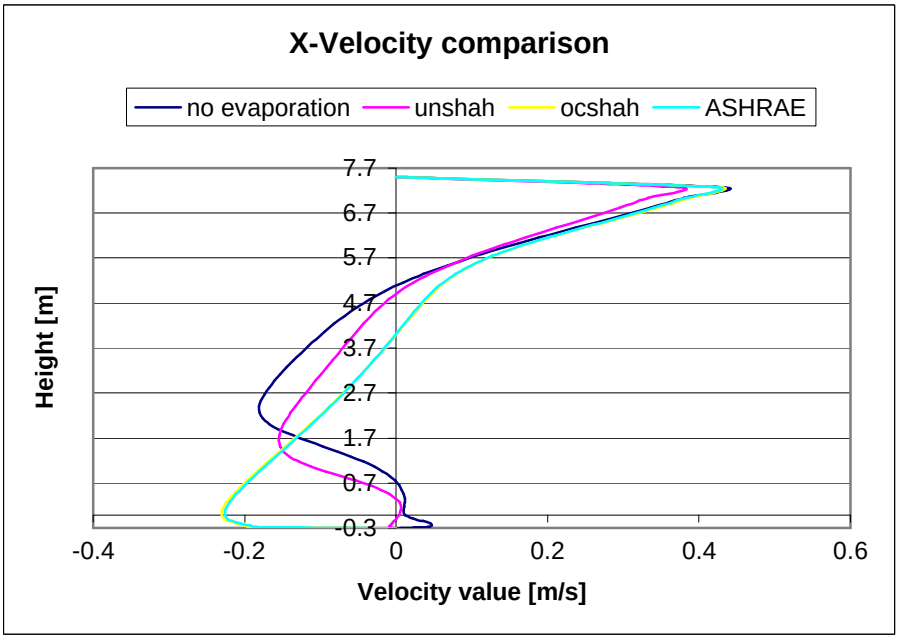

Figure 5.10: The comparison of X-velocity value distribution at X=9.25m for different evaporation models.

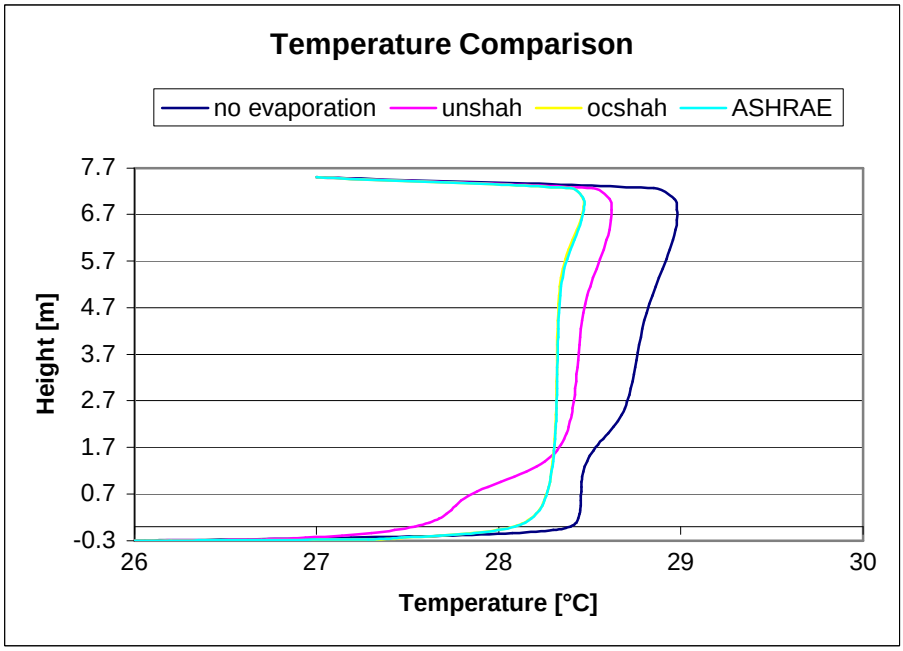

Figure 5.11: The comparison of temperature distribution at X=9.25m for different evaporation models.

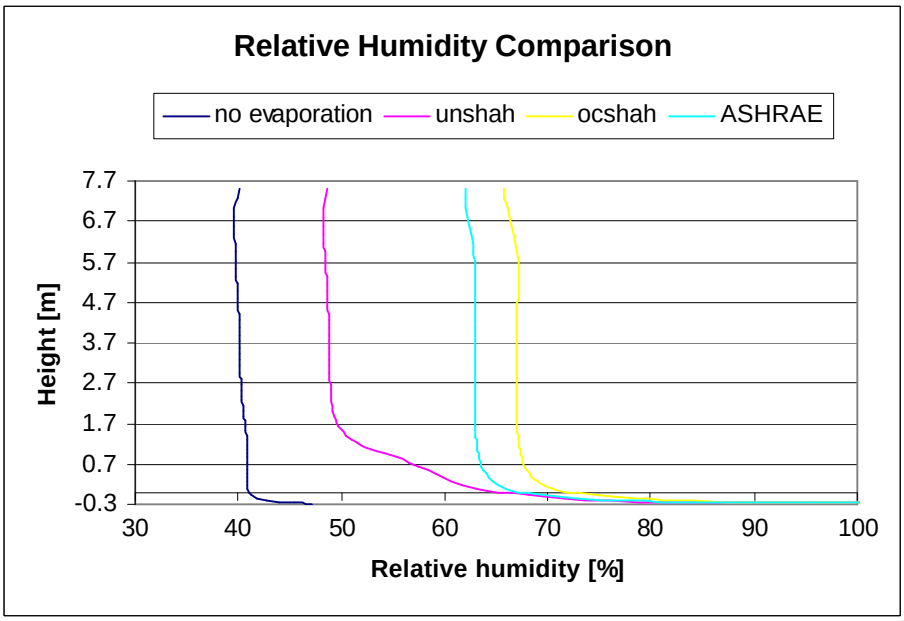

Figure 5.12: The comparison of relative humidity distribution at X=9.25m for different evaporation models.

5.4 Conclusions

It can be concluded from the 2D CFD simulation results that the water evaporation model works very well, therefore this model can be further used in 3D CFD simulations. Shah correlation and Shah empirical correlation can be used for unoccupied pools and occupied pools respectively.

The water evaporation rate influences relative humidity distribution very much inside the swimming hall, but the water evaporation rate for different models influences the air velocity and the temperature distributions very small inside the swimming.

6 3D simulations

6.1 Three-dimensional model

The geometry of the 3D model of the Korsør Svømmehal and the boundary conditions are appropriately represented in the CFD model based on the drawings of the Korsør Svømmehal and measurement results.

6.1.1 Geometry

The geometry of the CFD model in GAMBIT is simplified appropriately. The model geometry of Korsør Svømmehal is quite complicated, including slope roof, four swimming baths, 13 beams, one cafeteria, a long spectatory of staircases, walls, floors, windows and glass facades, 52 inlet grills and 2 outlet grills. The 52 inlet grills can be simplified as 5 long inlets in CFD model according to ventilation rate and inlet air velocity given by the drawings of ventilation system. The main dimensions of the model are shown in Table 6.1, Table 6.2 and Table 6.3 respectively, and the three dimensional models are shown in Figure 6.1 – Figure 6.3.

Building Length [m]	63
Building Width [m]	22.5
Building Height of low side wall [m]	6.5
Building Height of high side wall [m]	13
Slope angle of the roof [degree]	5.08
Slope angle of the roof over spring bath [degree]	18.43

Table 6.1: Main dimensions of the 3D geometry in CFD model.

Spring bath Length [m]	12.5
Spring bath width [m]	12.5
Swimming bath Length [m]	25
Swimming bath width [m]	12.5
Teaching bath Length [m]	11
Teaching bath width [m]	6
Small child bath Length [m]	9
Small child bath width [m]	3
Distance between floor and water surface [m]	0.3

Table 6.2: Main dimensions of the swimming baths in CFD model.

Inlet and Outlet	Size	View from +Z-direction
Length of inlet1 [m]	22.5	Right side in the hall
Width of inlet1 [m]	0.03	
Length of inlet2 [m]	22.5	Left side in the hall
Width of inlet2 [m]	0.03	
Length of inlet3 [m]	15	Front side in the hall
Width of inlet3 [m]	0.04	
Length of inlet4 [m]	43.5	Behind right side in the hall
Width of inlet4 [m]	0.04	
Length of inlet5 [m]	19.5	Behind left side in the hall
Width of inlet5 [m]	0.04	
Length of outlet1 and outlet2 [m]	1.4	
Width of outlet1 and outlet2 [m]	1.2	

Table 6.3: Main dimensions of the inlets and outlets in CFD model.

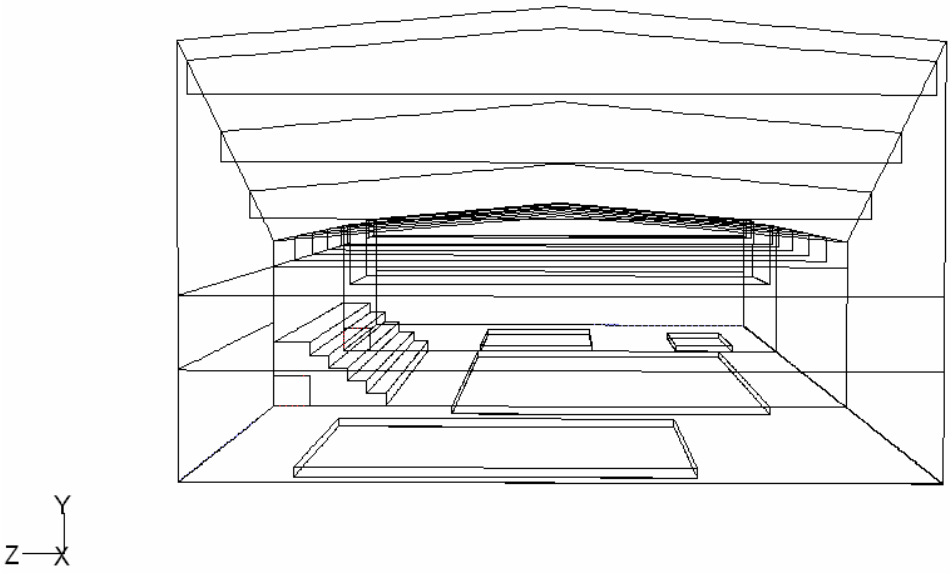

Figure 6.1: The geometry view in X-direction.

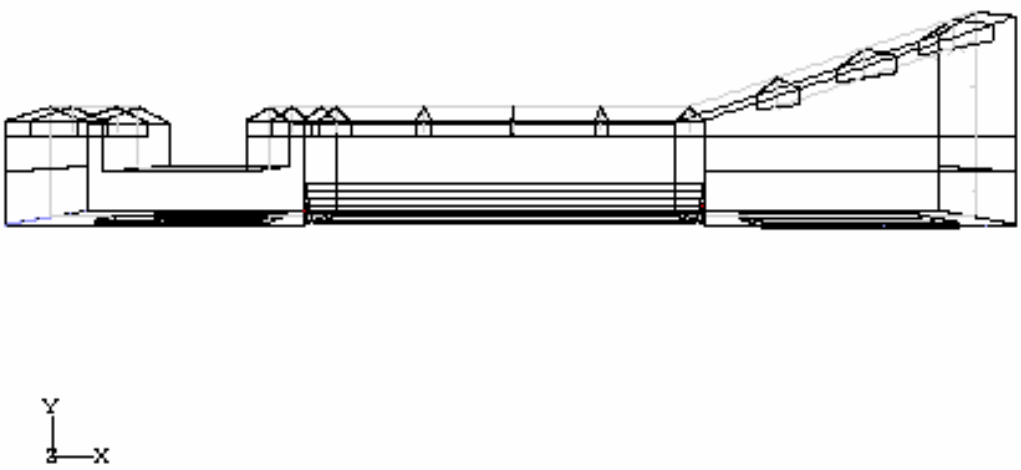

Figure 6.2: The geometry view in Z-direction.

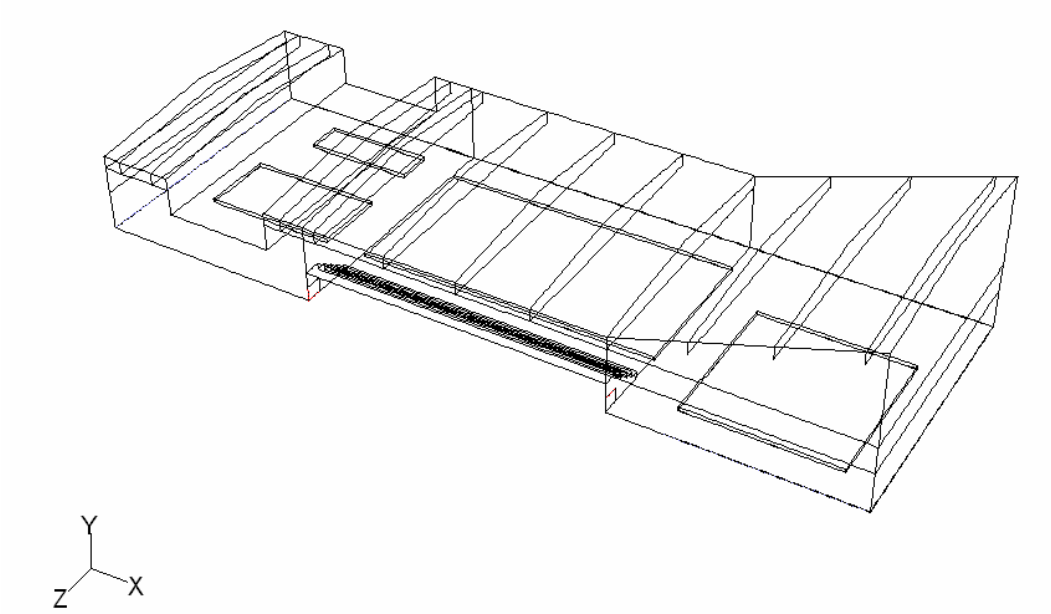

Figure 6.3: The geometry view in X, Y, Z-direction.

6.1.2 Boundary conditions

1. Thermal boundary conditions

The thermal boundary conditions are simplified and the calculated values are shown in Table 6.4 based on the second measurement data (19.05.2004) and heat balance equations of Korsør Svømmehal.

Wall type	Heat flux [W/m^2]	Temperature [°C]
Wall of the hall	-10	
Window	-45	
Glass facade	-45	
Roof	-5	
Wall of the water vapour source zone		28
All the other walls	0	adiabatic

Table 6.4: Thermal boundary conditions of the 3D model.

2. The supply moist air

The inlet fixed airflow rate of the ventilation system is set to be 18,000 m^3/h = 5 m^3/s according to the experiment results. The temperature of the supply airflow is 38°C, and the relative humidity is 29%. So the mass fraction of water vapour in the inlet

moist air is calculated to be 0.0119469. The inlet air velocities are calculated and shown in Table 6.5.

Inlet	Velocity [m/s]
Inlet1	1.14
Inlet2	0.633
Inlet3	1.327
Inlet4	1.395
Inlet5	0.771

Table 6.5: The inlet boundary conditions of the 3D model.

3. The water vapour source in swimming baths

The temperature of the water vapour source in swimming baths is set to be 28 °C same as the water temperature for unoccupied pool. But for occupied pool, the source temperature is set to be 34 °C in small child bath and 28 °C in the other three pools.

6.1.3 Grid

The domain is discretized to a non-uniform grid made of 645,408 grids totally. The refined grids are used for inlet, outlet, the water surface and water vapour source area.

Figure 6.4: The grid display at the plane Z = 11.25 m, the middle plane of the hall.

Figure 6.5: The grid display at the plane X = 31.5 m, the middle plane of the hall.

Figure 6.6: The grid display at the plane Y = 3 m.

6.1.4 Convergence

The converged solutions are obtained by the first order accuracy and the convergence criterion is set to be 10^{-3}. The average temperature and the average relative humidity of the middle plane Z = 11.25 m are monitored for the convergence.

6.1.5 Simulation cases

Table 6.6 shows the two CFD simulation cases where the evaporation rate calculations are based on T_w = 28°C, T_{air} = 30°C, f = 52% for unoccupied pool of the outlet moist air, which are given by the measurement results. And for occupied pool, the evaporation rate calculations are based on T_w = 28°C, T_{air} = 30°C, f = 82% for small child bath; T_w = 28°C, T_{air} = 30°C, f = 62% for the other three baths.

Model	Pool type	Evaporation rate of water vapour source [kg/m^{3}s]
Shah	Unoccupied pool	0.00437
Shah empirical	Occupied pool	0.01200 for small child bath 0.01002 for the other three baths

Table 6.6: Simulation cases in 3D simulations.

6.2 3D simulation results

The characteristics of moist air flow in the swimming hall can be understood by post-processing of the simulation results.

6.2.1 Results of unoccupied Shah correlation case

6.2.1.1 Velocity distribution

Figure 6.7 – Figure 6.21 show the velocity vector distributions for different planes in the swimming hall. The air flow movement is quite complicated due to the complicated model geometry, the ventilation grills distribution. The different air flow velocities from inlet, the wall boundary conditions, the cafeteria and the beams influence the air flow field largely.

The main air flow along X direction can be seen in the figures of velocity distributions at plane Z = = 5 m, Z = 11.25 m and Z = 21.5 m. The inlet airflow from left side flows up and turns right against roof then turns down to the floor, the airflow meets the airflow from right side and then flows up to right side along the upper part of the room. The inlet airflow from right side flows up and meets the flow from left side, then flows down to the left side along the lower part of the room.

The main air flow along Z direction can be seen in the figures of velocity distributions at plane X = 10 m, X = 31.5 m and X = 55m. In the zone of the small child bath and sport bath, the airflow seems to be regular because the inlet is located at the right side and the outlet located at the left side. The inlet airflow from right side flows up and turns left along the roof then turns down to the floor along the left side wall, then the airflow flows to right side along the lower part of the room. In the zone of the spring bath, the airflow is very complicated because there are three inlets around this zone and the inlet air velocities are different.

The inlet air velocity and air flow rate in spring bath area are higher than them in the other zones. This situation will give rise to little higher room temperature and little lower relative humidity. For the same reason, the inlet air velocity and air flow rate in small child bath area are lower, this situation will produce lower temperature and higher relative humidity. Therefore, the gradient of the temperature and relative humidity along X direction are very clear.

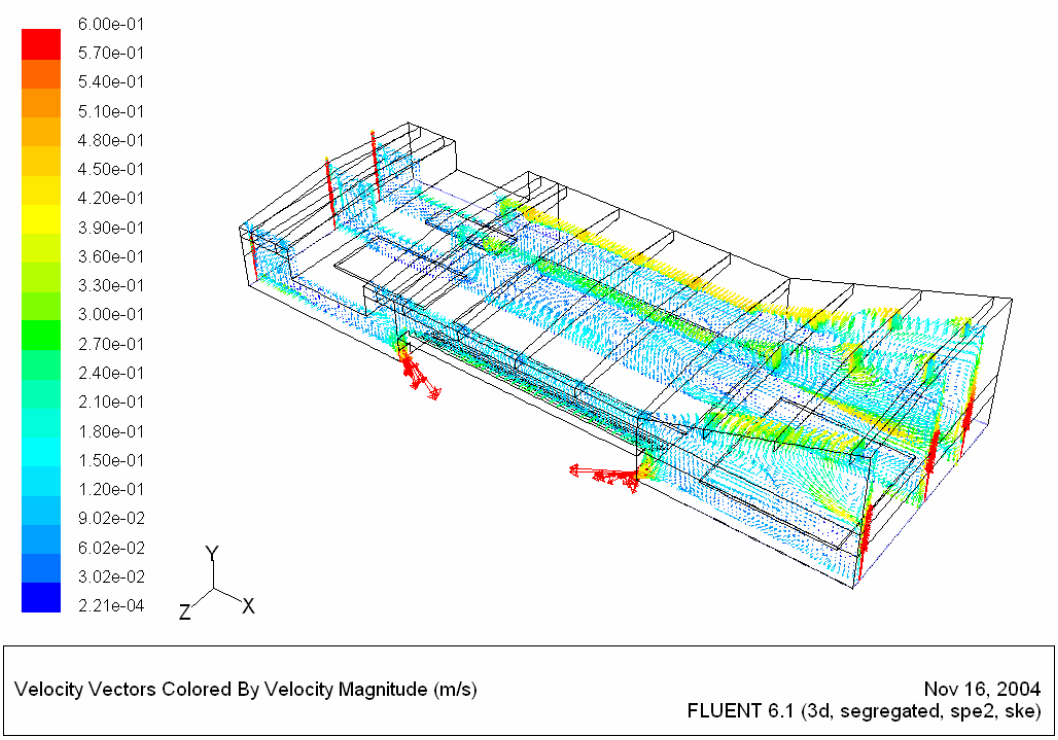

Figure 6.7: Velocity distributions at plane Z = 5 m, Z = 11.25 m and Z = 21.5 m.

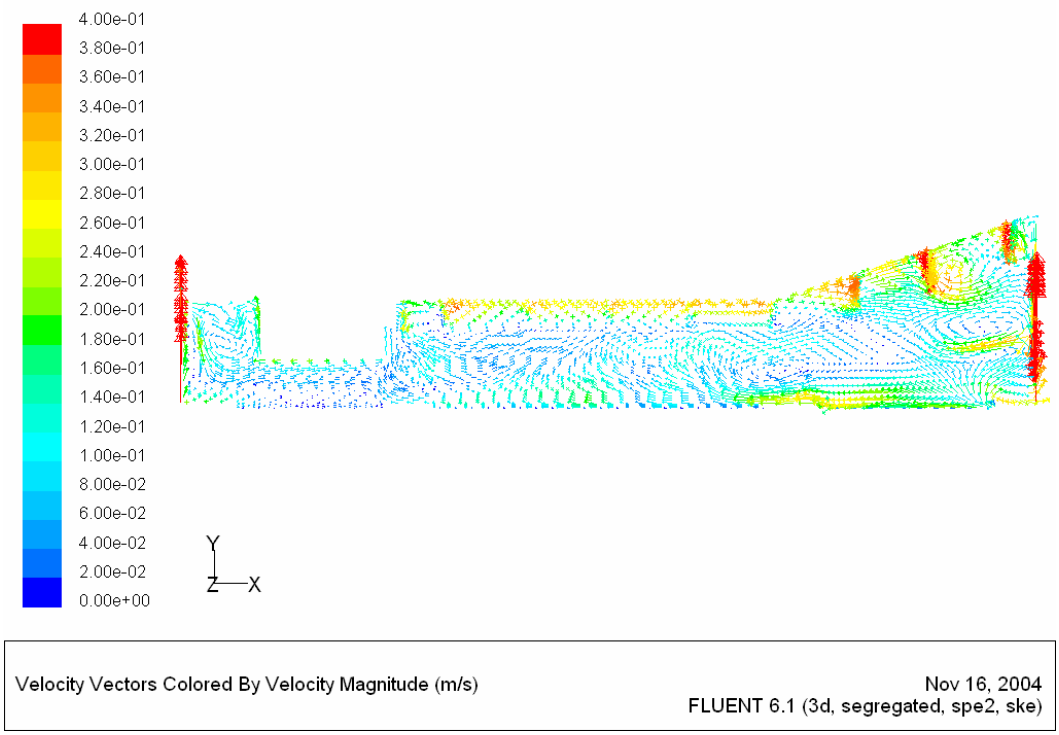

Figure 6.8: Velocity distributions at plane Z = 11.25 m.

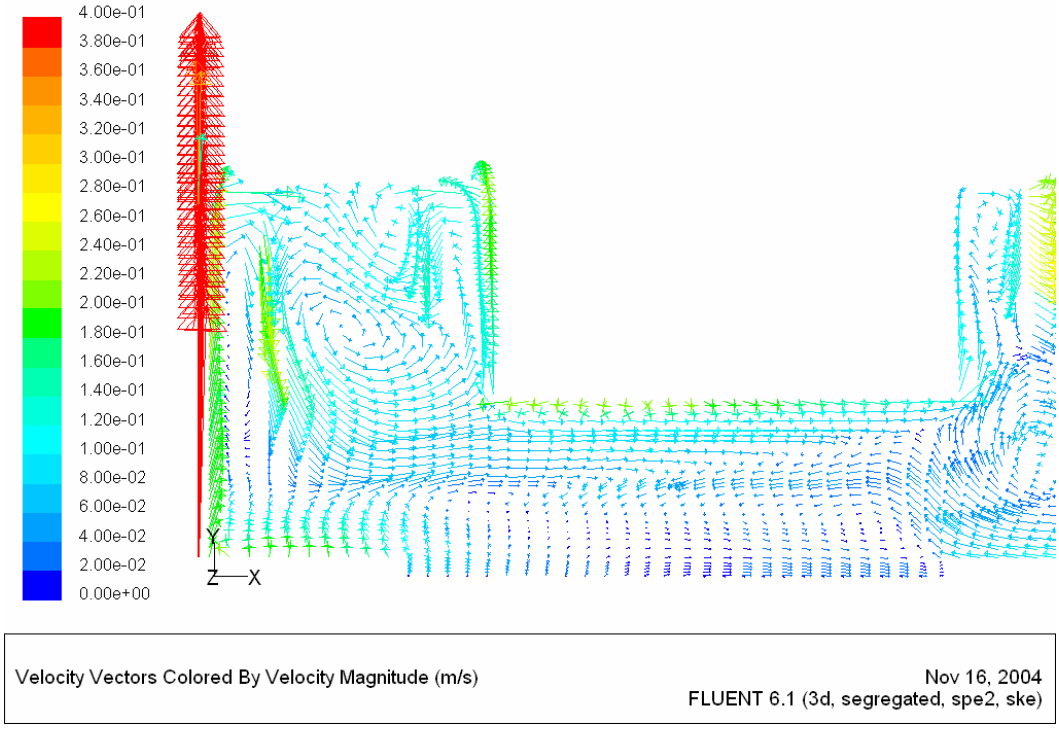

Figure 6.9: Velocity distributions of left part in the hall at plane Z = 11.25 m.

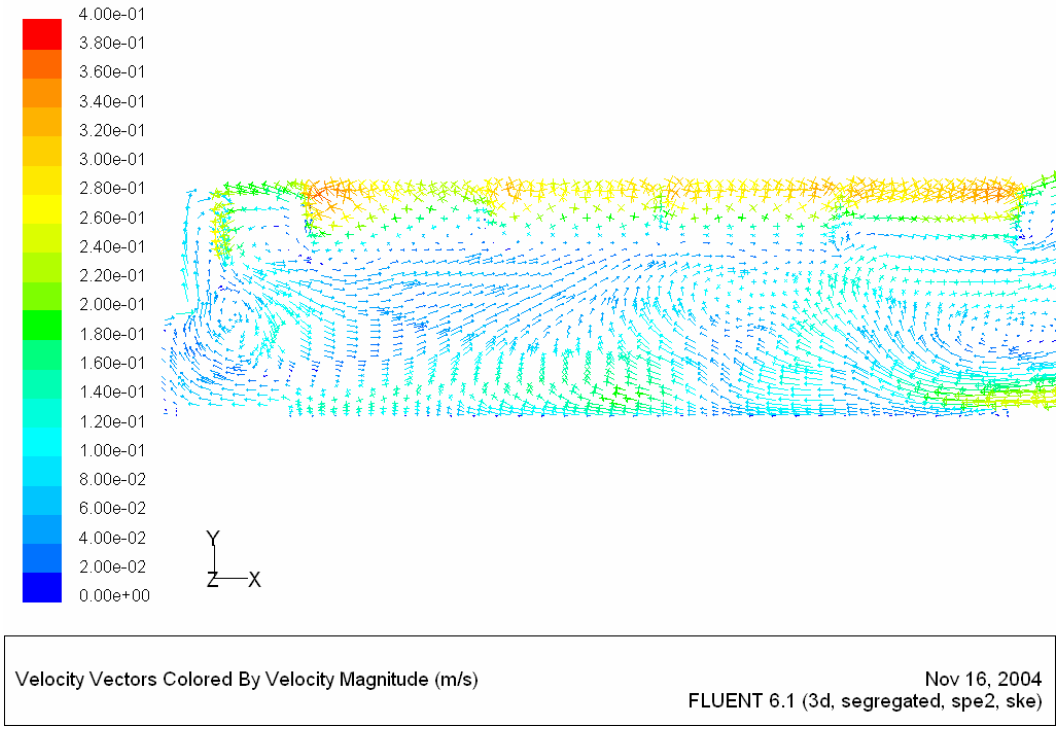

Figure 6.10: Velocity distributions of middle part in the hall at plane Z = 11.25 m.

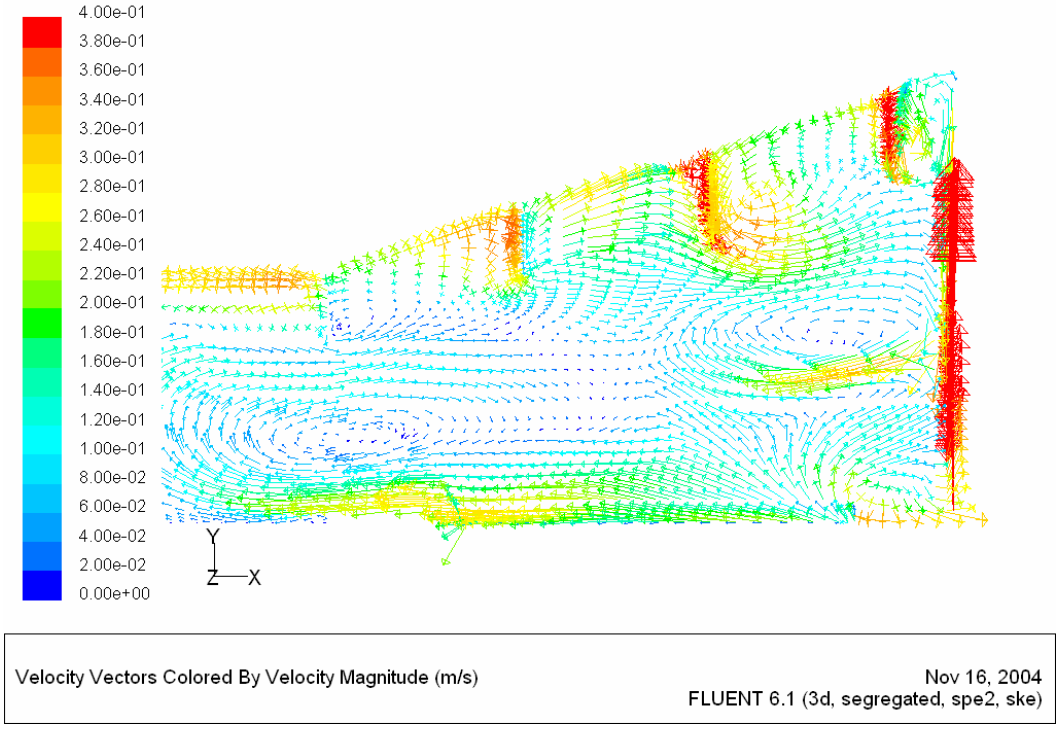

Figure 6.11: Velocity distributions of right part in the hall at plane Z = 11.25 m.

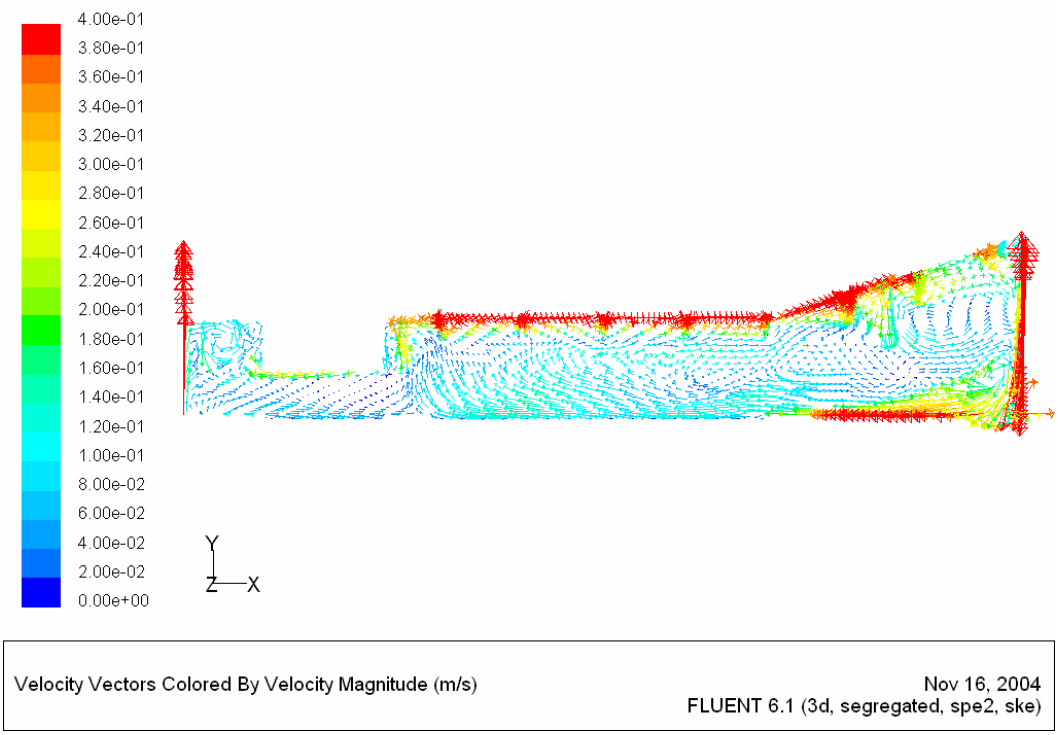

Figure 6.12: Velocity distributions at plane Z = 5 m.

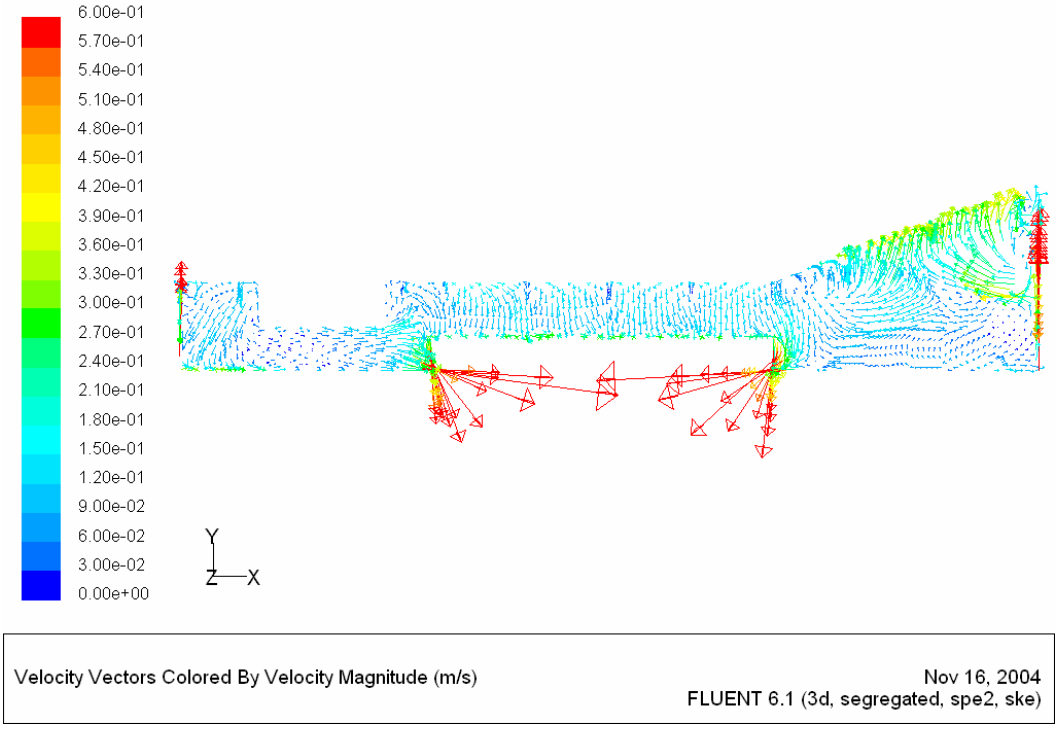

Figure 6.13: Velocity distributions at plane Z = 21.5 m.

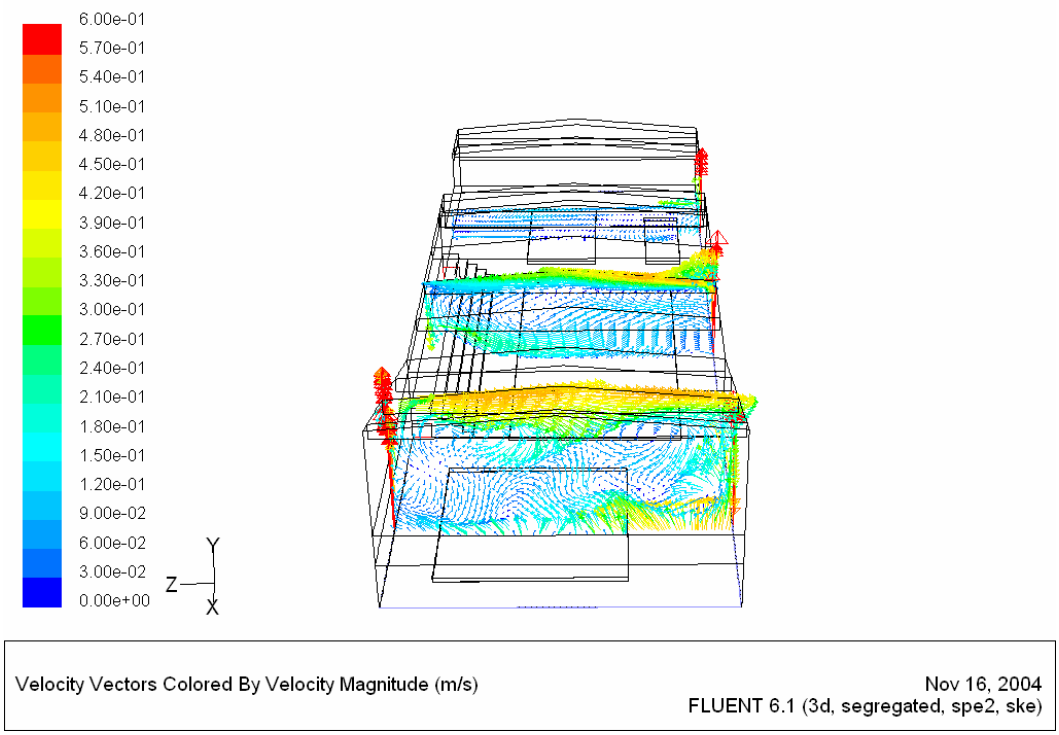

Figure 6.14: Velocity distributions at plane X = 10 m, X = 31.5 m and X = 55m.

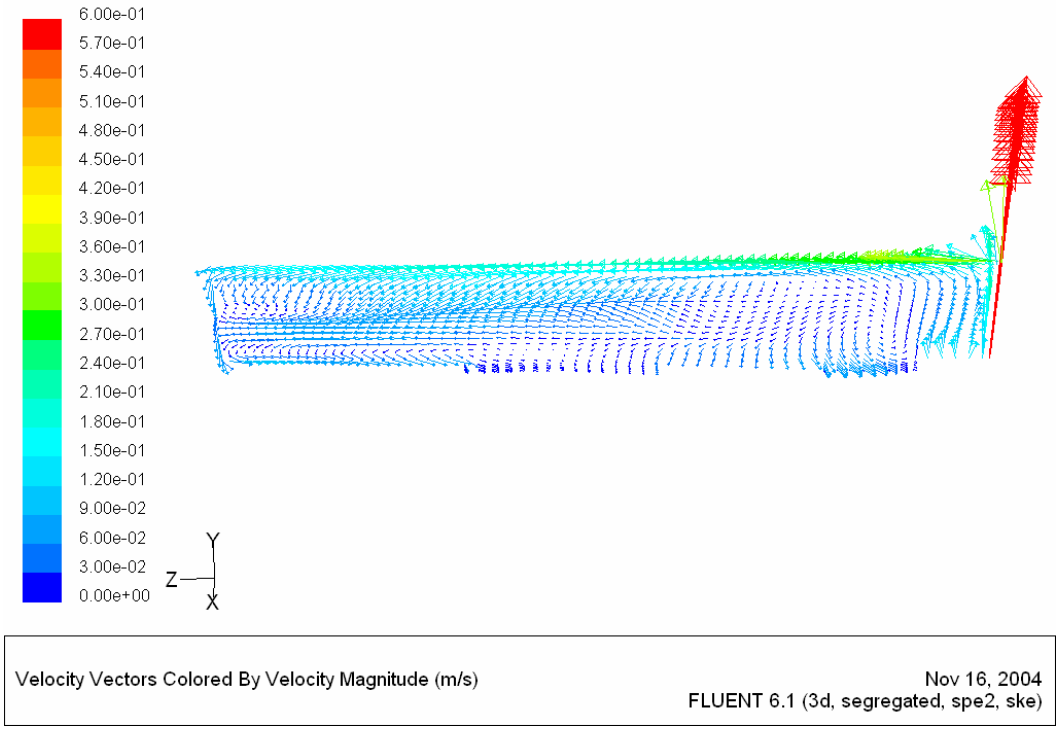

Figure 6.15: Velocity distributions at plane X = 10 m.

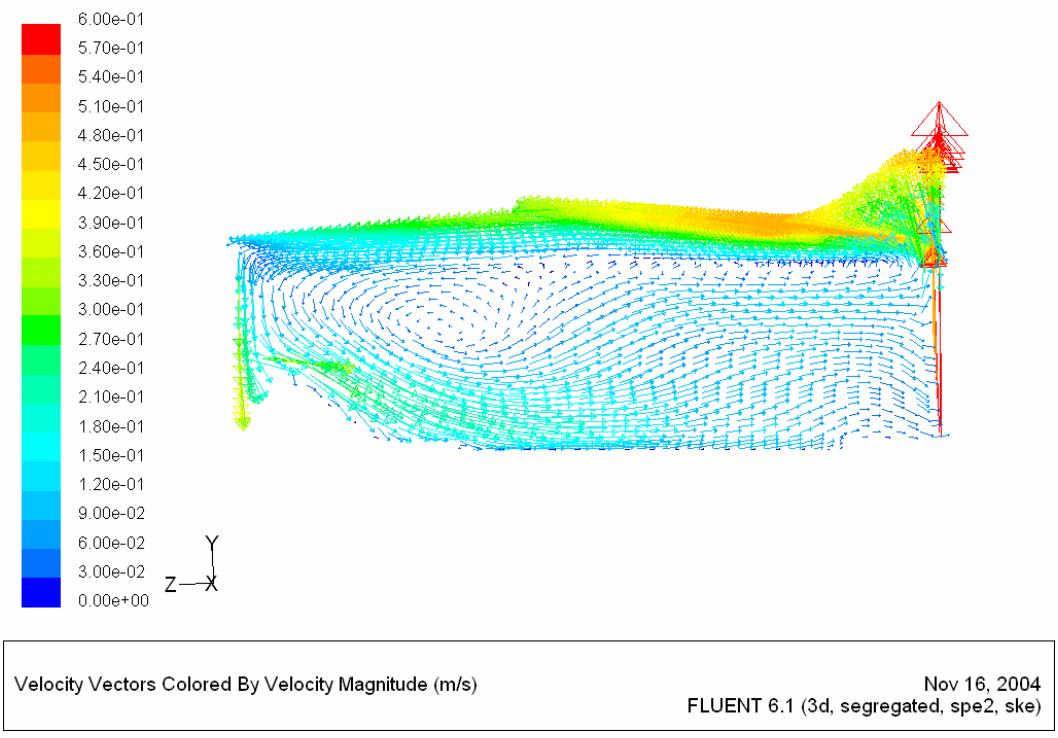

Figure 6.16: Velocity distributions at plane X = 31.5 m.

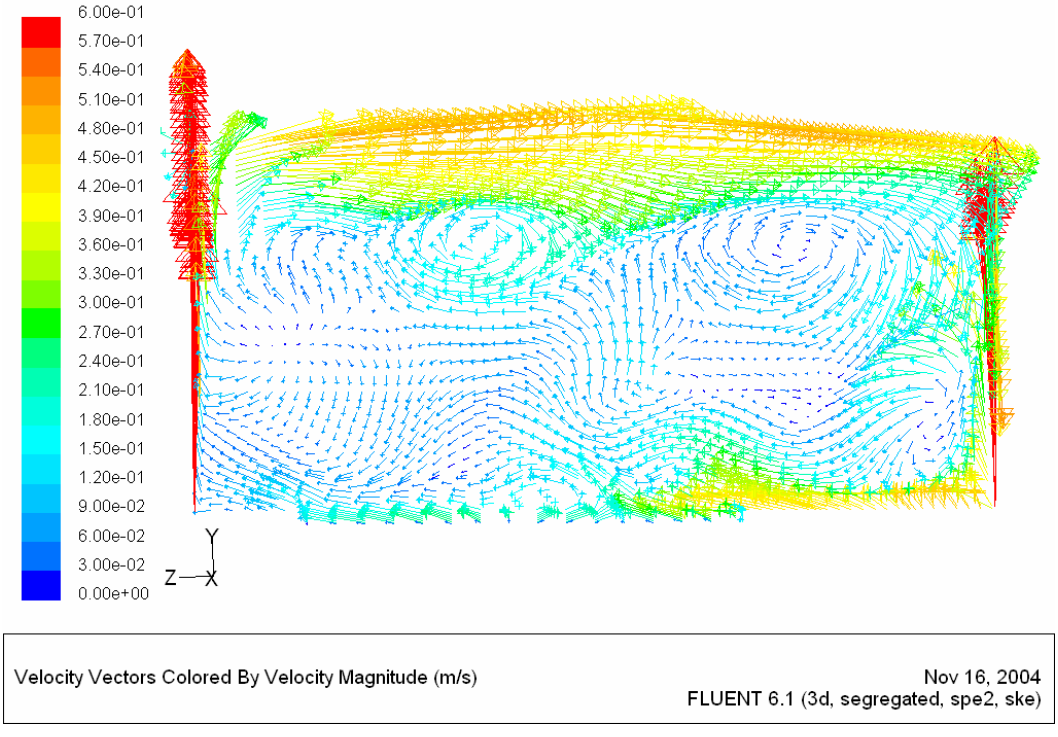

Figure 6.17: Velocity distributions at plane X = 55 m.

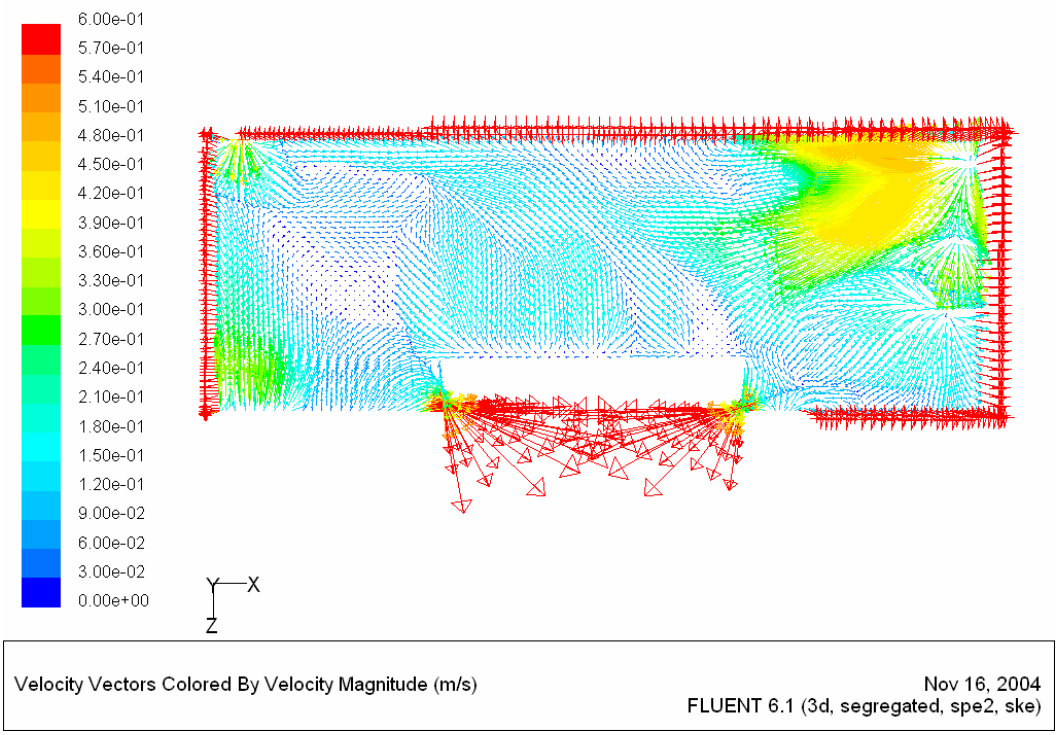

Figure 6.18: Velocity distributions at plane Y = 0.1 m.

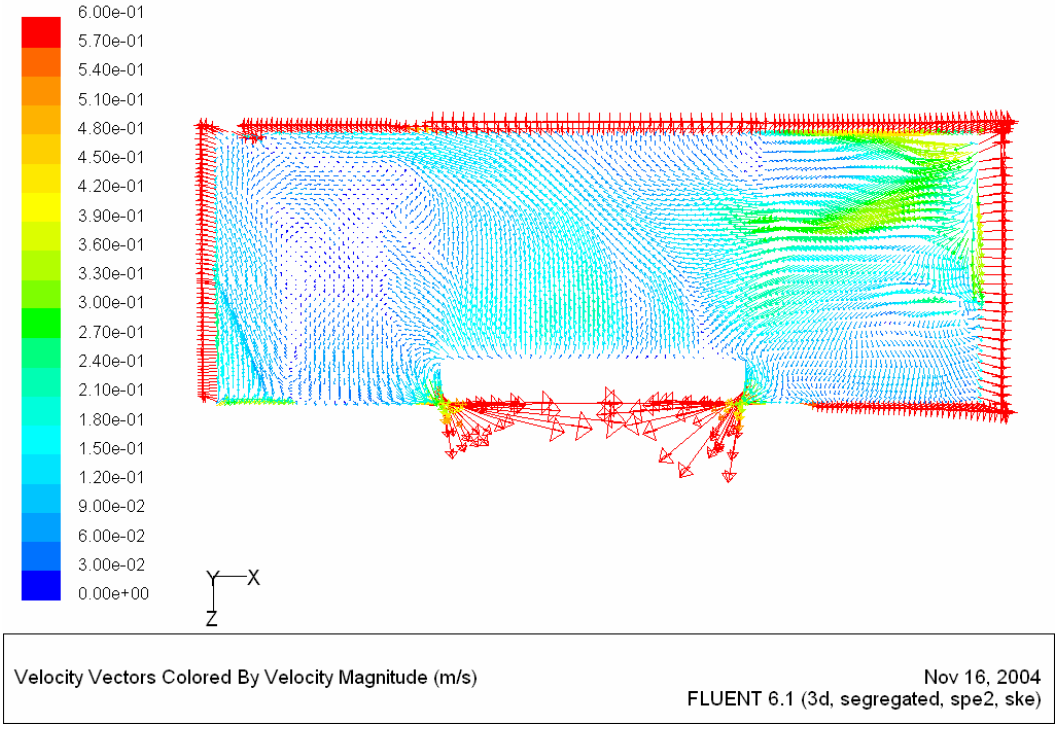

Figure 6.19: Velocity distributions at plane Y = 0.77 m.

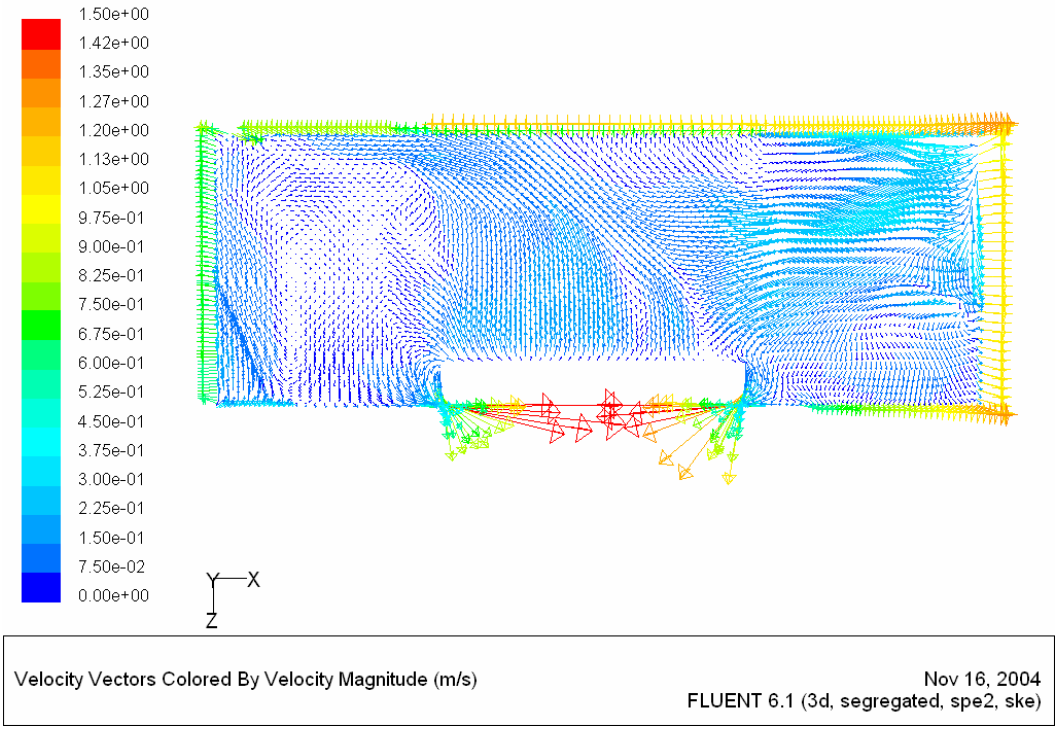

Figure 6.20: Velocity distributions at plane Y = 0.77 m.

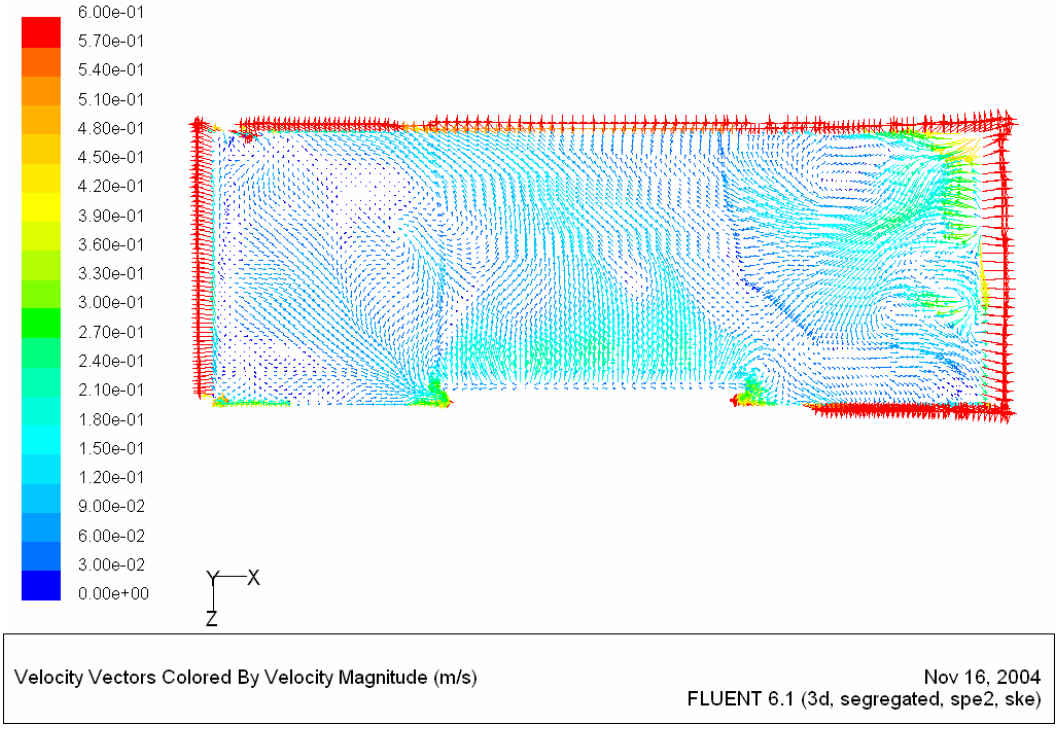

Figure 6.21: Velocity distributions at plane Y = 2 m.

6.2.1.2 Temperature distribution

Figure 6.22 – Figure 6.29 show the air temperature distributions for different planes in the swimming hall. Generally, the air temperature keeps about 30 °C, but it is little lower close to the water surface because the water temperature is 28 °C. Along the Y direction of the building, the temperature shows clear gradient because the warmer air will flow up.

The inlet air velocity and air flow rate in spring bath area are higher than them in the other zones. This situation will give rise to little higher room temperature in the spring bath zone. For the same reason, the inlet air velocity and air flow rate in small child bath area are lower, this situation will produce lower temperature. Therefore, the gradient of the temperature along X direction are very clear.

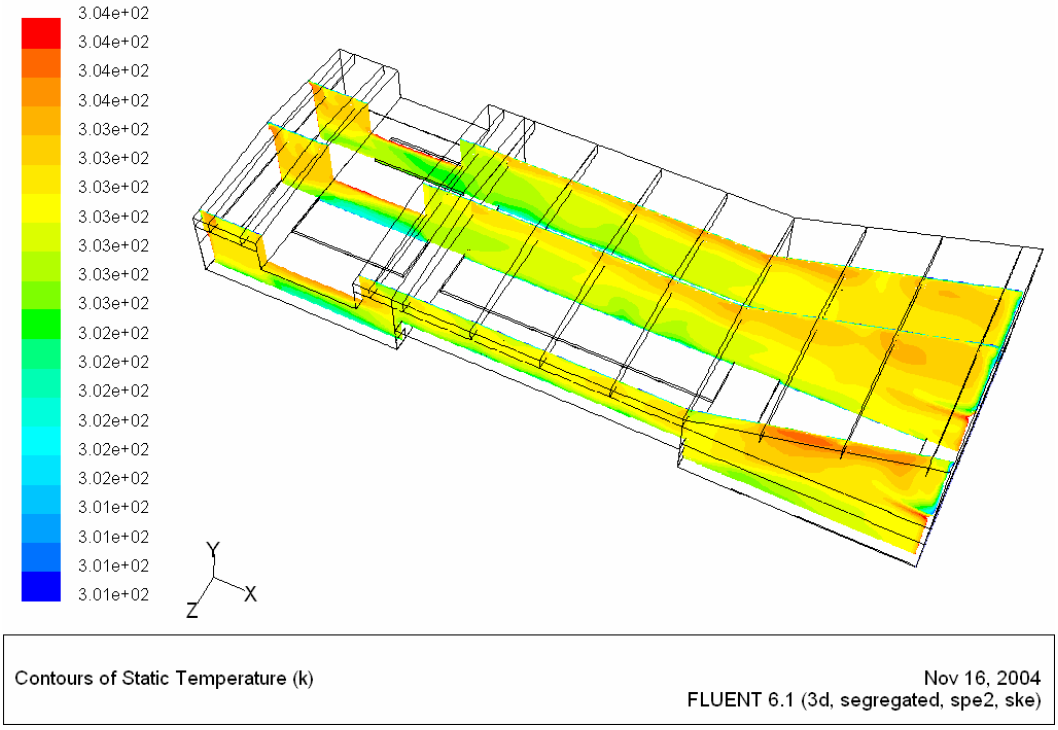

Figure 6.22: Temperature distributions at plane Z = 5 m, Z = 11.25 m and Z = 21.5 m.

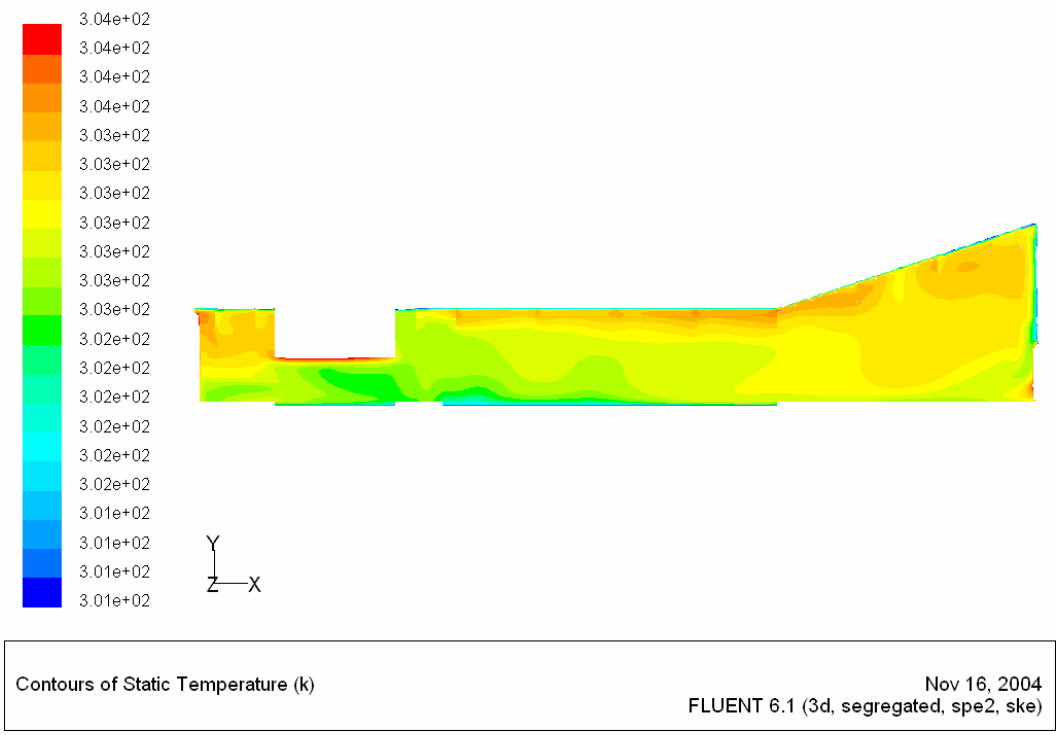

Figure 6.23: Temperature distributions at plane Z = 5 m.

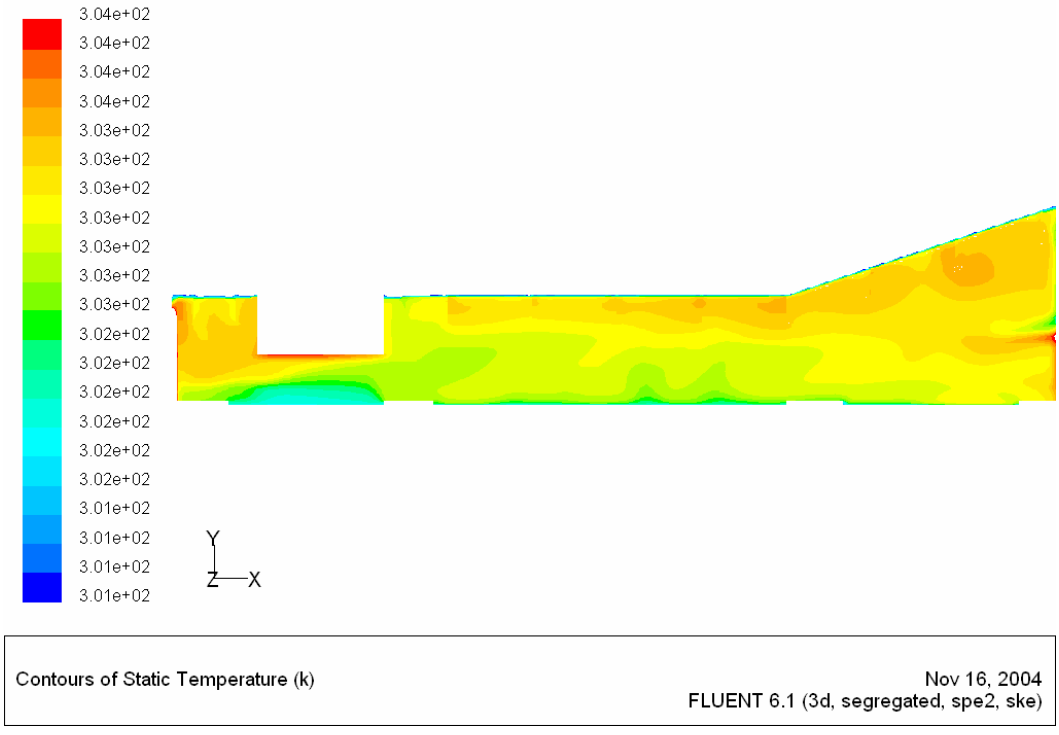

Figure 6.24: Temperature distributions at plane Z = 11.25 m.

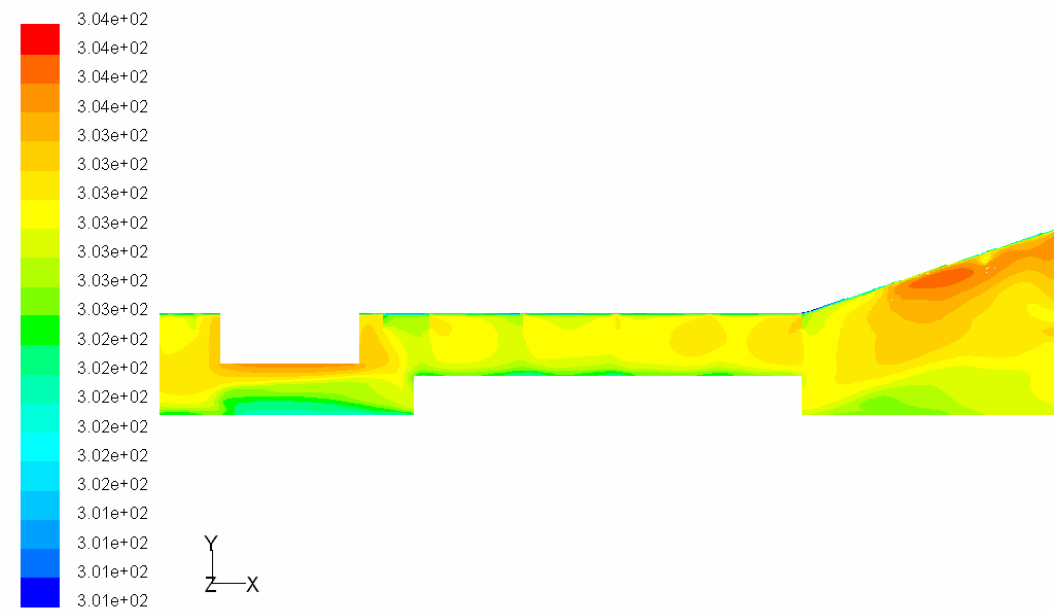

Figure 6.25: Temperature distributions at plane Z = 21.5 m.

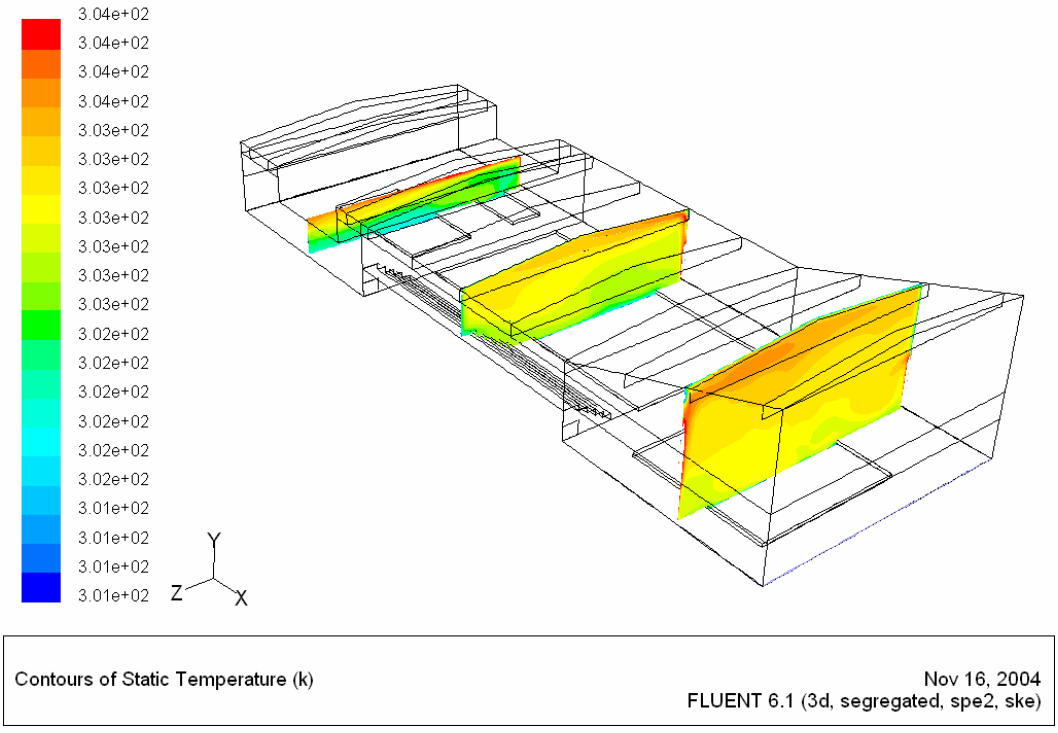

Figure 6.26: Temperature distributions at plane X = 10 m, X = 31.5 m and X = 55 m.

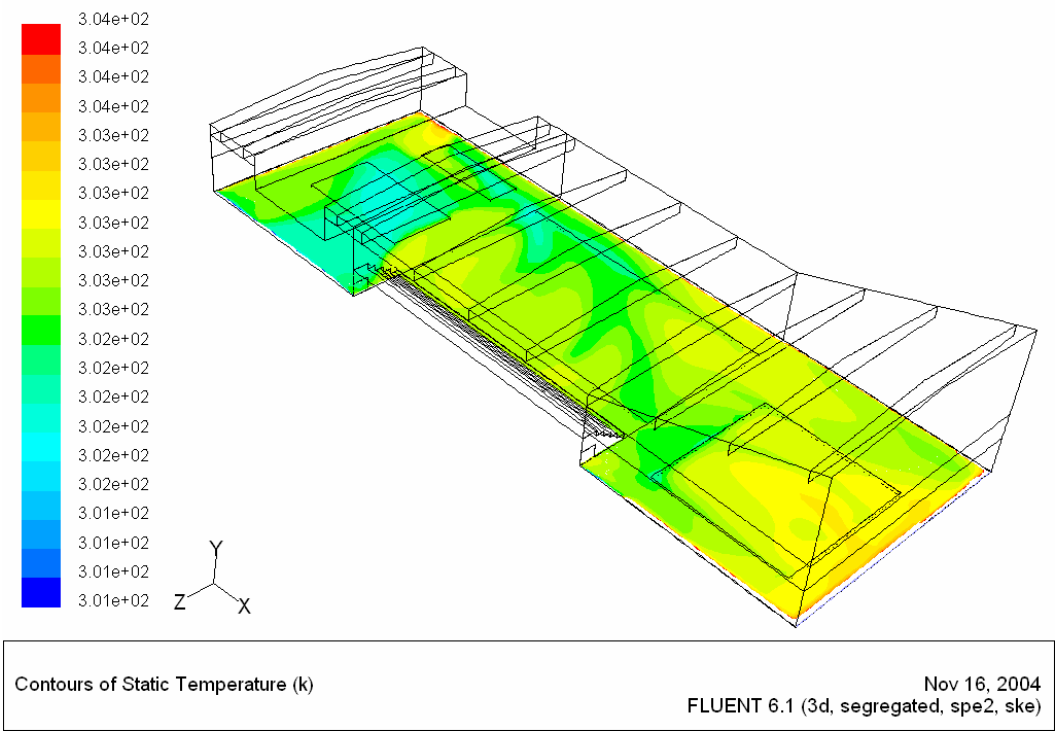

Figure 6.27: Temperature distributions at plane Y = 0.1 m.

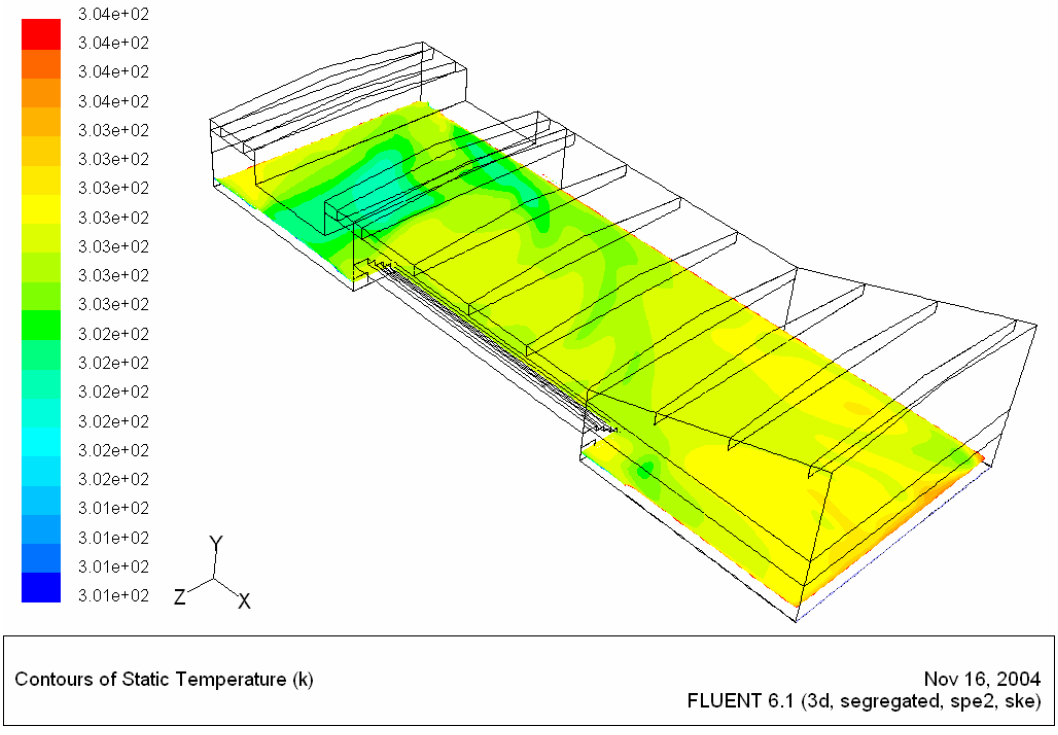

Figure 6.28: Temperature distributions at plane Y = 0.77 m.

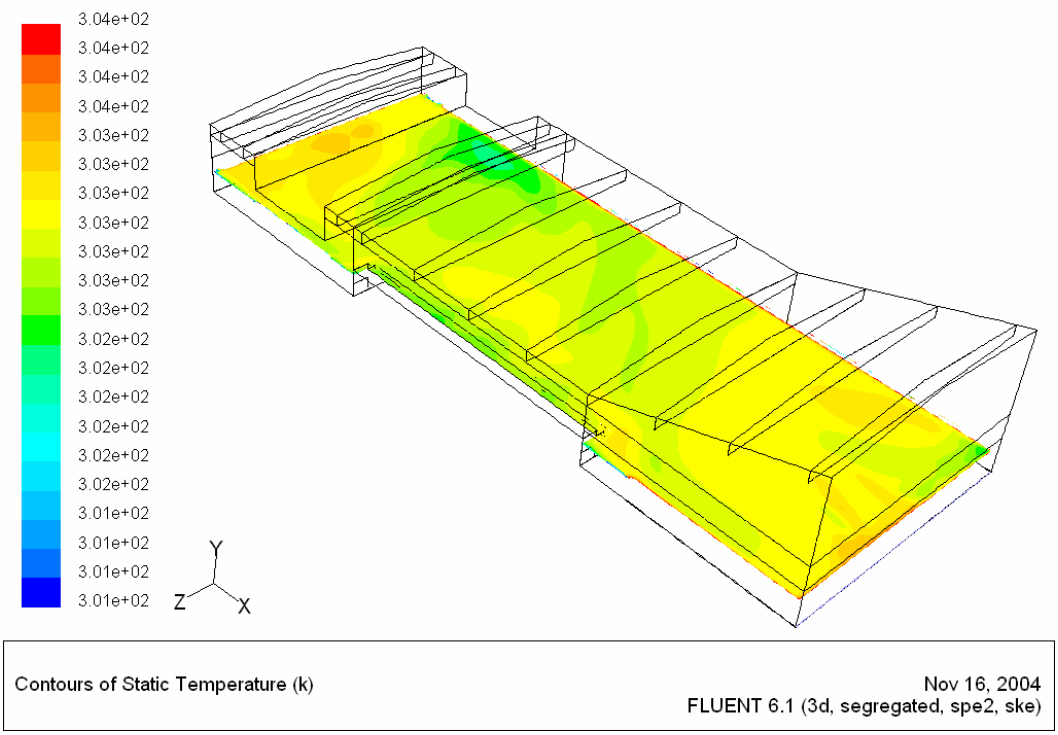

Figure 6.29: Temperature distributions at plane Y = 2 m.

6.2.1.3 Relative humidity distribution

Figure 6.30 – Figure 6.37 show the relative humidity distributions for different planes in the swimming hall. It is clear to see that the relative humidity varies greatly inside the building. The relative humidity is quite lower in the spring bath part of the building because of the higher ventilation rate, and the relative humidity is higher in the small child bath part because of the lower ventilation rate. The relative humidity is very higher close to the water surface because the water vapour evaporates. Over a certain height in the Y direction, it seems that the relative humidity does not change so much.

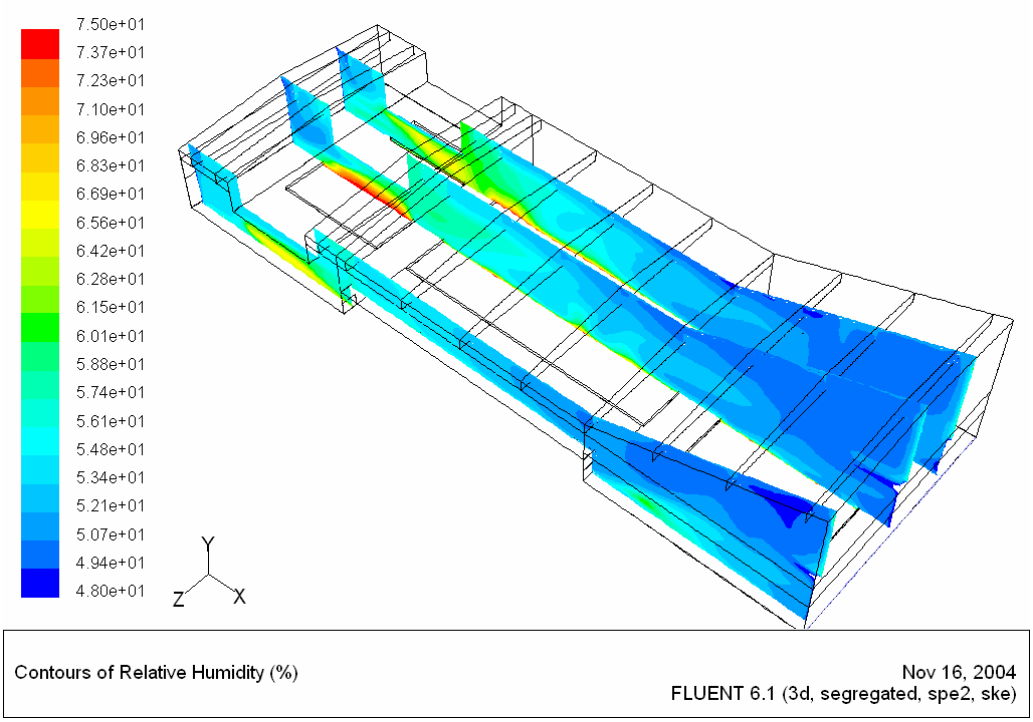

Figure 6.30: Relative humidity distributions at plane Z = 5 m, Z = 11.25 m and Z = 21.5 m.

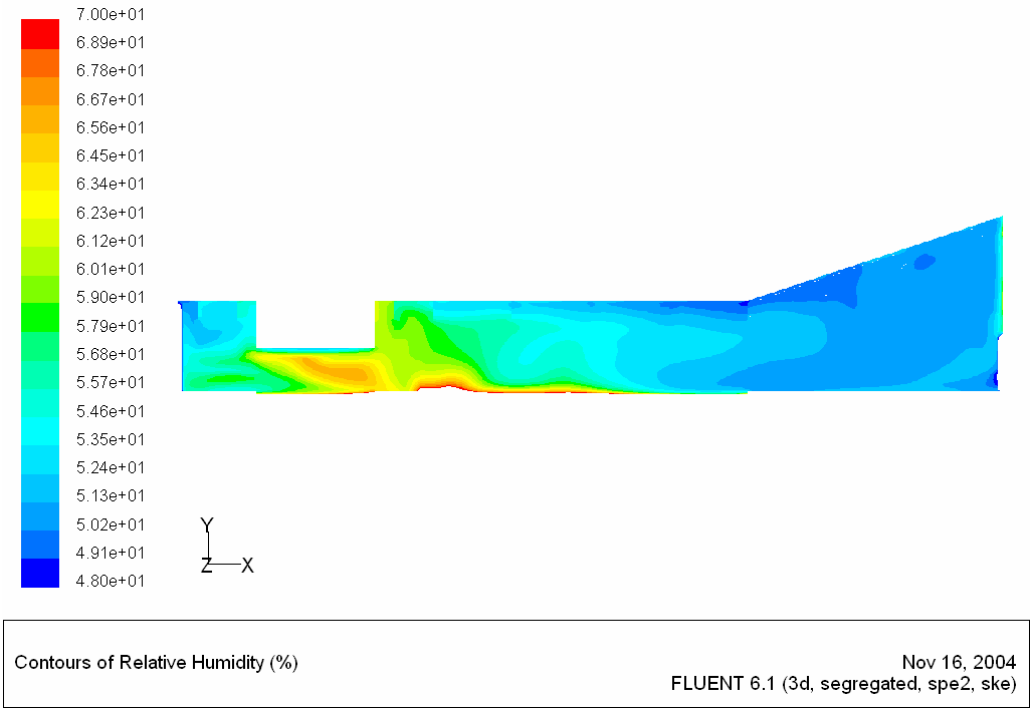

Figure 6.31: Relative humidity distributions at plane Z = 5 m.

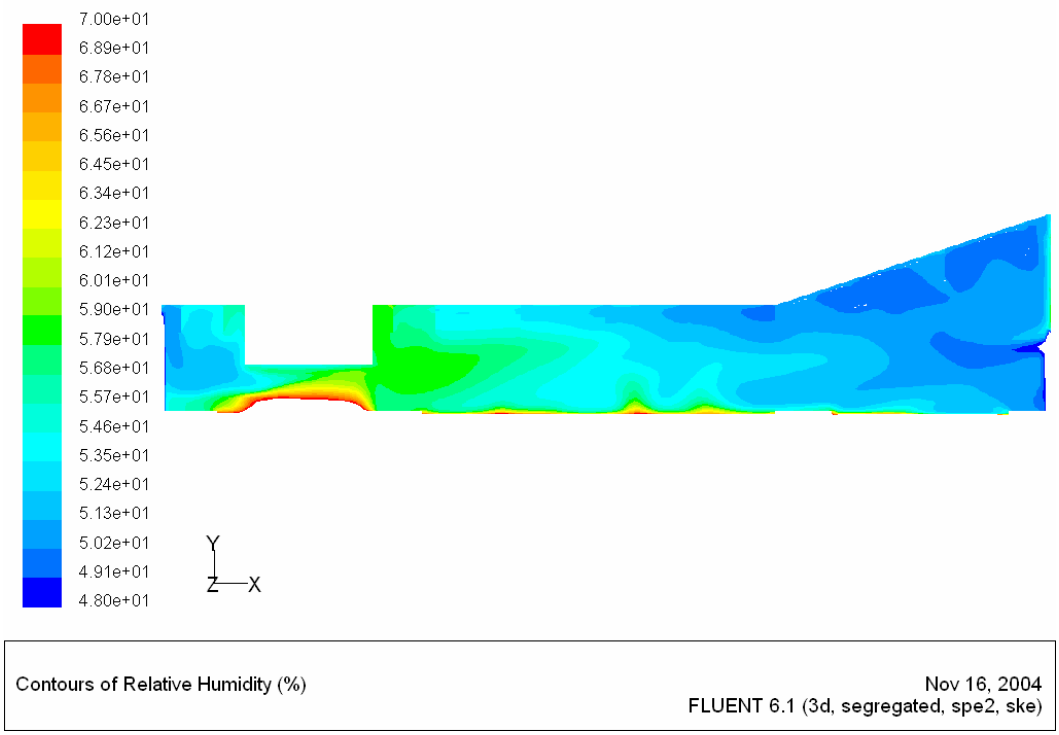

Figure 6.32: Relative humidity distributions at plane Z = 11.25 m.

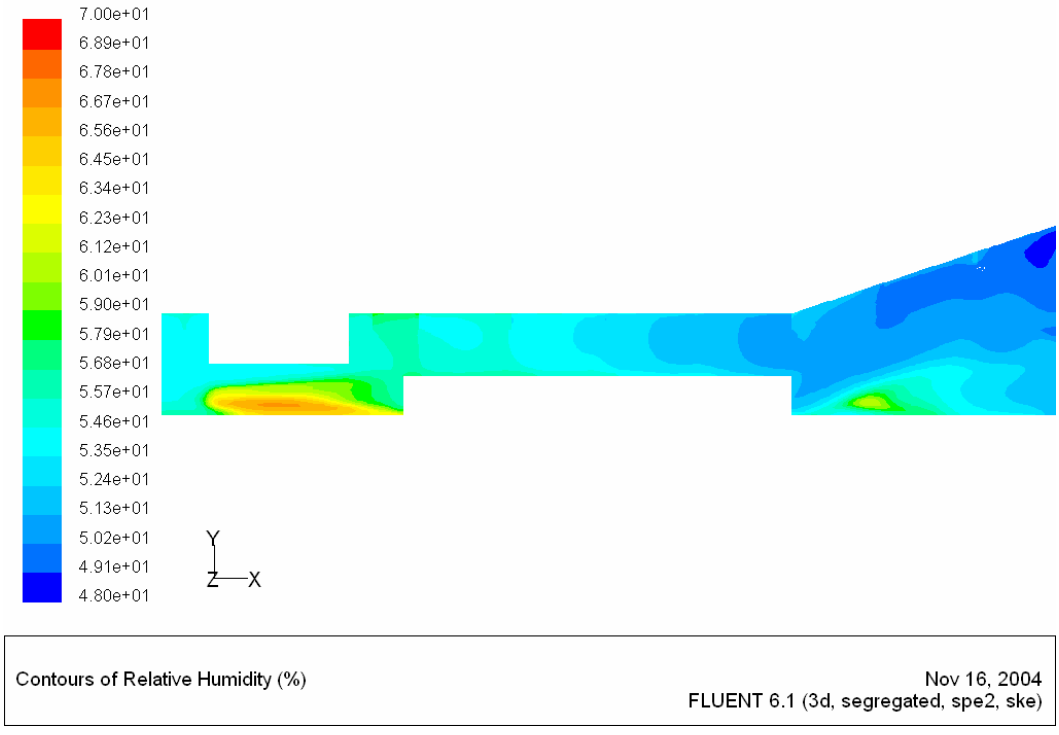

Figure 6.33: Relative humidity distributions at plane Z = 21.5 m.

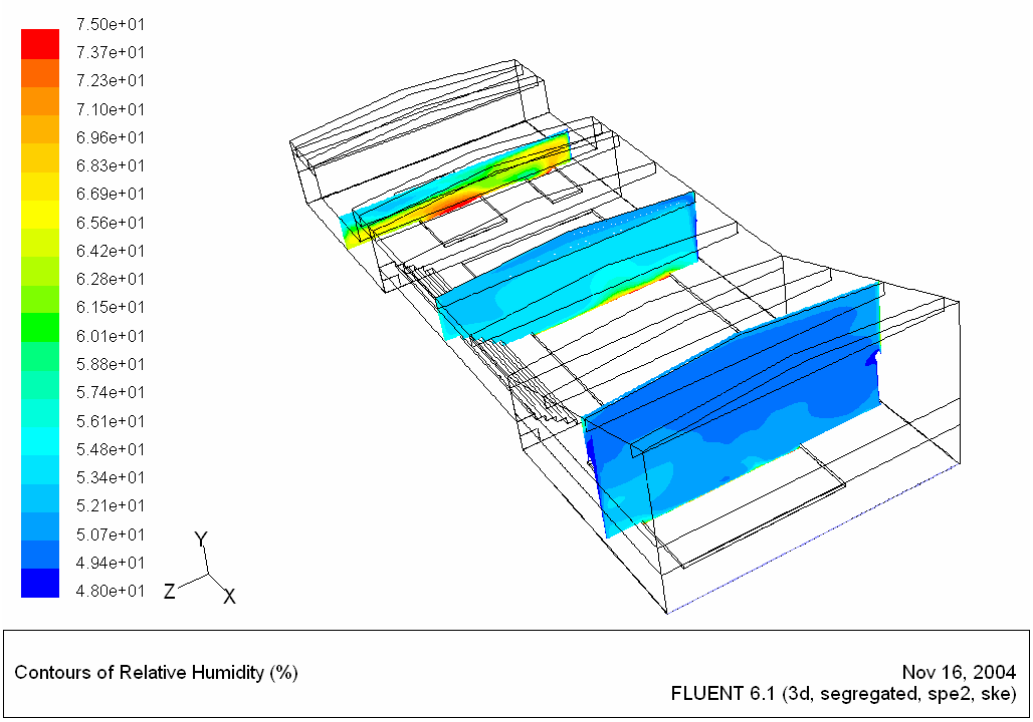

Figure 6.34: Relative humidity distributions at plane X = 10 m, X = 31.5 m and X = 55 m.

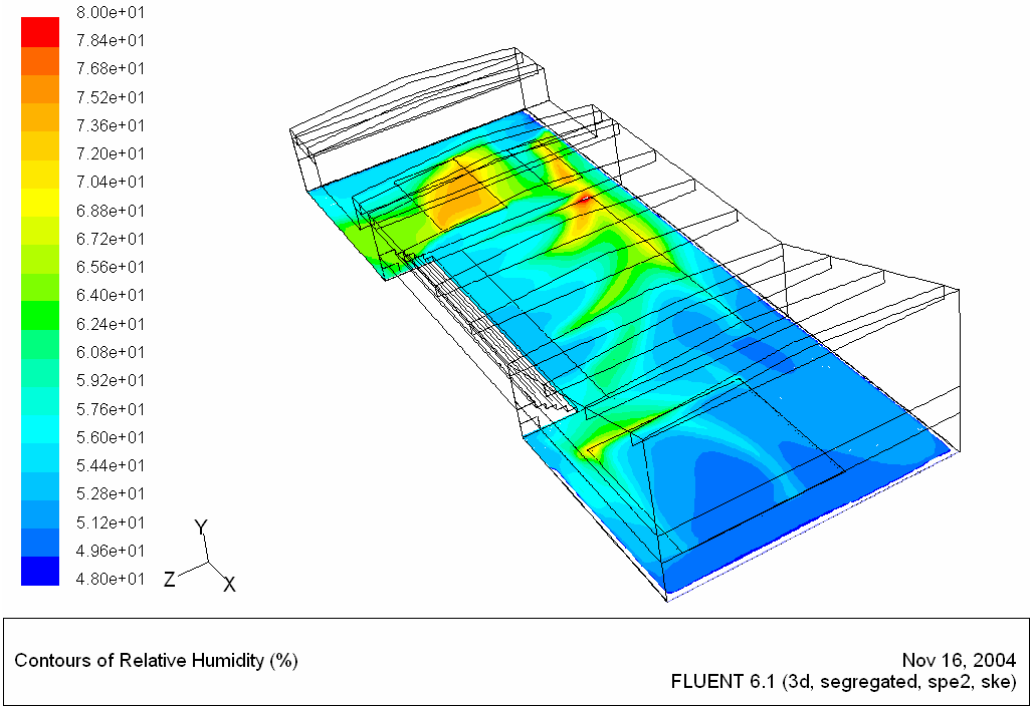

Figure 6.35: Relative humidity distributions at plane Y = 0.1 m.

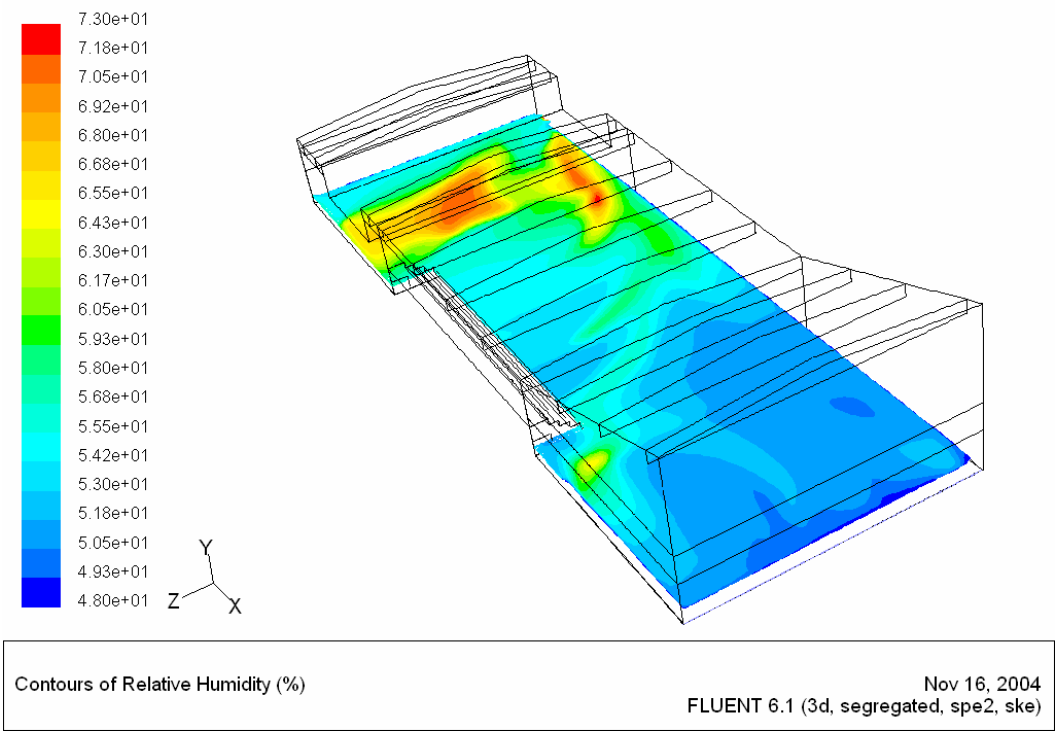

Figure 6.36: Relative humidity distributions at plane Y = 0.77 m.

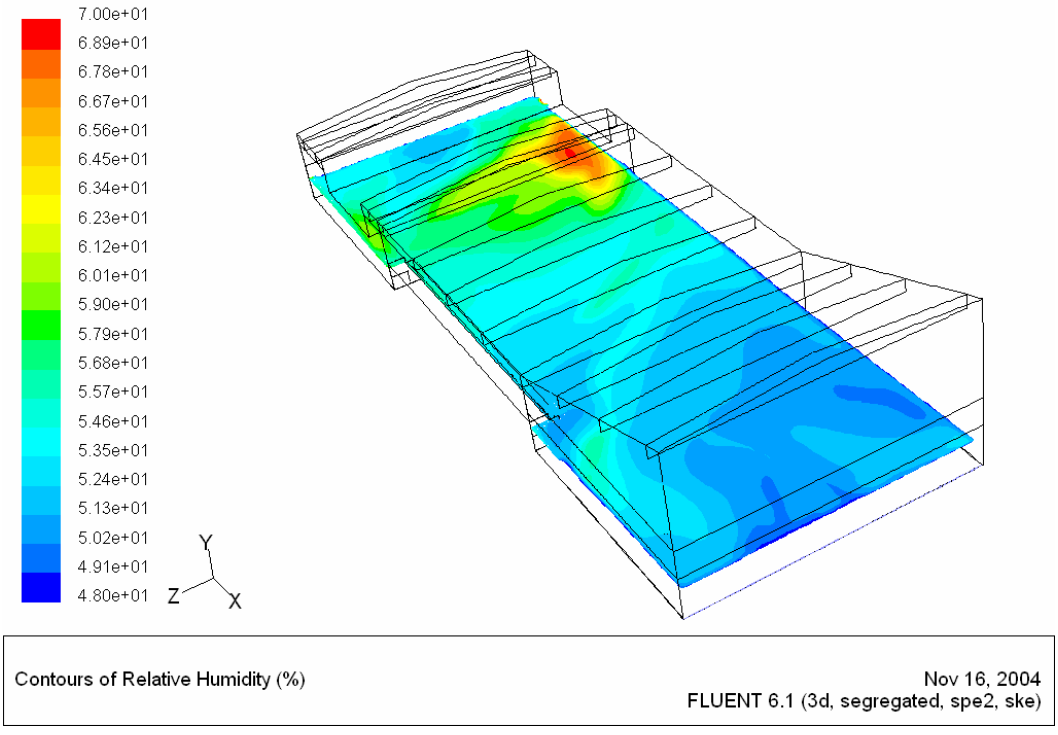

Figure 6.37: Relative humidity distributions at plane Y = 2 m.

6.2.1.4 Profiles

The air velocity, air temperature and air relative humidity at different lines in the middle plane are shown in Figure 6.38 – Figure 6.40 in order to compare them with the measurement results. The simulation results show that the Shah correlation is very good to calculate the water evaporation rate from unoccupied baths.

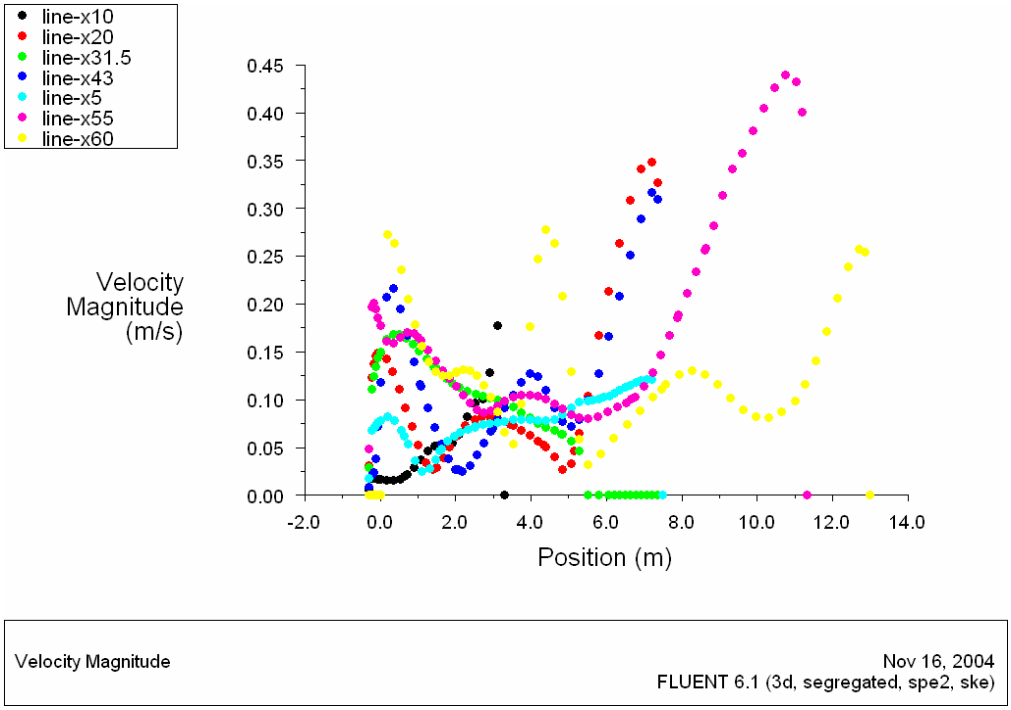

Figure 6.38: Velocity magnitude profile at line X = 5 m, 10 m, 20 m, 31.5 m, 43 m, 55 m and 60 m of the middle plane Z = 11.25m.

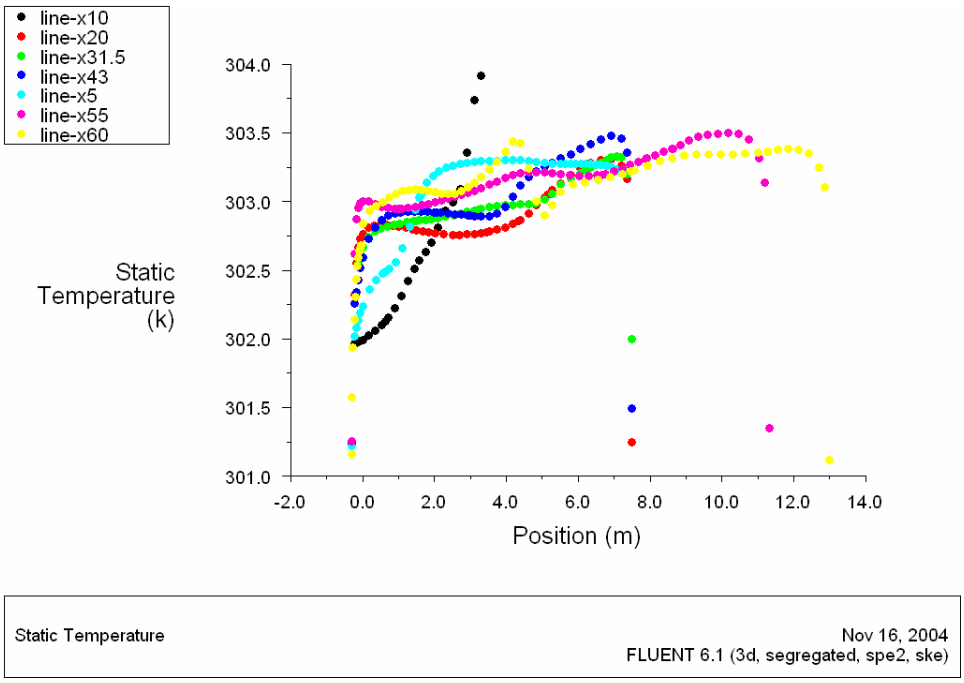

Figure 6.39: Temperature profile at line X = 5 m, 10 m, 20 m, 31.5 m, 43 m, 55 m and 60 m of the middle plane Z = 11.25m.

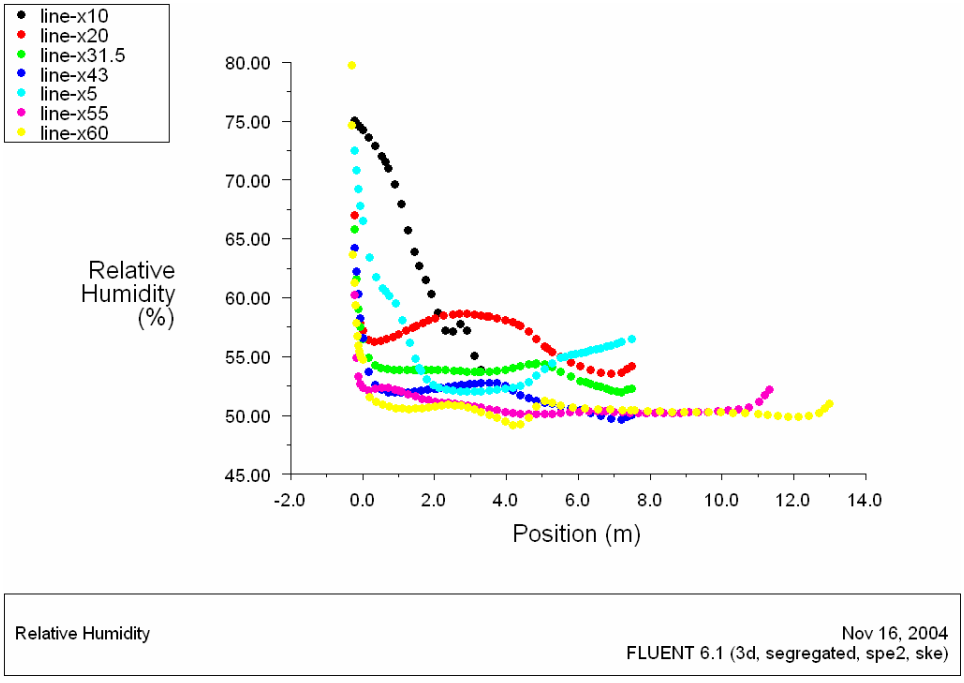

Figure 6.40: Relative humidity profile at line X = 5 m, 10 m, 20 m, 31.5 m, 43 m, 55 m and 60 m of the middle plane Z = 11.25m.

6.2.2 Results of occupied Shah empirical correlation case

6.2.2.1 Velocity distribution

Figure 6.41 – Figure 6.51 show the velocity vector distributions for different planes in the occupied swimming hall. The air flow movement is similar with the air flow in the unoccupied swimming hall, because the mass fraction of water vapour in the air is very low and it influences the air flow very little.

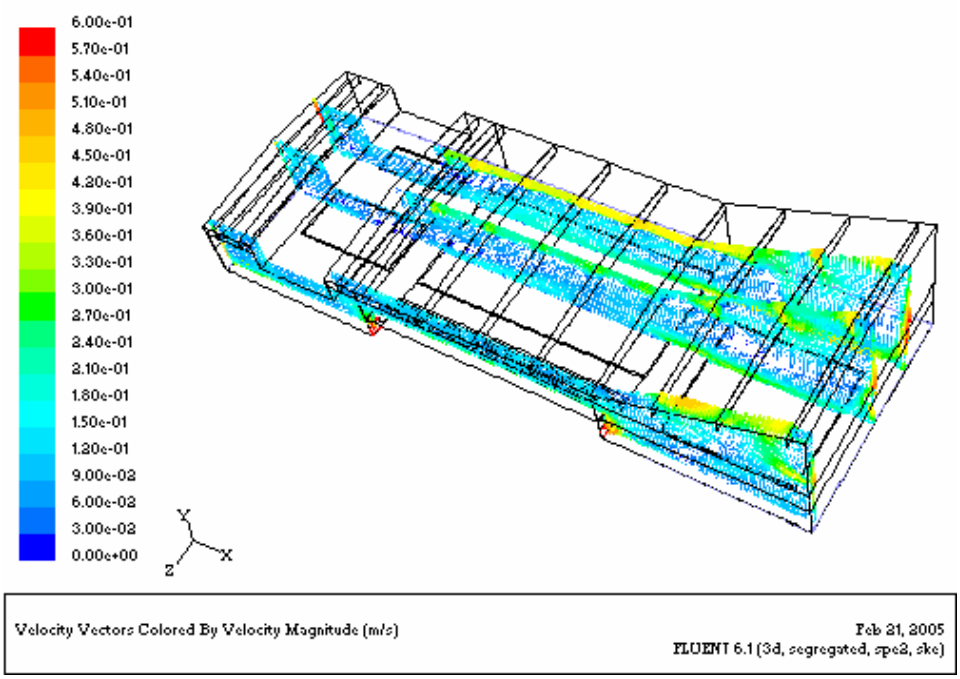

Figure 6.41: Velocity distributions at plane Z = 5 m, Z = 11.25 m and Z = 21.5 m.

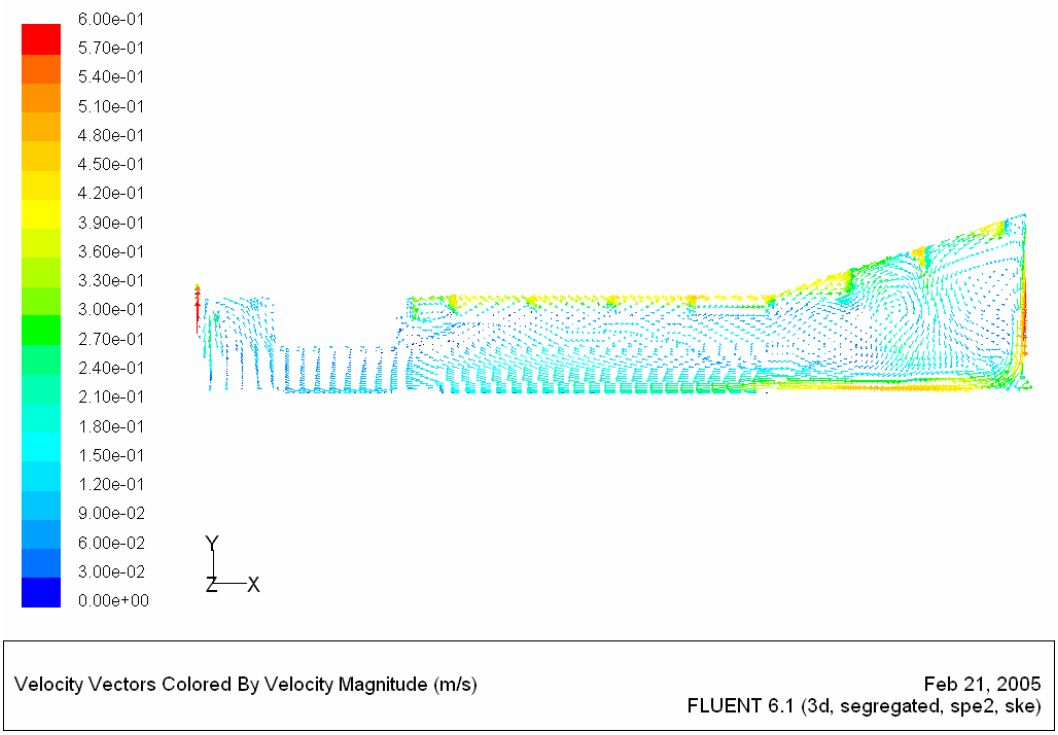

Figure 6.42: Velocity distributions at plane Z = 5 m.

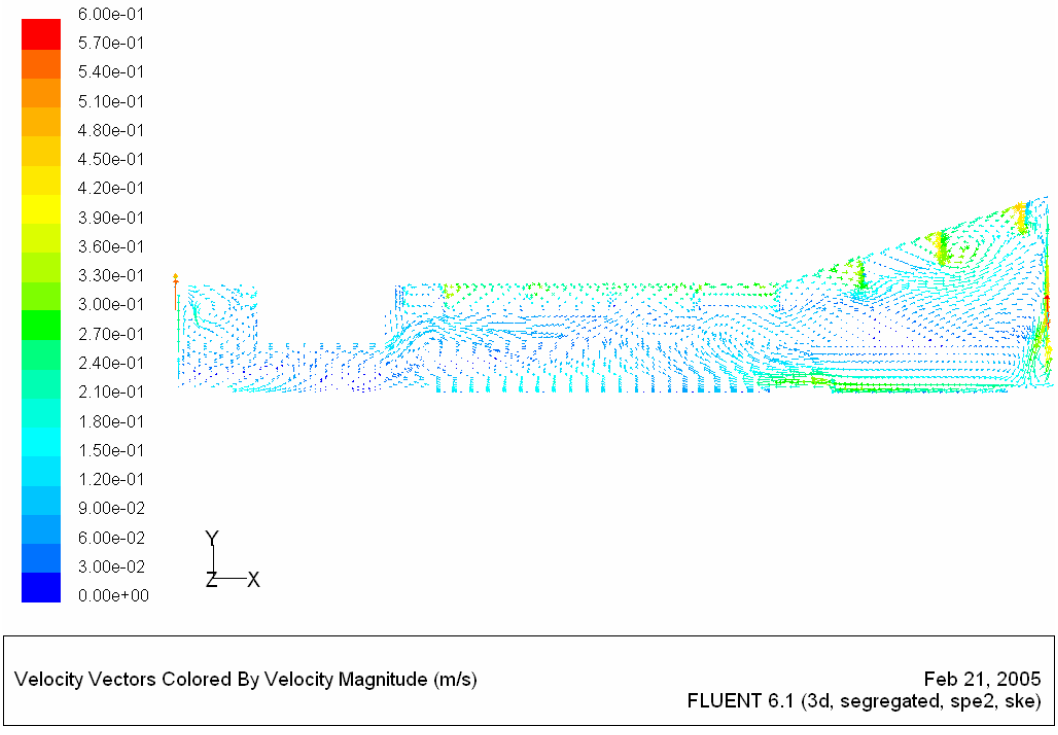

Figure 6.43: Velocity distributions at plane Z = 11.25 m.

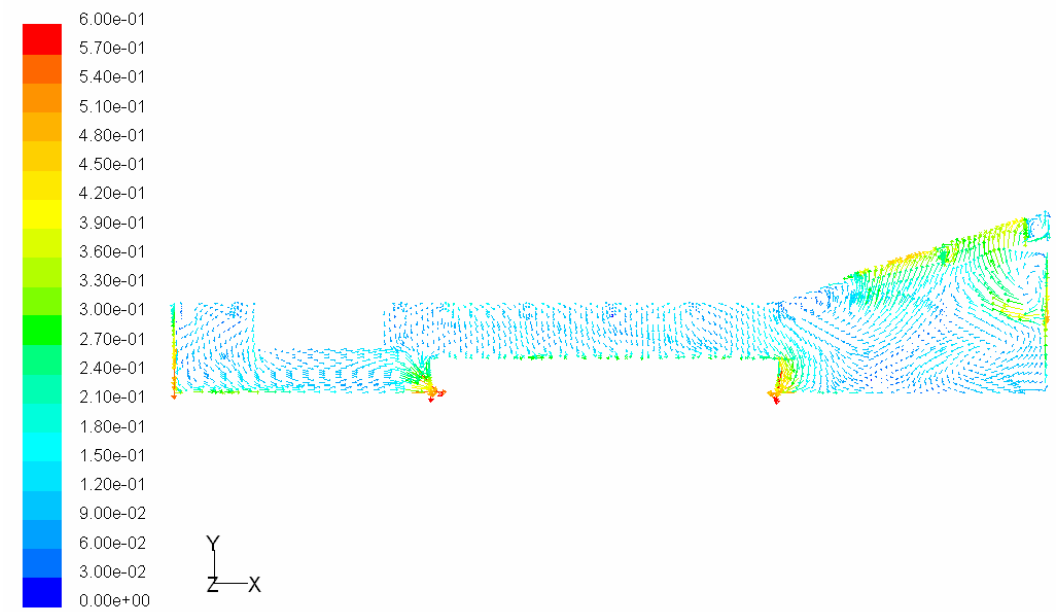

Figure 6.44: Velocity distributions at plane Z = 21.5 m.

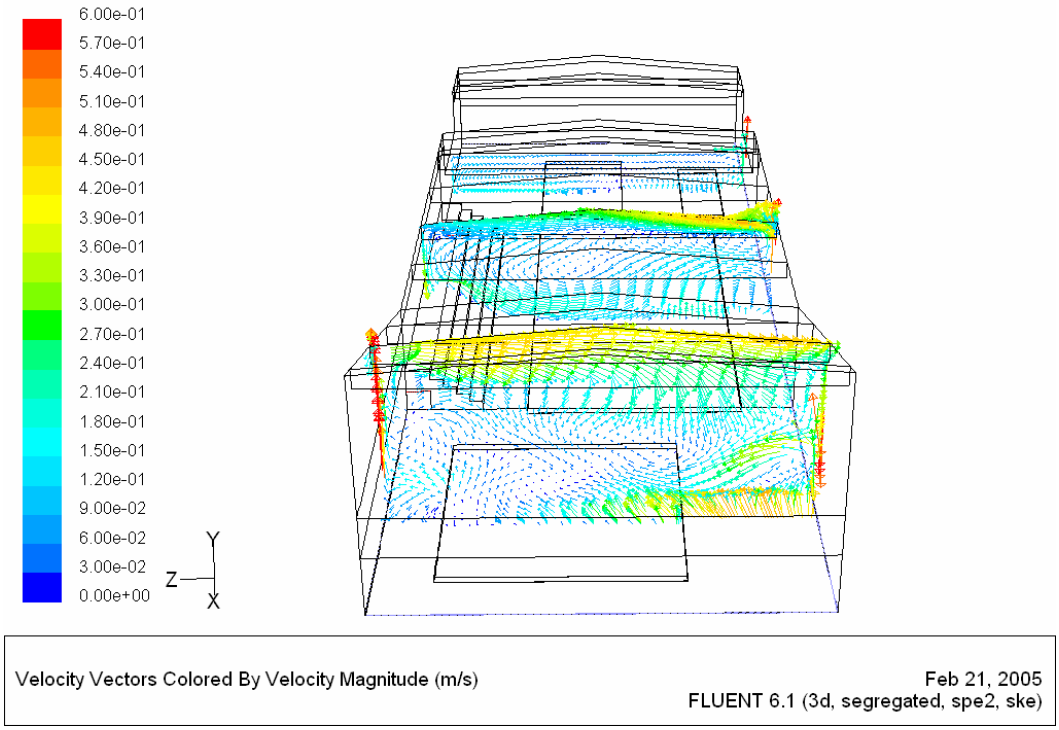

Figure 6.45: Velocity distributions at plane X = 10 m, X = 31.5 m and X = 55m.

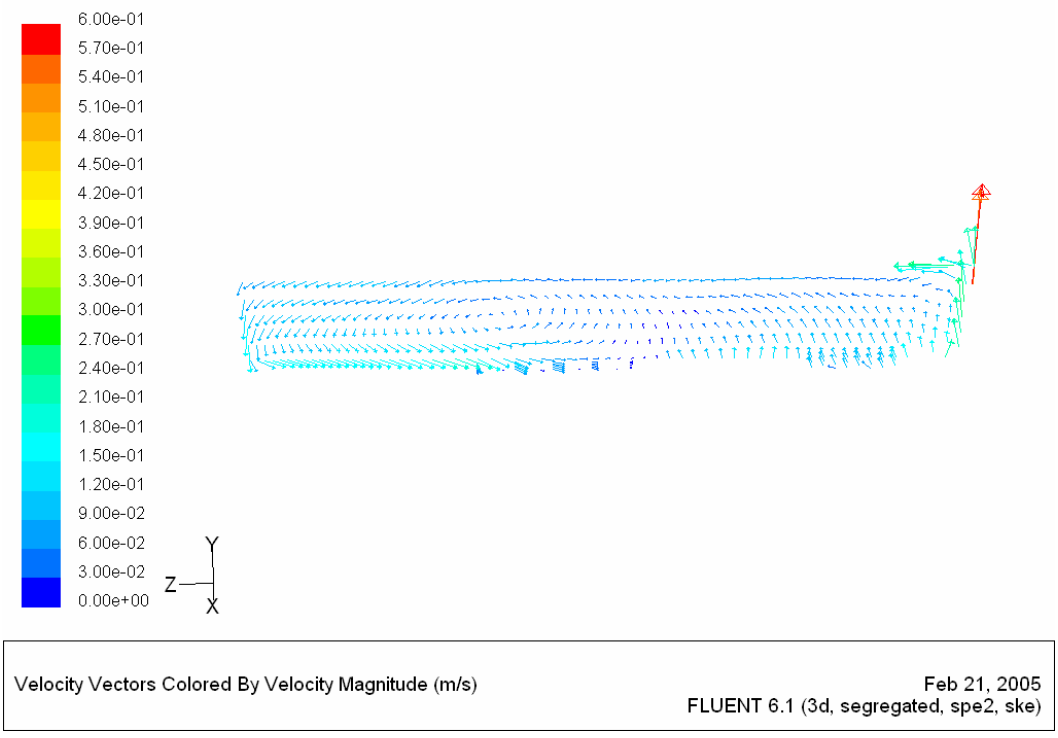

Figure 6.46: Velocity distributions at plane X = 10 m.

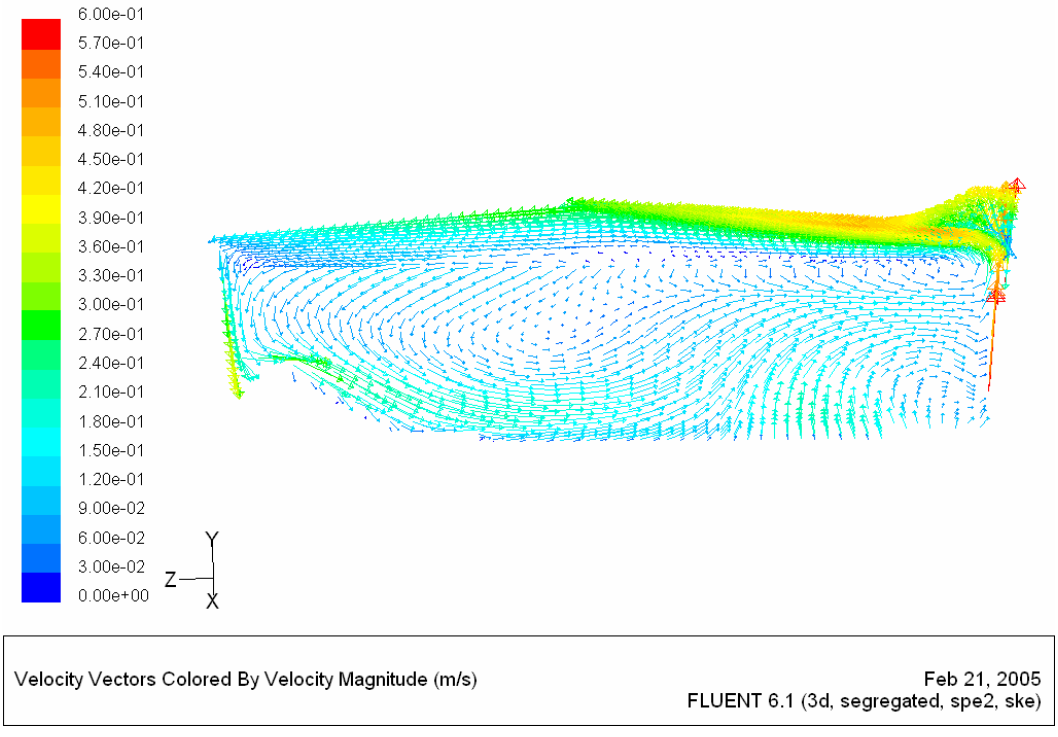

Figure 6.47: Velocity distributions at plane X = 31.5 m.

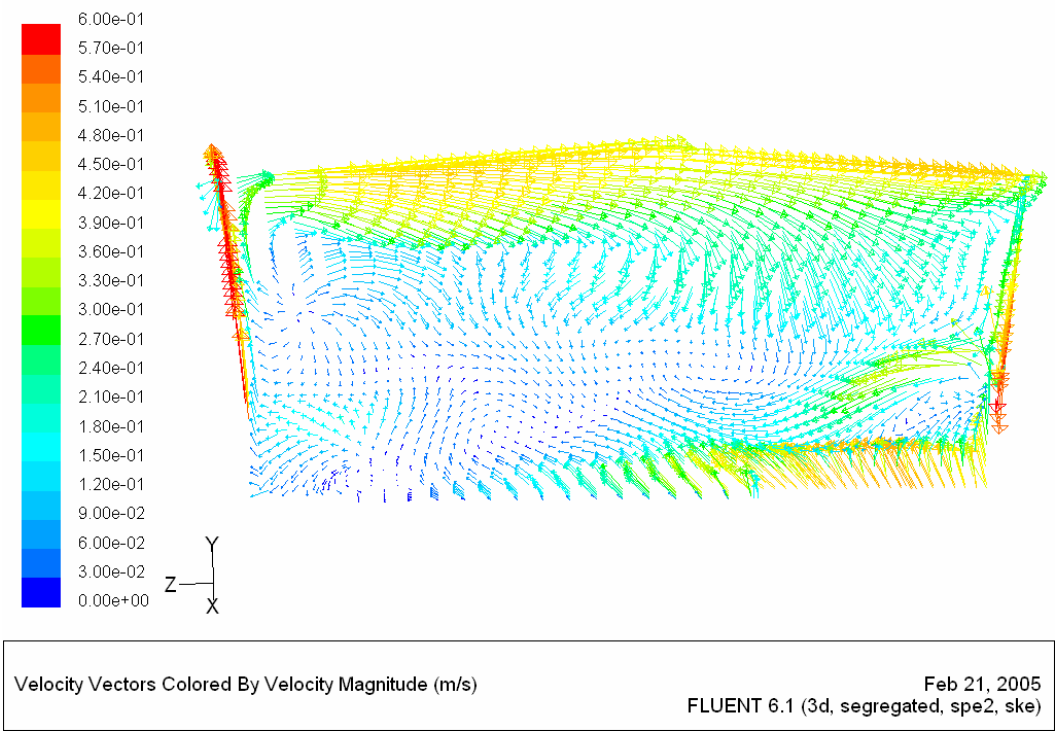

Figure 6.48: Velocity distributions at plane X = 55m.

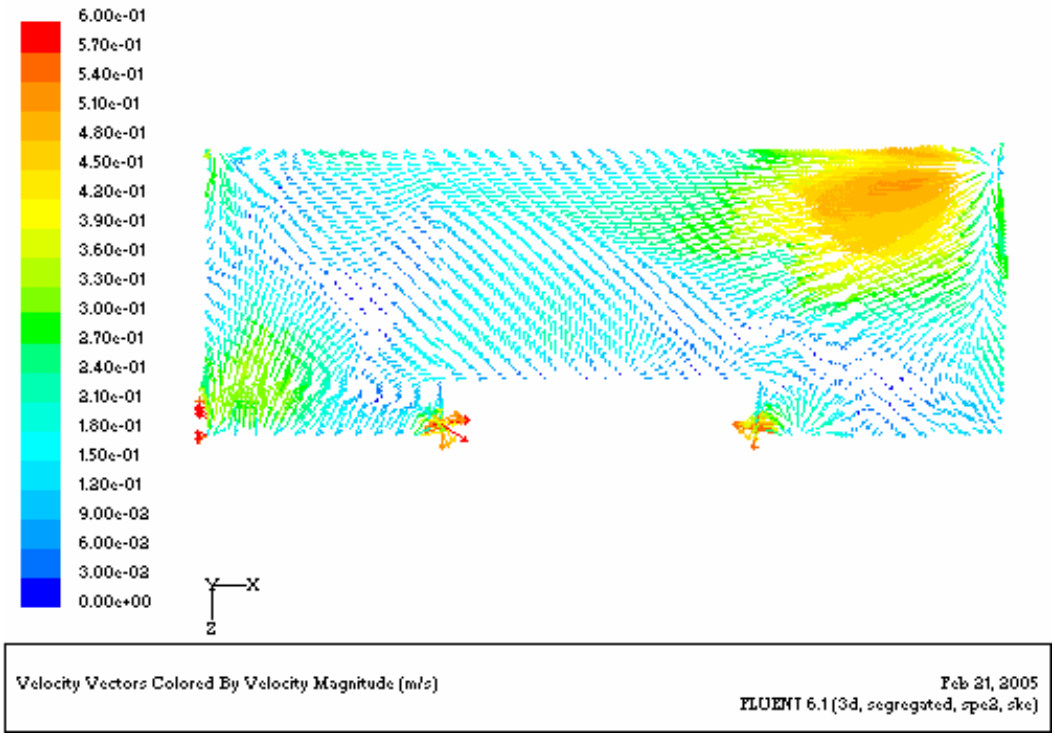

Figure 6.49: Velocity distributions at plane Y = 0.1 m.

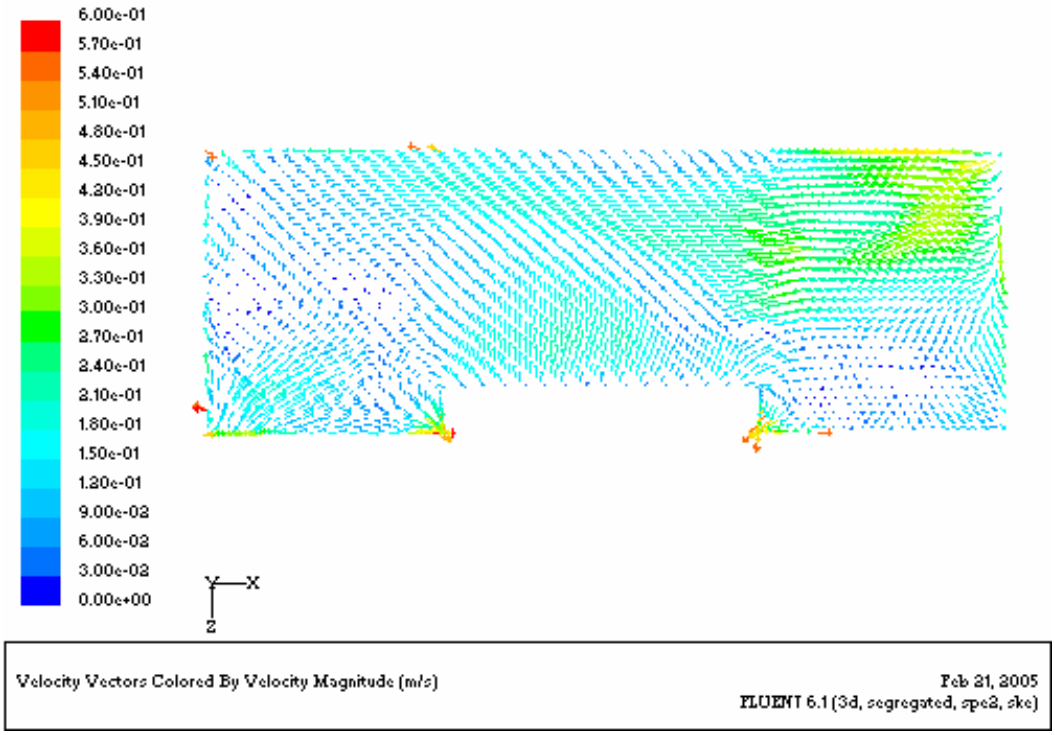

Figure 6.50: Velocity distributions at plane Y = 0.77 m.

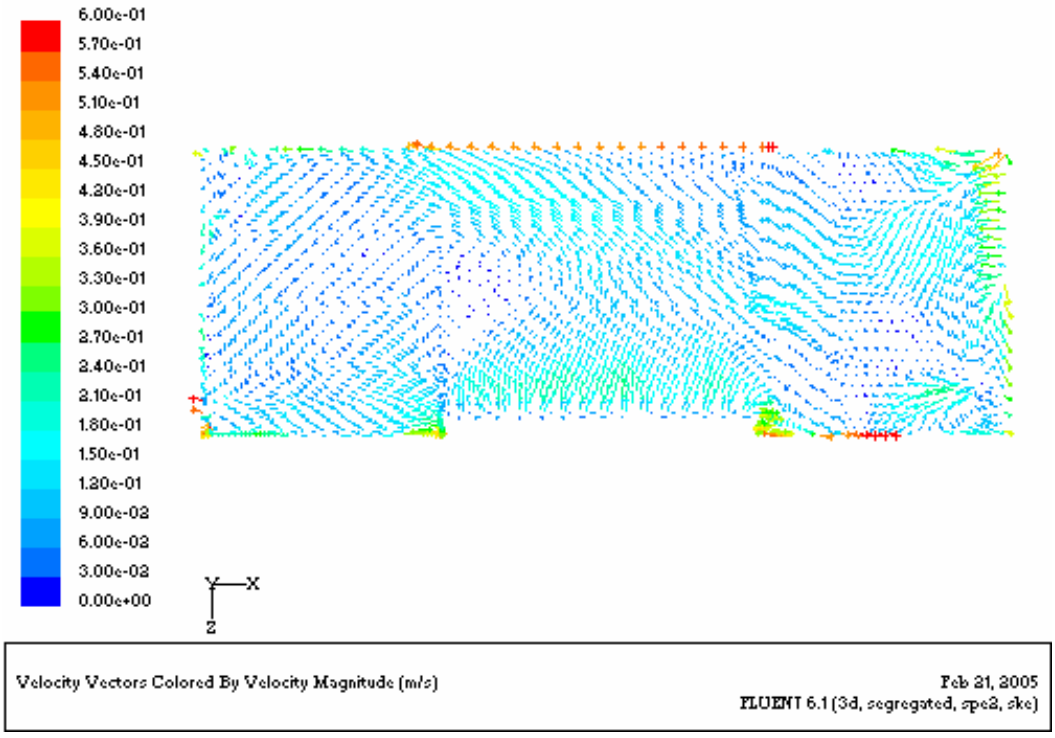

Figure 6.51: Velocity distributions at plane Y = 2 m.

6.2.2.2 Temperature distribution

Figure 6.52 – Figure 6.59 show the air temperature distributions for different planes in the occupied swimming hall. The air temperature distribution is similar with the temperature distribution in the unoccupied pool. But certainly the air temperature should be little lower than it in the unoccupied case because of the higher water evaporation rate. The air temperature also keeps about 30 °C, and it is little lower close to the water surface.

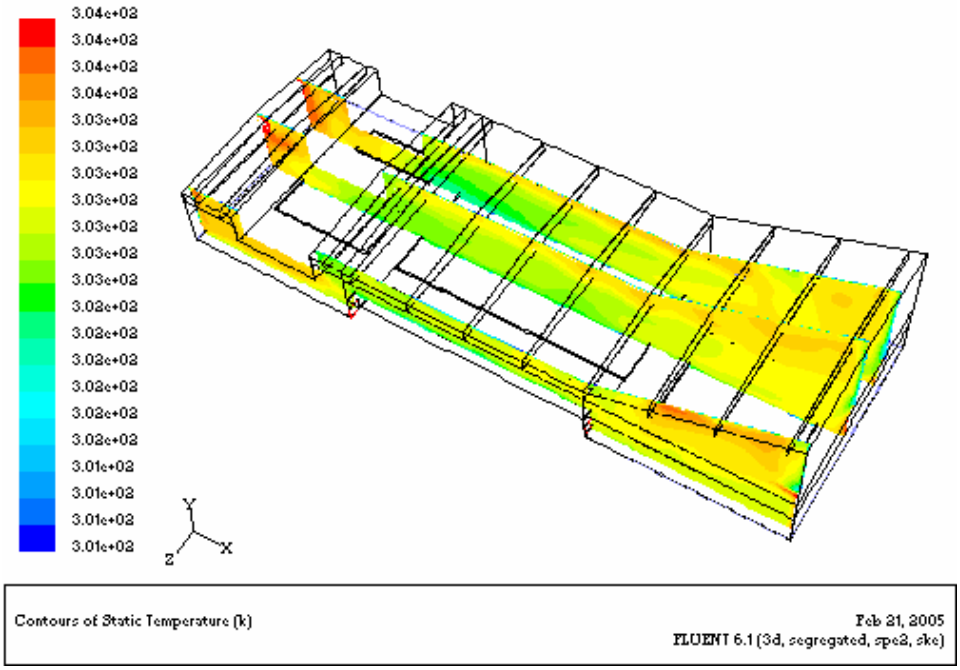

Figure 5.52: Temperature distributions at plane Z = 5 m, Z = 11.25 m and Z = 21.5 m.

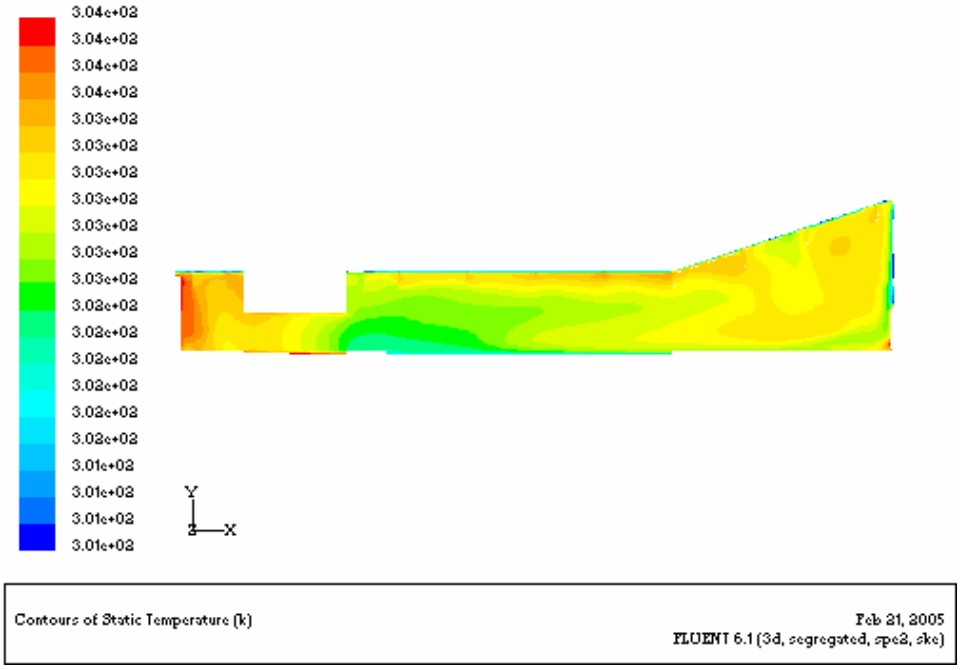

Figure 6.53: Temperature distributions at plane Z = 5 m.

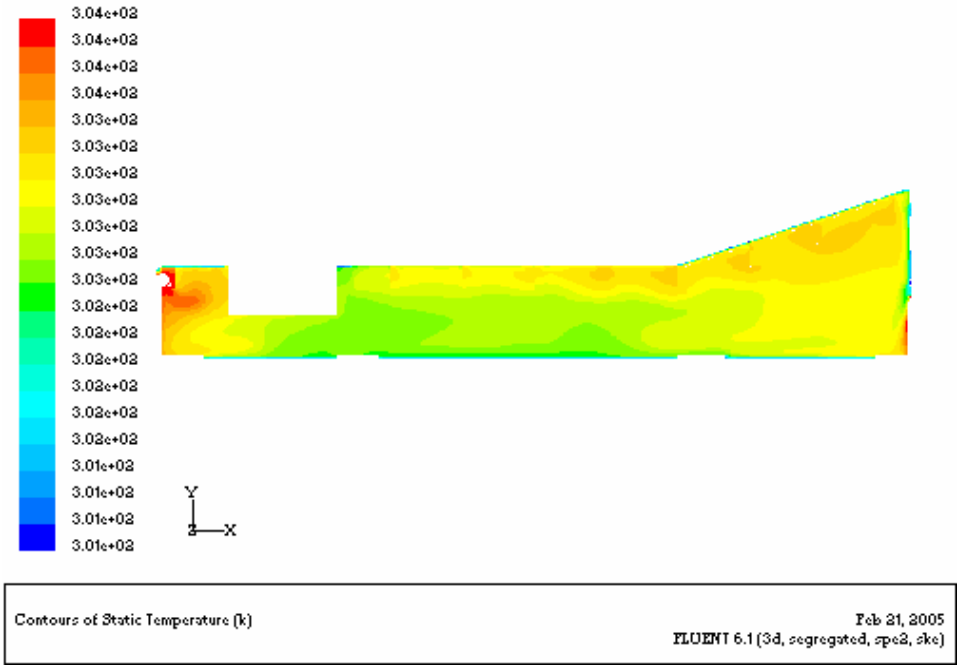

Figure 6.54: Temperature distributions at plane Z = 11.25 m.

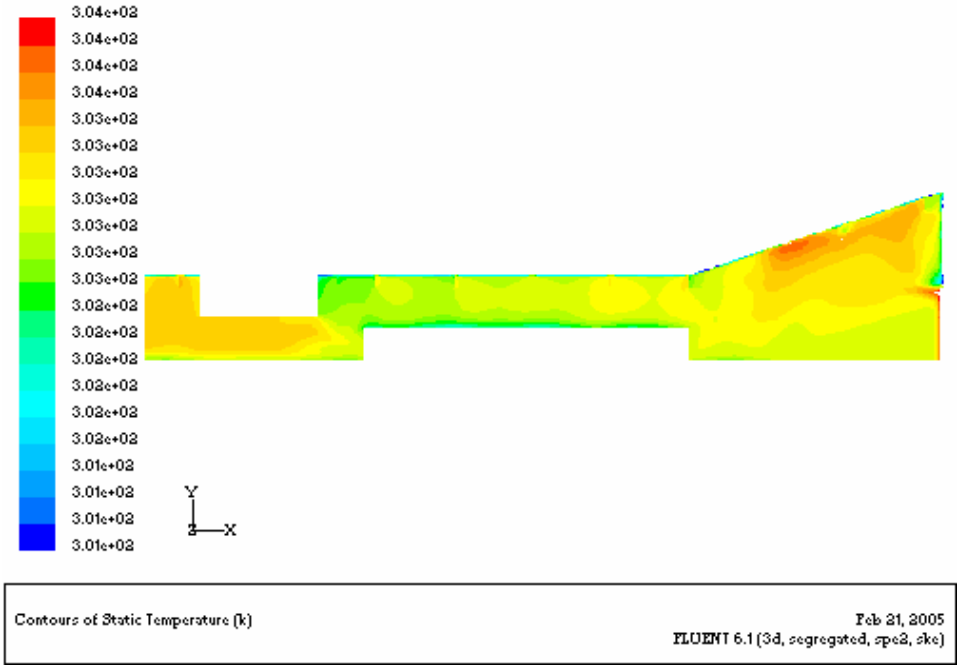

Figure 6.55: Temperature distributions at plane Z = 21.5 m.

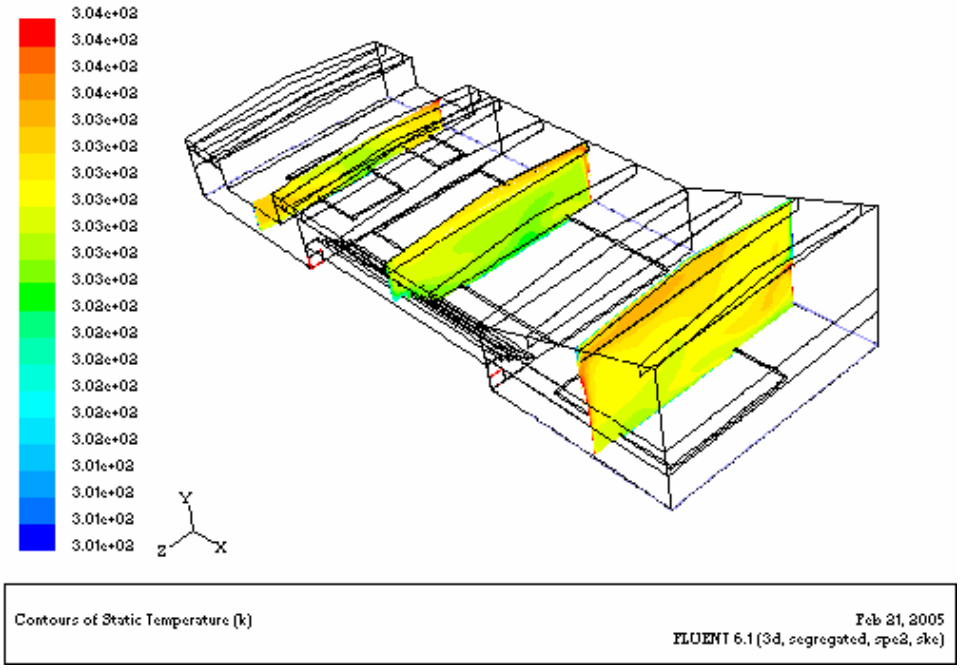

Figure 6.56: Temperature distributions at plane X = 10 m, X = 31.5 m and X = 55 m.

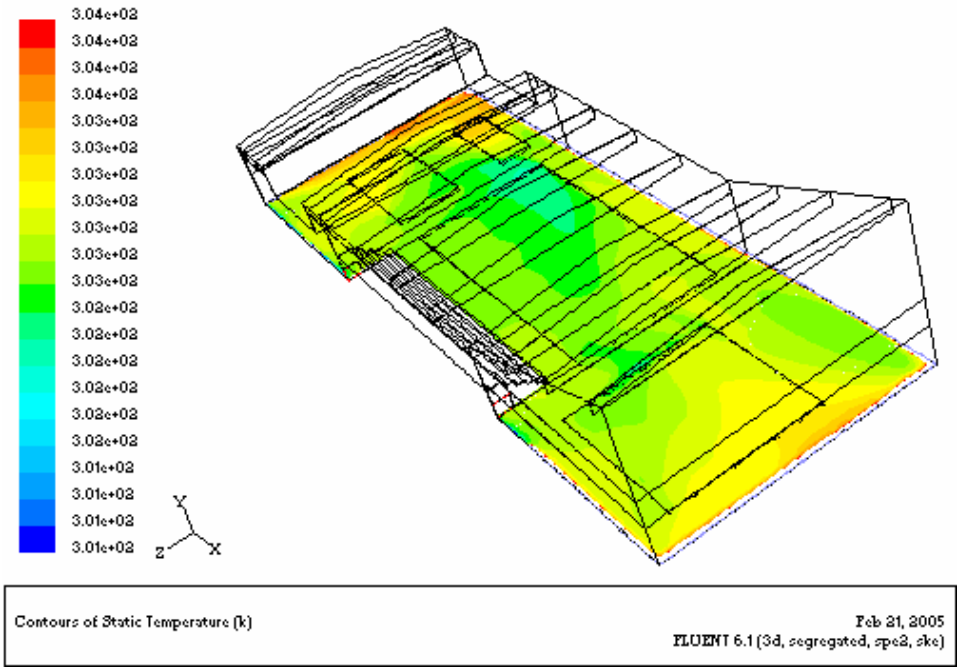

Figure 6.57: Temperature distributions at plane Y = 0.1 m.

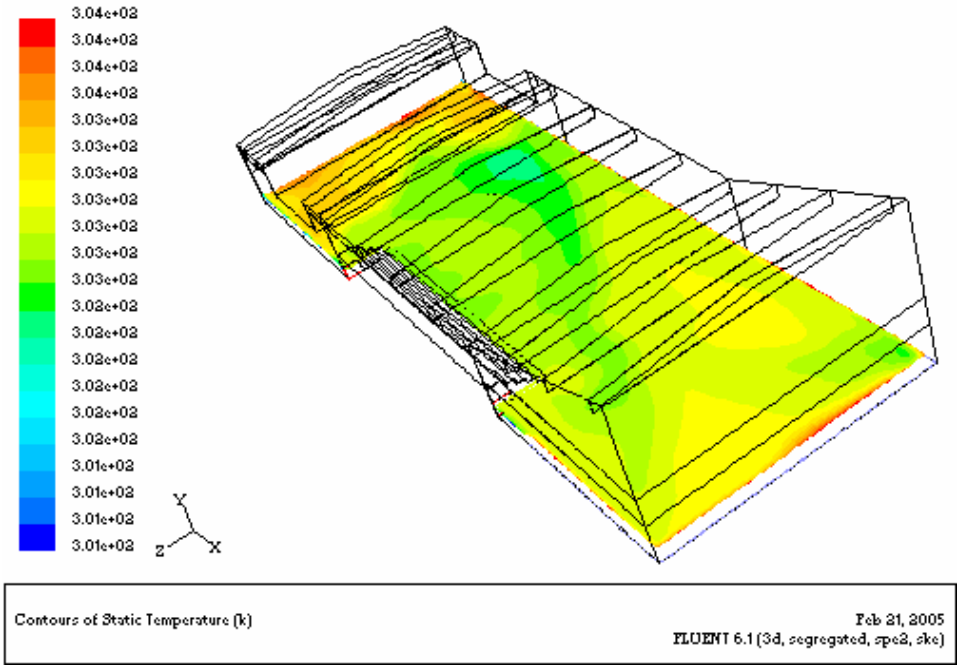

Figure 6.58: Temperature distributions at plane Y = 0.77 m.

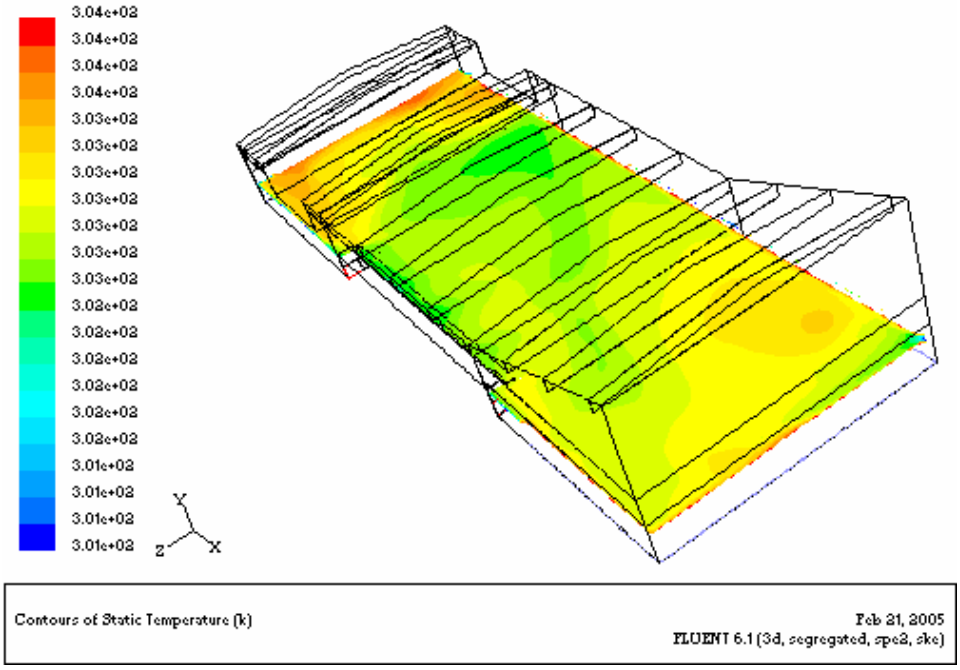

Figure 6.59: Temperature distributions at plane Y = 2 m.

6.2.2.3 Relative humidity distribution

Figure 6.60 – Figure 6.67 show the relative humidity distributions for different planes in the swimming hall. It is clear to see that the relative humidity varies greatly inside the building and the relative humidity is higher than it of the unoccupied case because of the higher water evaporation rate. The relative humidity is lower in the spring bath part of the building because of the higher ventilation rate, and the relative humidity is higher in the small child bath part because of the higher water temperature and higher water evaporation rate. The relative humidity is very higher close to the water surface because the water vapour evaporates. Over a certain height in the Y direction, it seems that the relative humidity does not change so much.

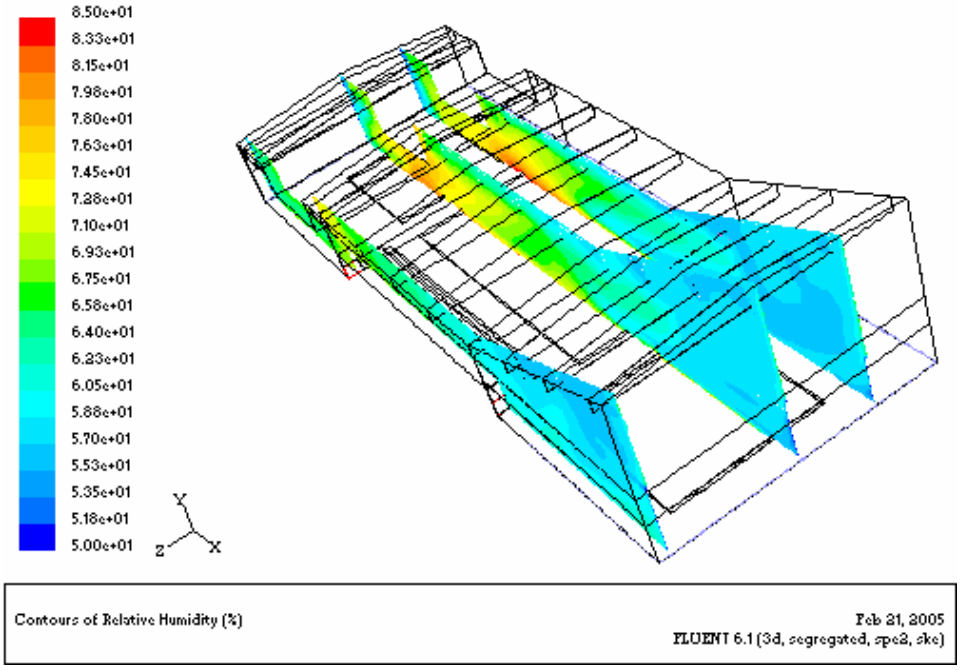

Figure 6.60: Relative humidity distributions at plane Z = 5 m, Z = 11.25 m and Z = 21.5 m.

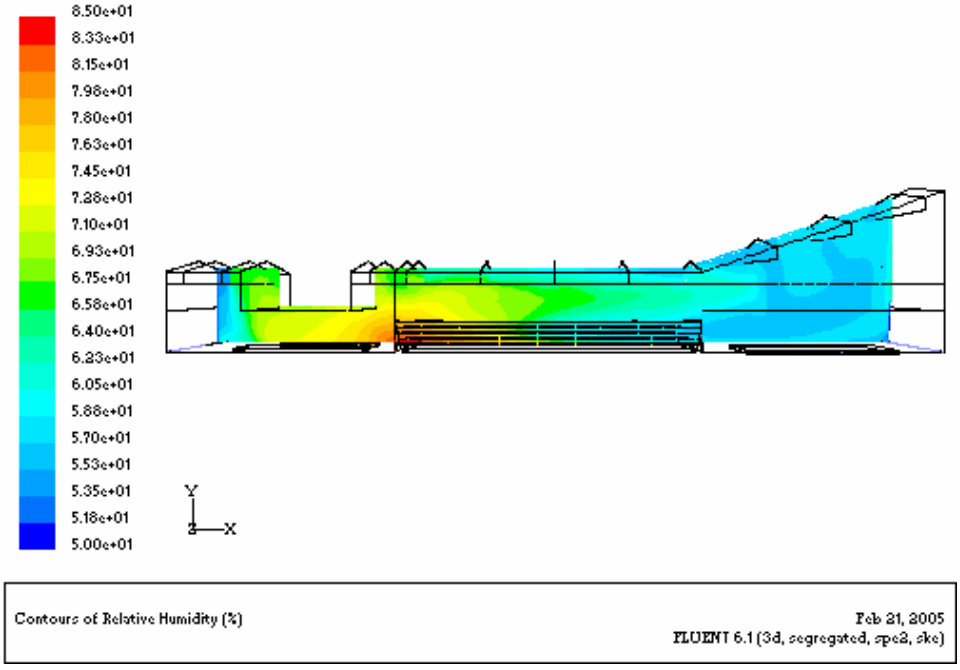

Figure 6.61: Relative humidity distributions at plane Z = 5 m.

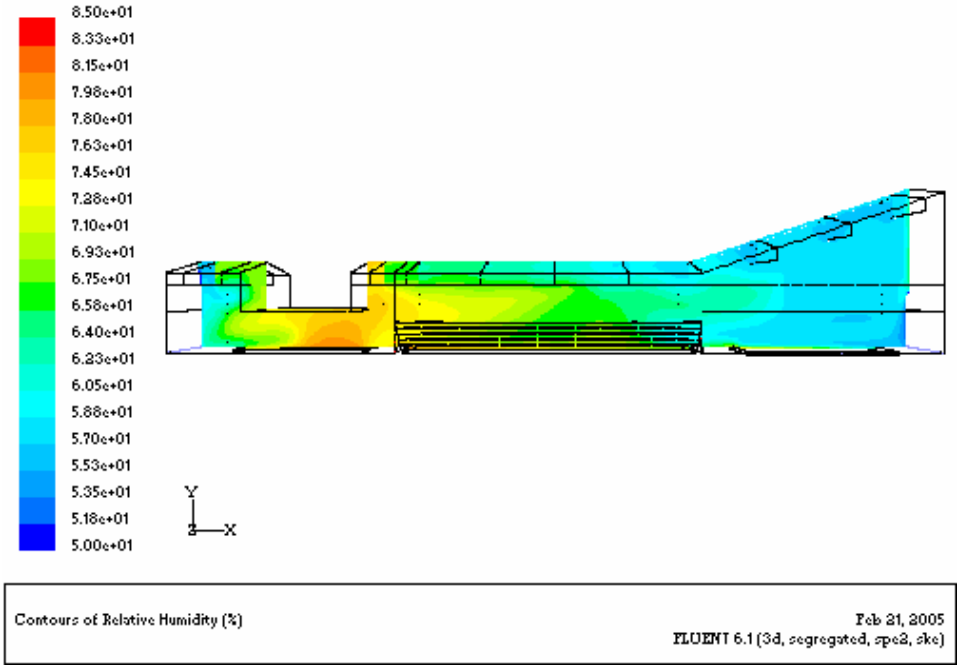

Figure 6.62: Relative humidity distributions at plane Z = 11.25 m.

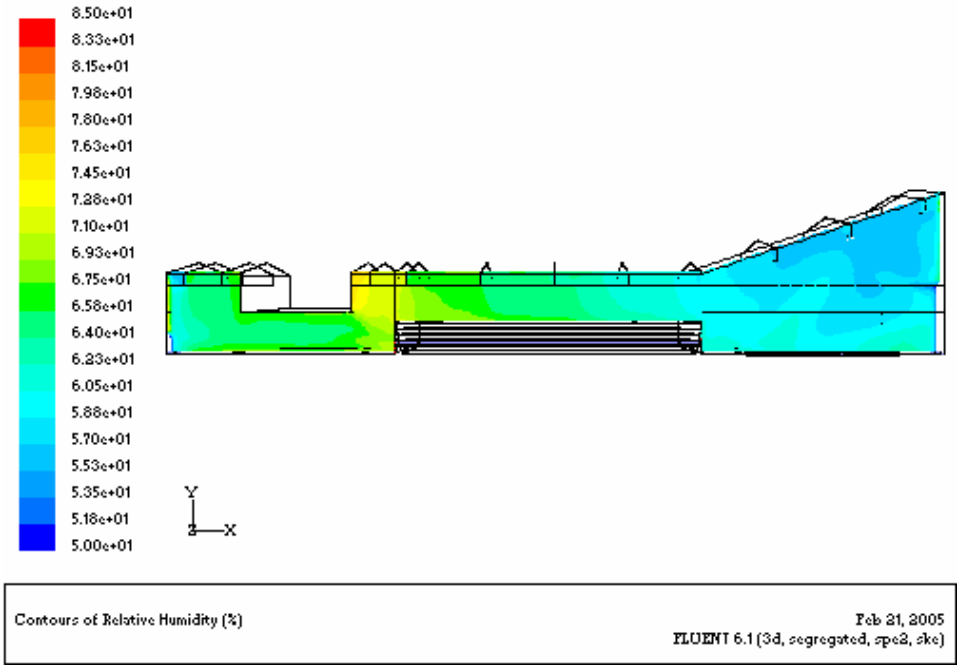

Figure 6.63: Relative humidity distributions at plane Z = 21.5 m.

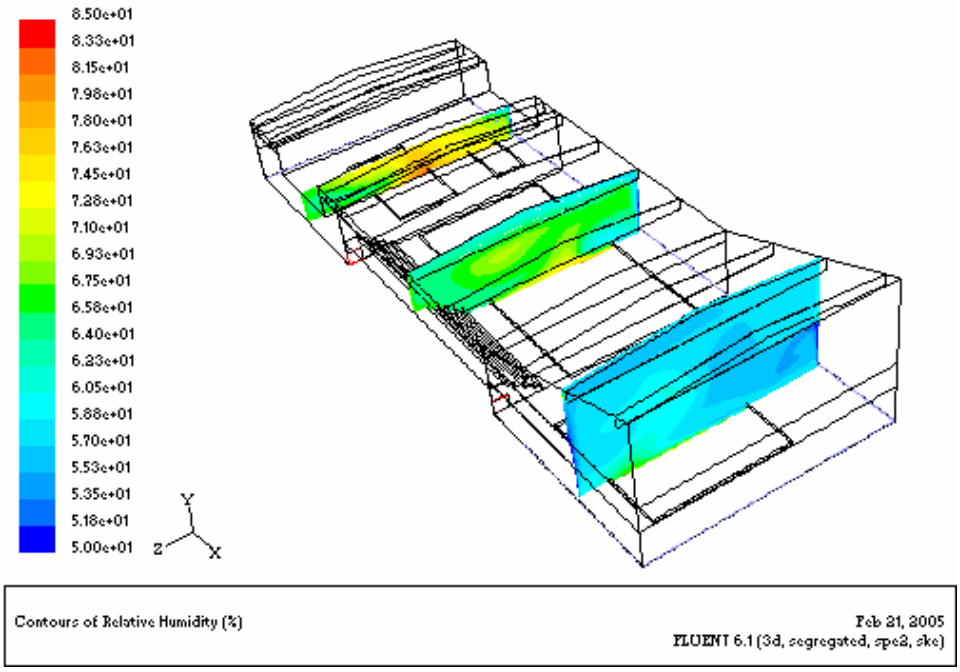

Figure 6.64: Relative humidity distributions at plane X = 10 m, X = 31.5 m and X = 55 m.

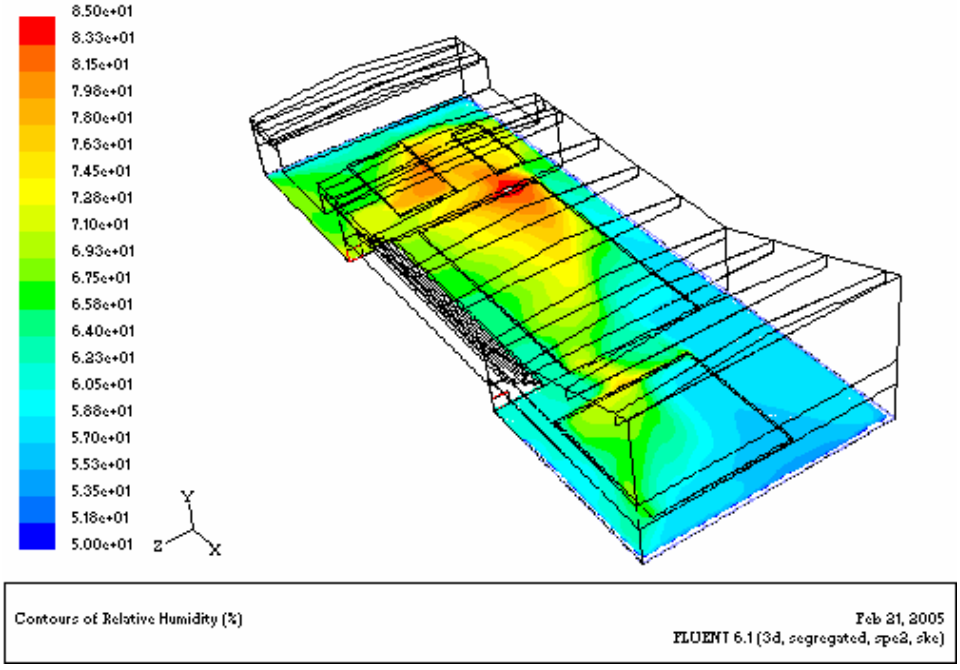

Figure 6.65: Relative humidity distributions at plane Y = 0.1 m.

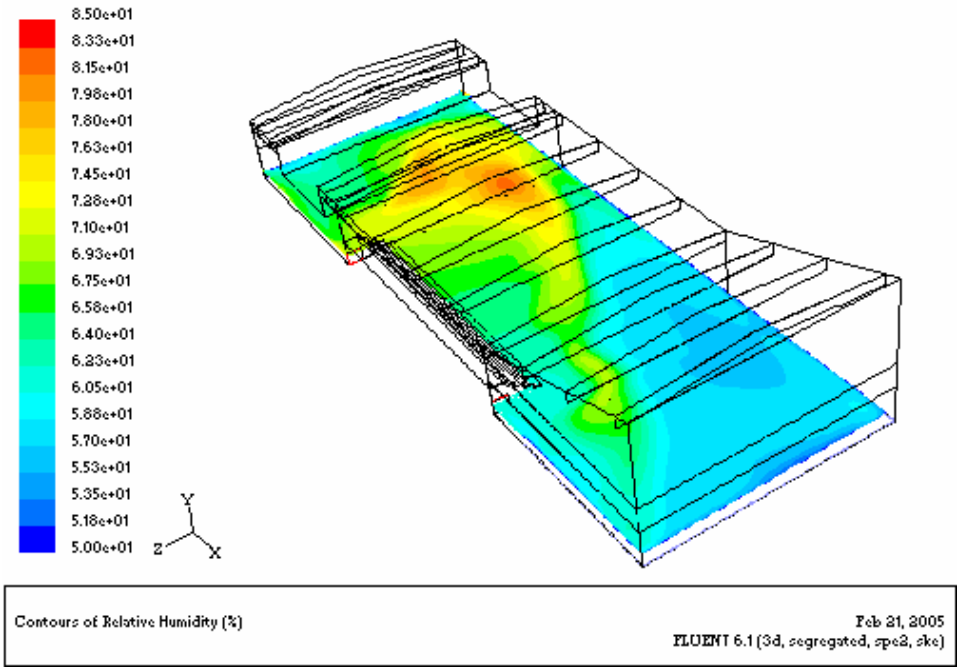

Figure 6.66: Relative humidity distributions at plane Y = 0.77 m.

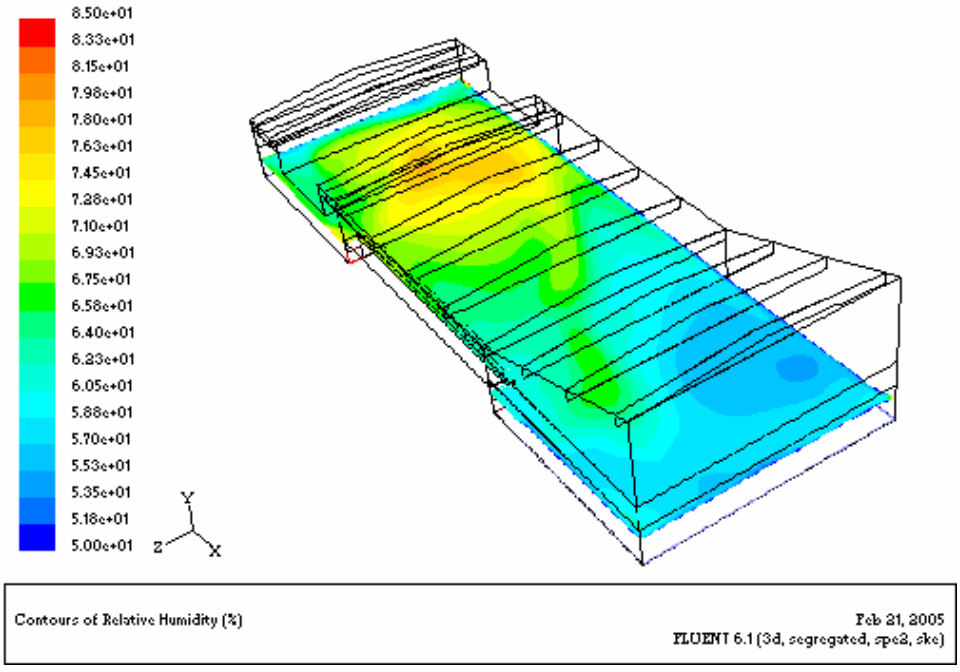

Figure 6.67: Relative humidity distributions at plane Y = 2 m.

6.2.2.4 Profiles

The air velocity, air temperature and air relative humidity at different lines in the middle plane are shown in Figure 6.68 – Figure 6.70 in order to compare them with

the measurement results. The simulation results show that the Shah empirical correlation is reasonable to calculate the water evaporation rate from occupied baths.

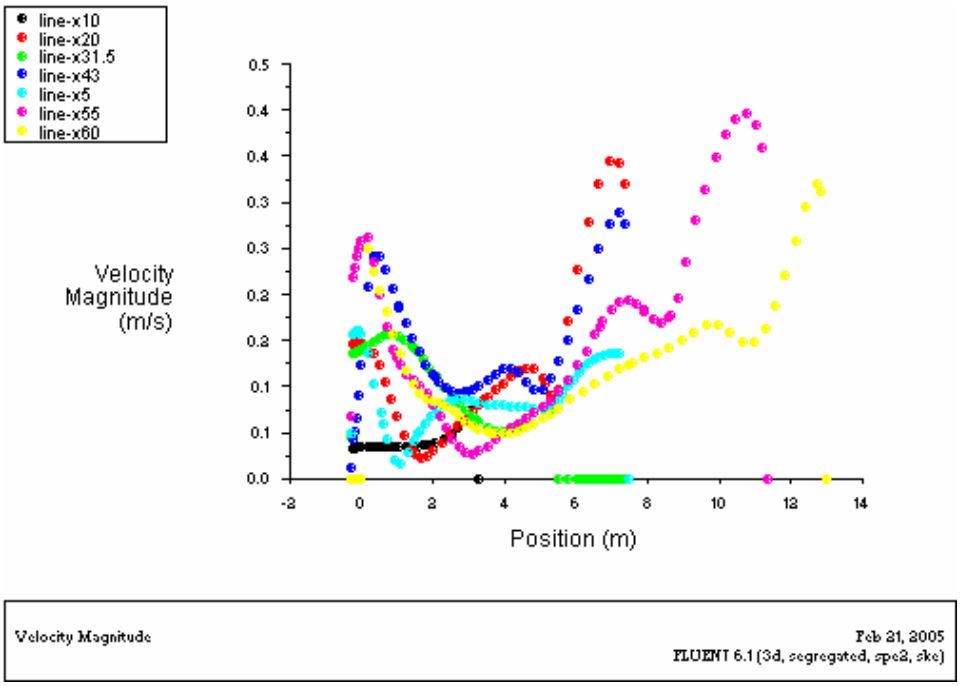

Figure 6.68: Velocity magnitude profile at line X = 5 m, 10 m, 20 m, 31.5 m, 43 m, 55 m and 60 m of the middle plane Z = 11.25m.

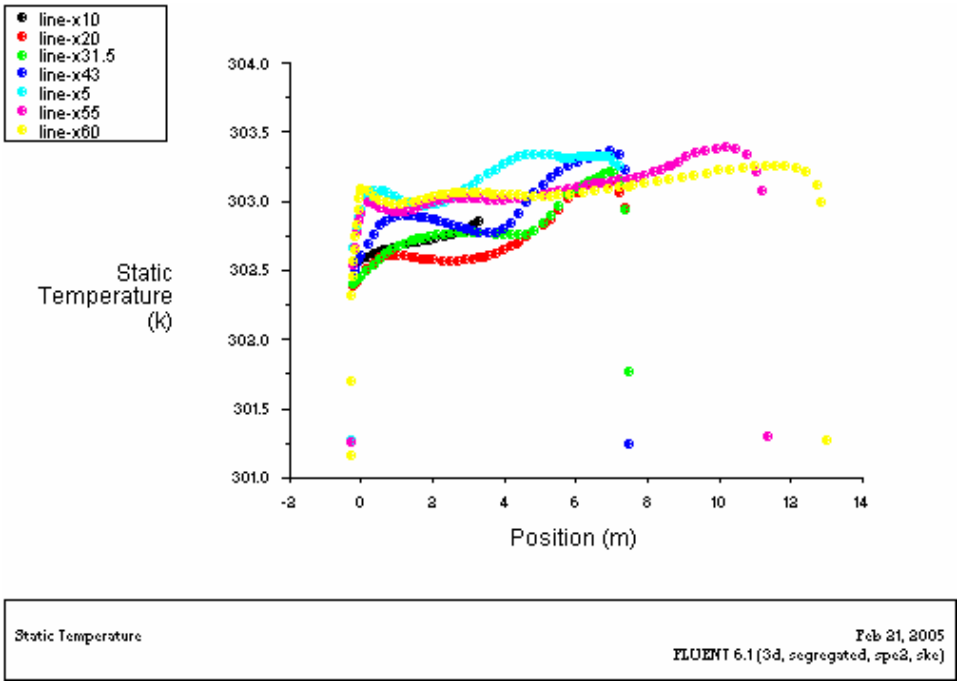

Figure 6.69: Temperature profile at line X = 5 m, 10 m, 20 m, 31.5 m, 43 m, 55 m and 60 m of the middle plane Z = 11.25m.

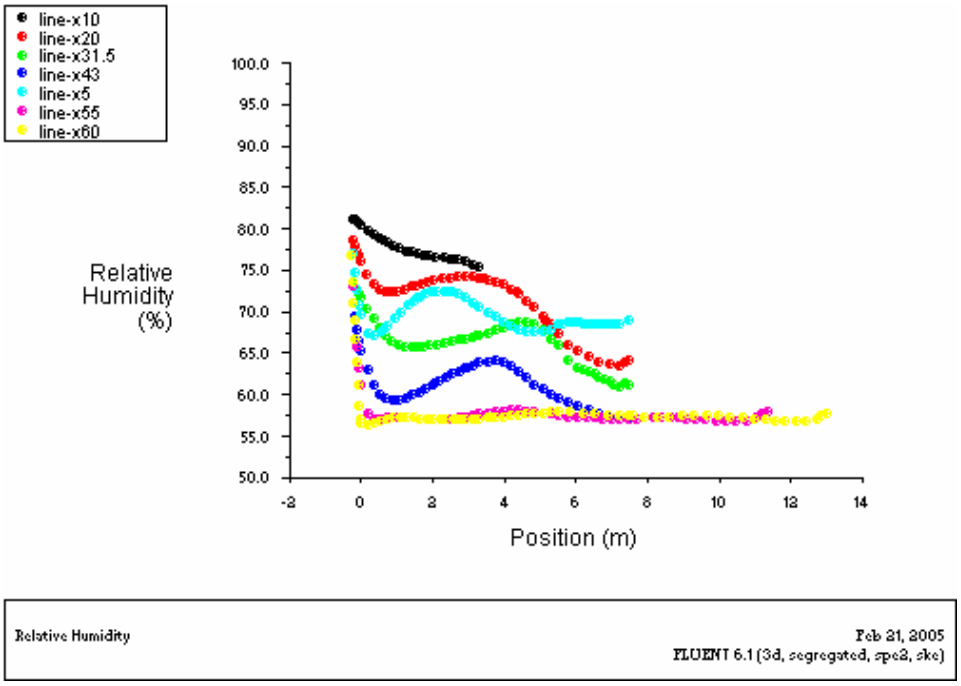

Figure 6.70: Relative humidity profile at line X = 5 m, 10 m, 20 m, 31.5 m, 43 m, 55 m and 60 m of the middle plane Z = 11.25m.

6.2.2.5 Relative humidity comparison

Relative humidity						
Model	Pool type	Measurement value	Simulation set value	3D simulation results value		
		outlet	for the other three baths	outlet-left close to teaching bath zone	outlet-right close to spring bath zone	room average value
Shah	Unoccupied	52%	52%	57.7%	52.4%	53.6%
Shah empirical	Occupied	58%	62%	70.3%	61.0%	63.2%

Table 6.7: Relative humidity comparison.

Table 6.7 shows the relative humidity simulation results compared with the measurement results. The CFD simulations are based on the measurement of outlet air relative humidity. From the CFD results the room average humidity and the two outlets air humidity can be obtained. The shah correlation seems to be quite good agreement with the measurement value. The Shah empirical results show some difference with the measurement value. Certainly, the shah empirical correlation should show some uncertainty because this correlation is influenced by the occupant's

number and different activities in the baths. Another reason for this little higher room average humidity value because no condensation model used in this CFD modeling. Summarily, the shah empirical correlation is quite reasonable to calculate the water evaporation from occupied baths according to the CFD simulation results.

7 3D supplement simulation cases

7.1 Two more simulation cases

Two more cases are simulated for the occupied swimming pool.

7.1.1 New Case1

The supply air flow rate is reduced to 75% and the supply air temperature is increased to 40.6 °C. According to the energy balance, the average air temperature in the swimming pool still keeps to 30 °C, and the water evaporation rate and relative humidity distribution will change in the swimming pool. Table 7.1 shows this 3D CFD simulation case where the Shah empirical evaporation rate calculations are based on T_w = 34°C, T_{air} = 30°C, f = 84% for the small child bath and T_w = 28°C, T_{air} = 30°C, f = 68% for the other three baths.

Bath	Evaporation rate of water vapour source [kg/m^{3}s]
Spring bath	0.0092
Swimming bath	0.0092
Teaching bath	0.0092
Small child bath	0.0120

Table 7.1: New 3D simulation case1 for Shah empirical occupied pool model.

7.1.2 New Case2

The supply air flow rate does not change and keeps 100% but the supply air temperature is reduced to 35.5 °C. According to the energy balance, the average air temperature in the swimming pool changes to 28 °C, and the water evaporation rate and relative humidity distribution will change in the swimming pool as well. Table 7.2 shows this 3D CFD simulation case where the Shah empirical evaporation rate calculations are based on T_w = 34°C, T_{air} = 28°C, f = 76% for the small child bath and T_w = 28°C, T_{air} = 28°C, f = 69% for the other three baths.

Bath	Evaporation rate of water vapour source [kg/m^{3}s]
Spring bath	0.010
Swimming bath	0.010

Teaching bath	0.010
Small child bath	0.014

Table 7.2: New 3D simulation case2 for Shah empirical occupied pool model.

7.2 Simulation results

7.2.1 Results of occupied Shah empirical correlation new case1

7.2.1.1 Velocity distribution

Figure 7.1 – Figure 7.11 show the velocity vector distributions for different planes in the occupied swimming hall.

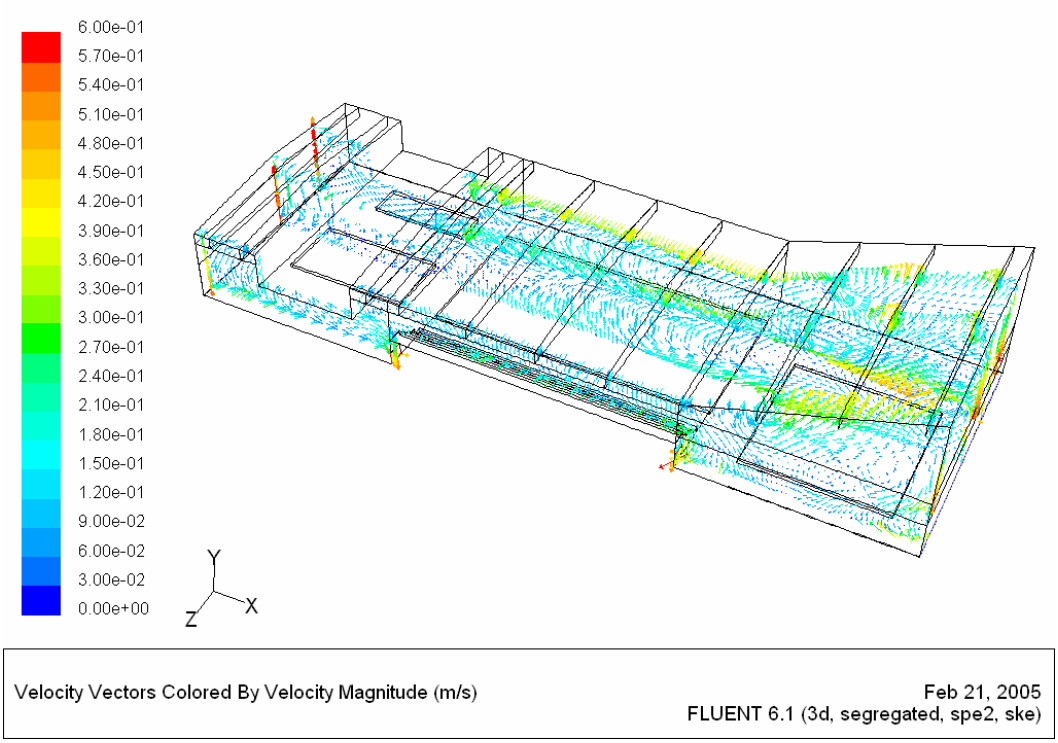

Figure 7.1: Velocity distributions at plane Z = 5 m, Z = 11.25 m and Z = 21.5 m.

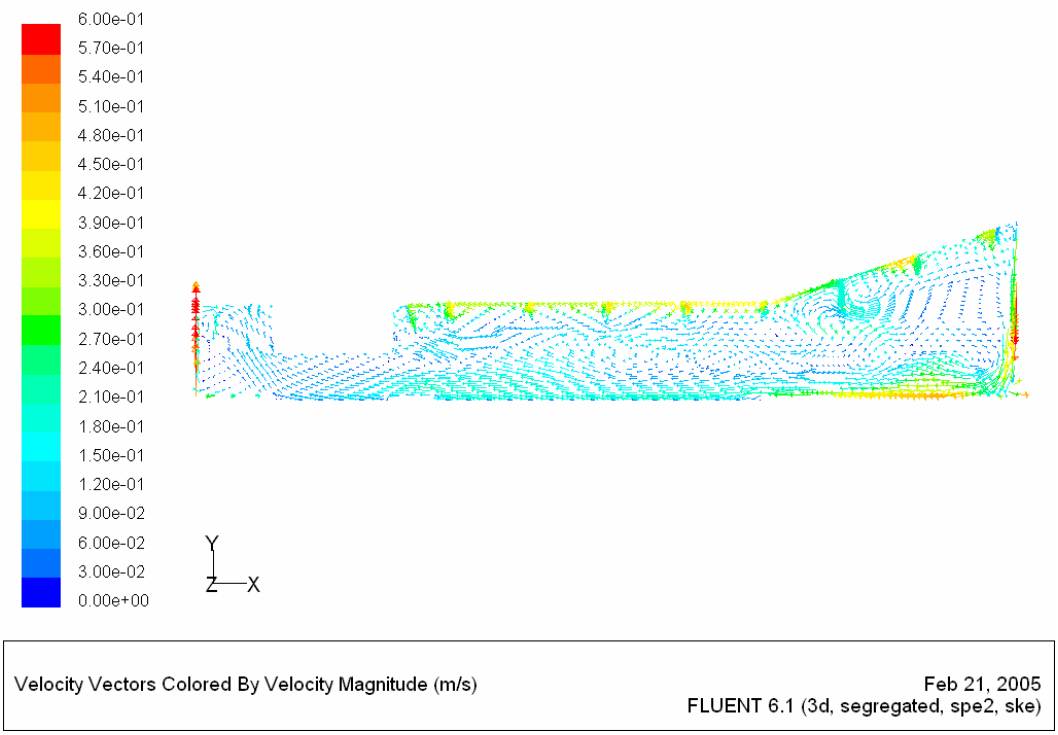

Figure 7.2: Velocity distributions at plane Z = 5 m.

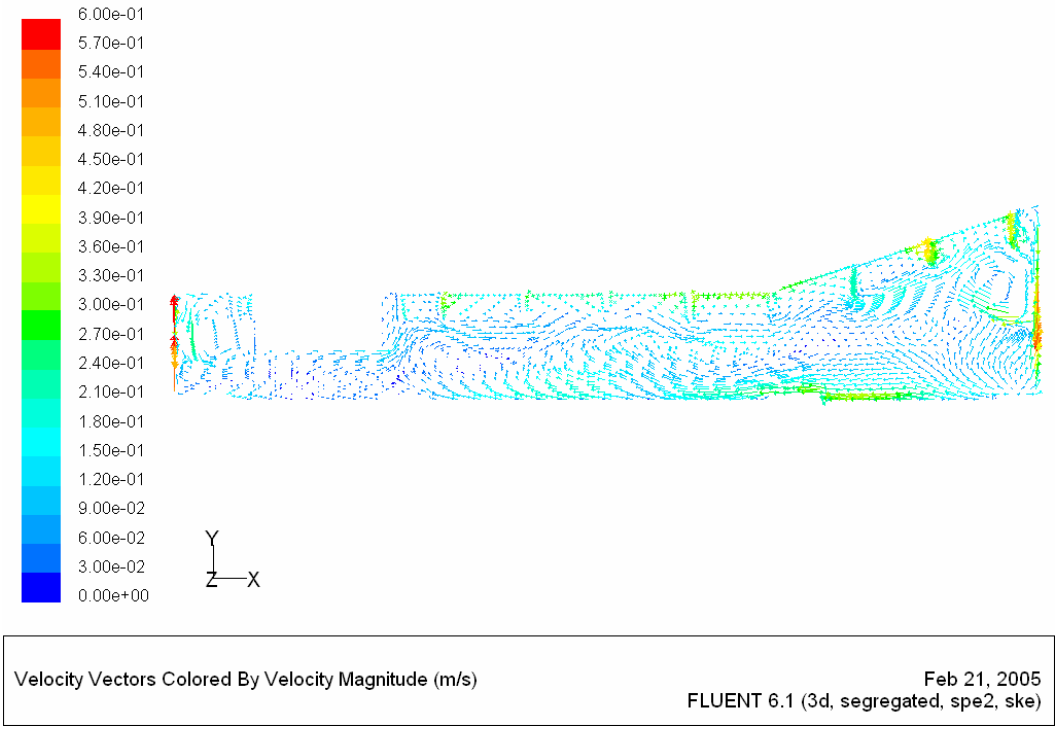

Figure 7.3: Velocity distributions at plane Z = 11.25 m.

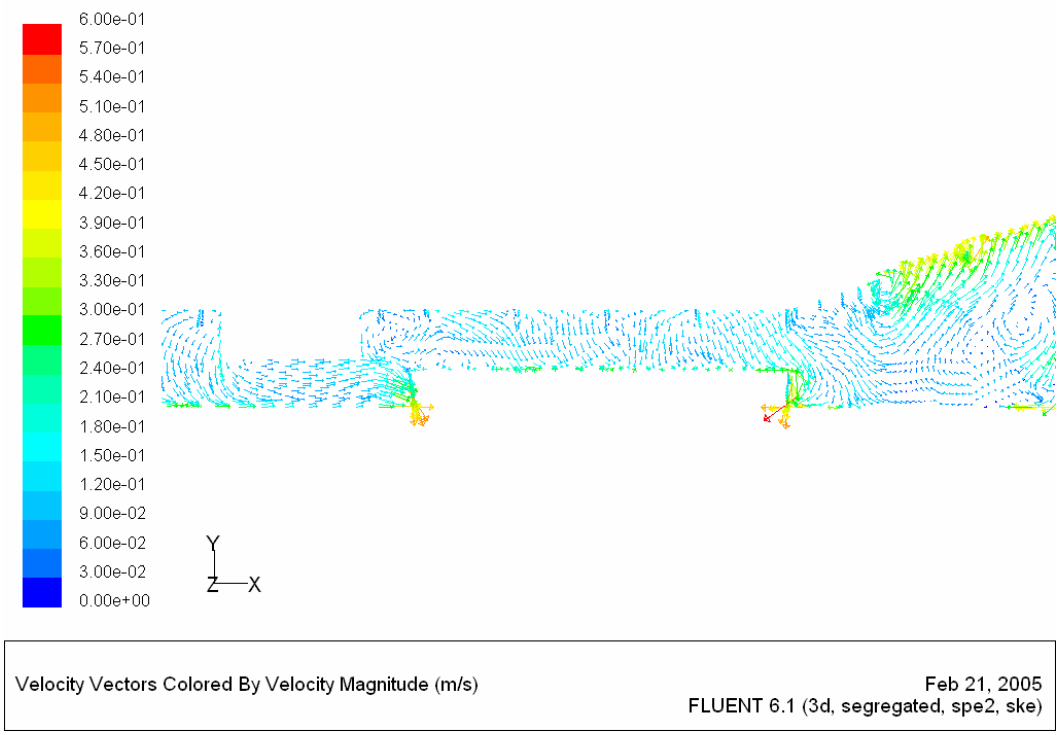

Figure 7.4: Velocity distributions at plane Z = 21.5 m.

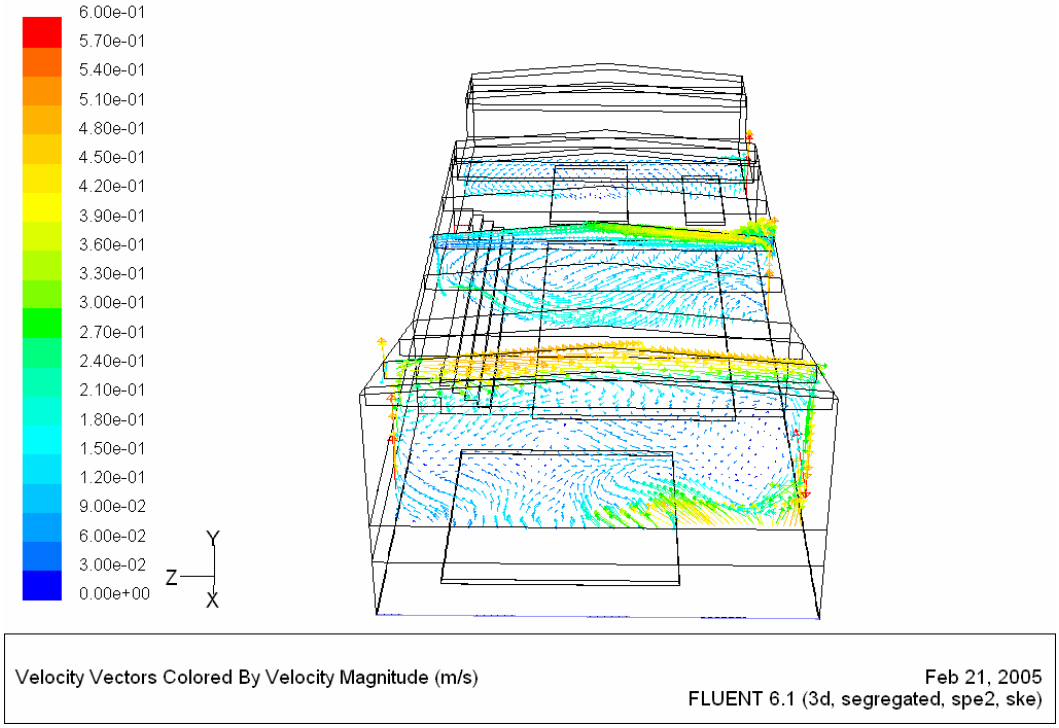

Figure 7.5: Velocity distributions at plane X = 10 m, X = 31.5 m and X = 55m.

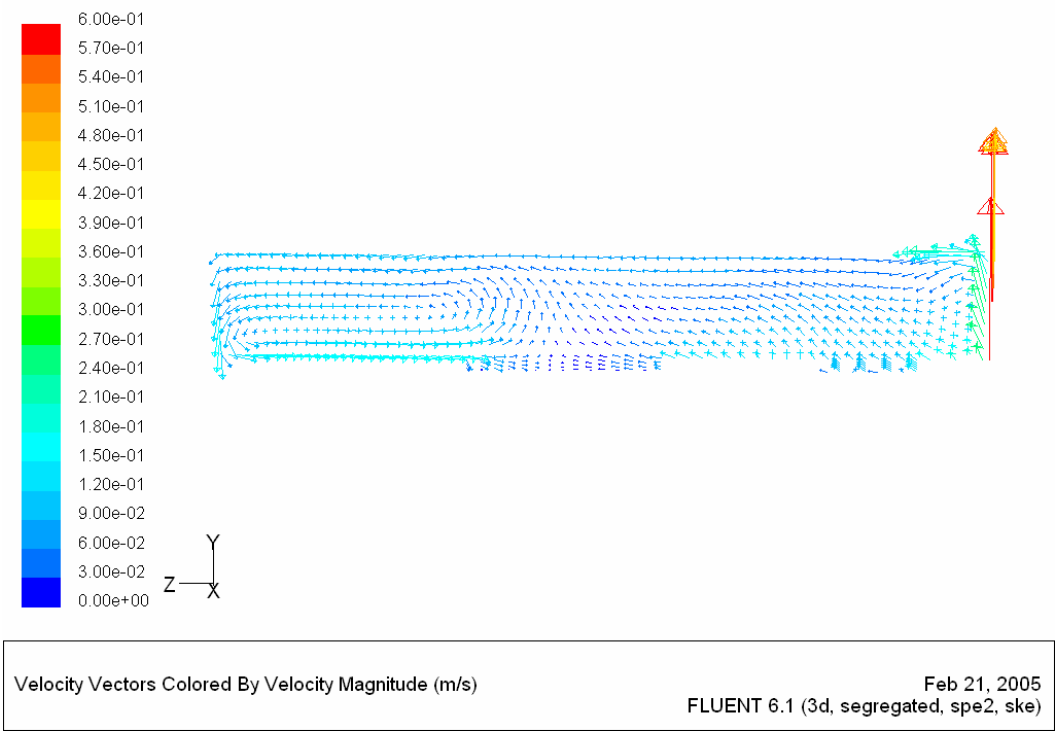

Figure 7.6: Velocity distributions at plane X = 10 m.

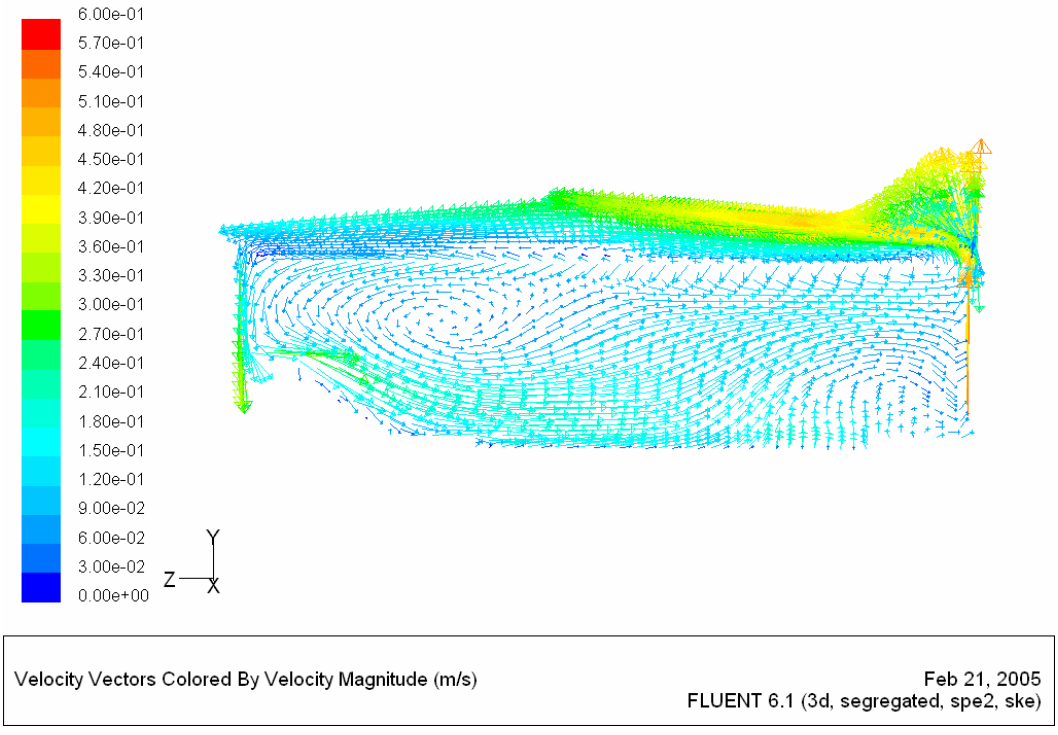

Figure 7.7: Velocity distributions at plane X = 31.5 m.

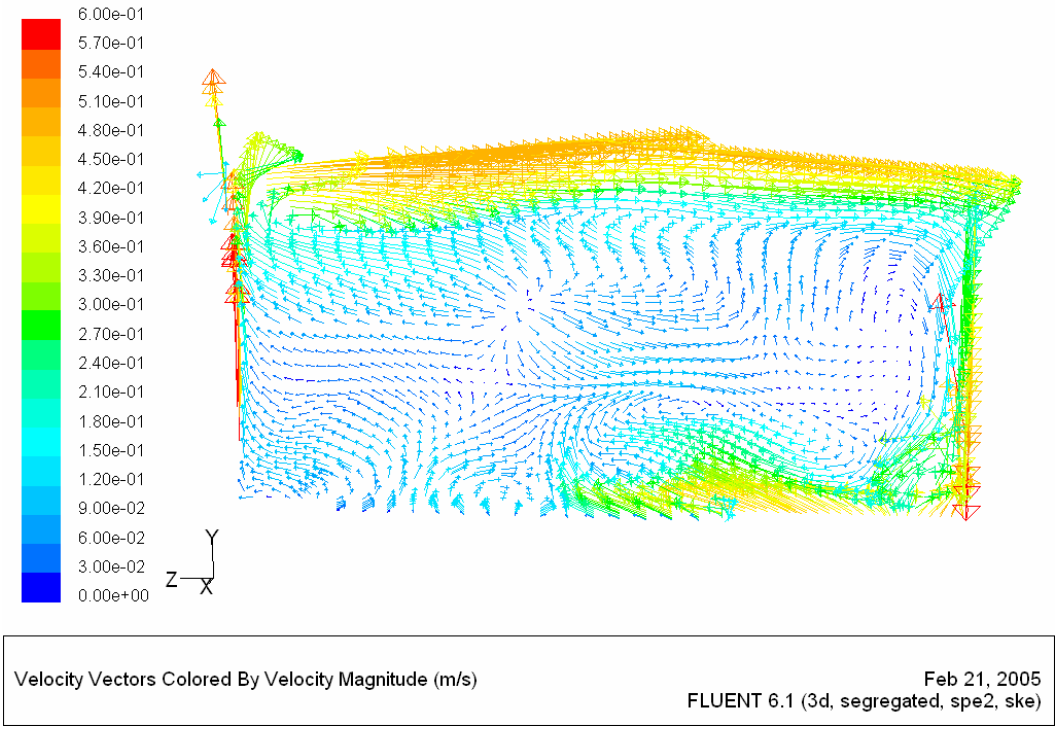

Figure 7.8: Velocity distributions at plane X = 55m.

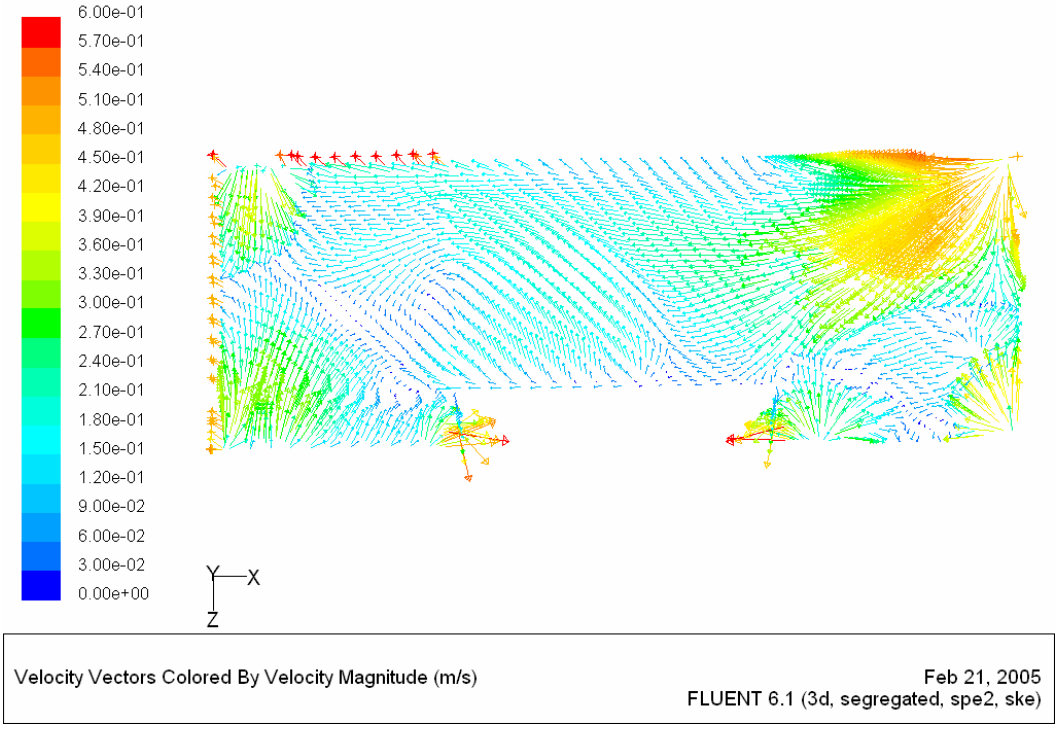

Figure 7.9: Velocity distributions at plane Y = 0.1 m.

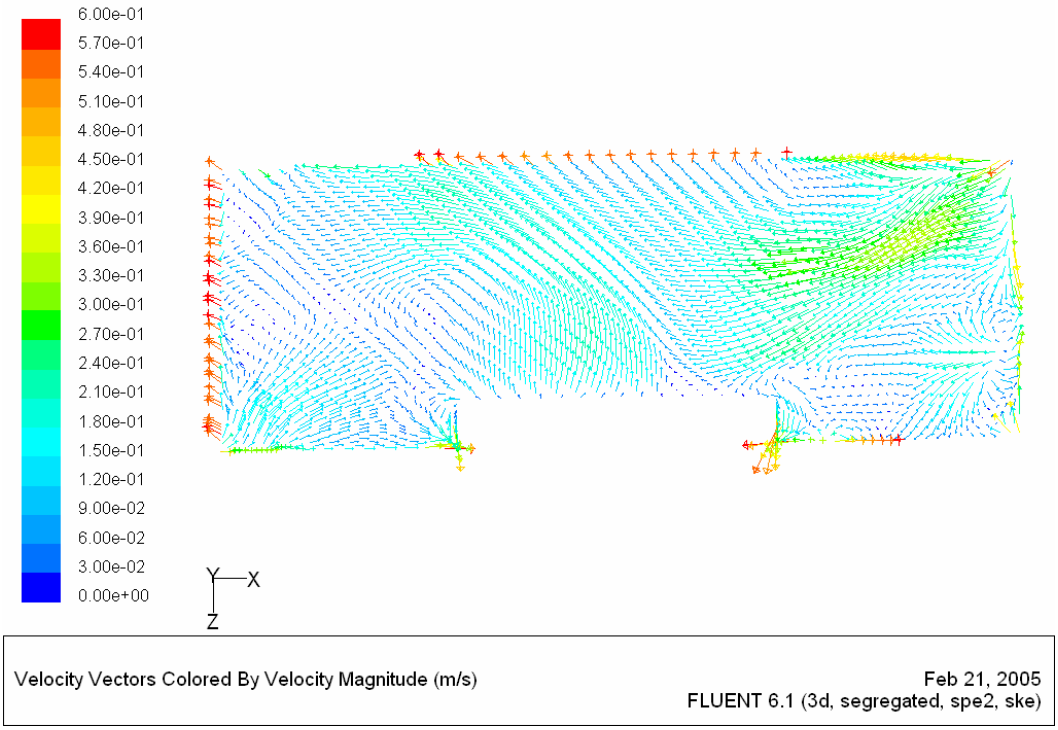

Figure 7.10: Velocity distributions at plane Y = 0.77 m.

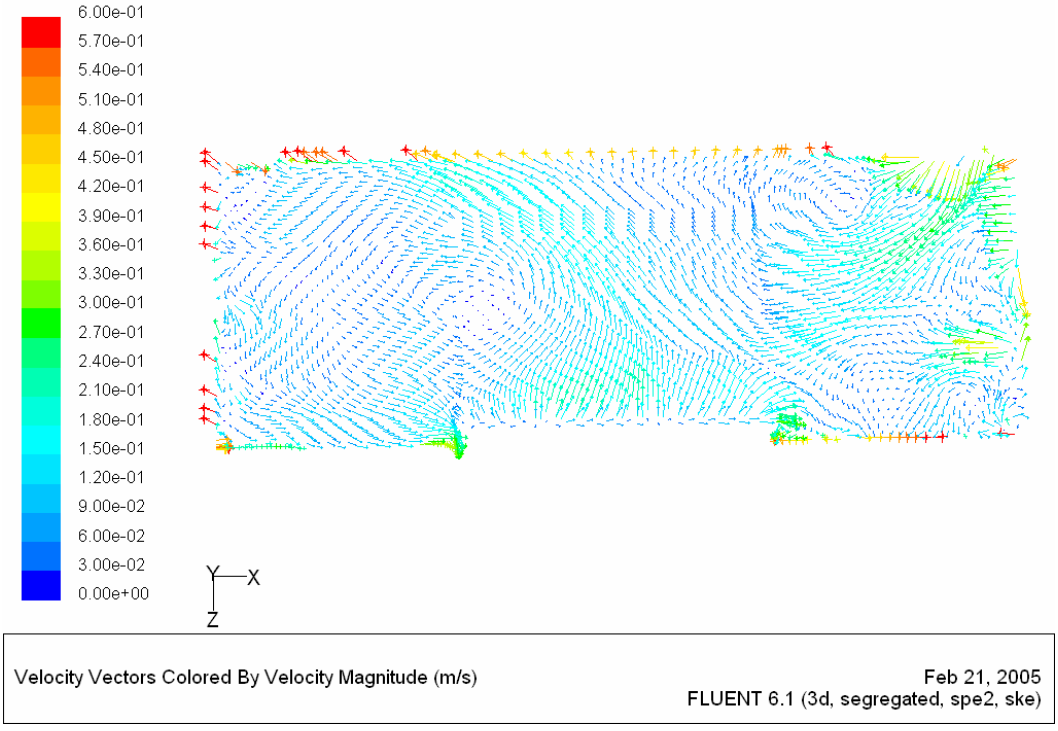

Figure 7.11: Velocity distributions at plane Y = 2 m.

7.2.1.2 Temperature distribution

Figure 7.12 – Figure 7.19 show the air temperature distributions for different planes in the occupied swimming hall.

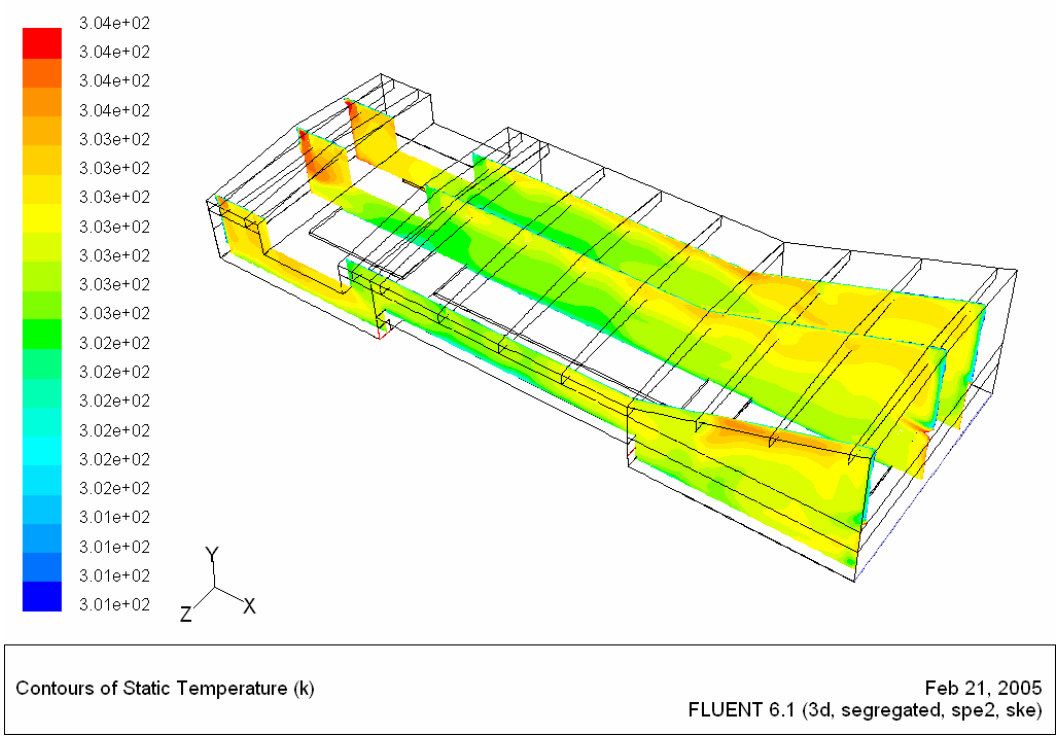

Figure 7.12: Temperature distributions at plane Z = 5 m, Z = 11.25 m and Z = 21.5 m.

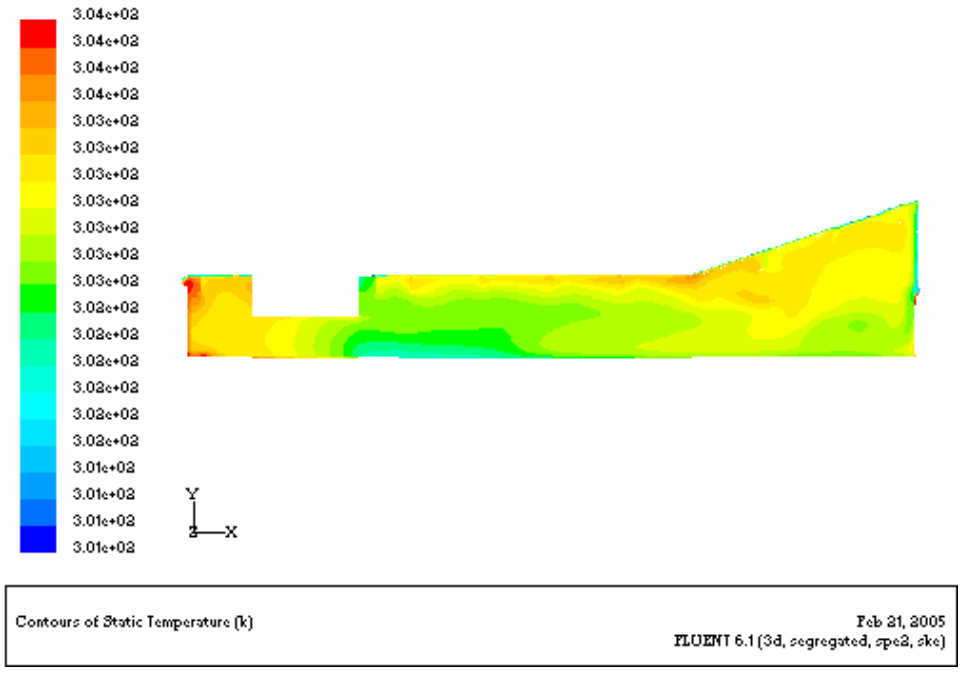

Figure 7.13: Temperature distributions at plane Z = 5 m.

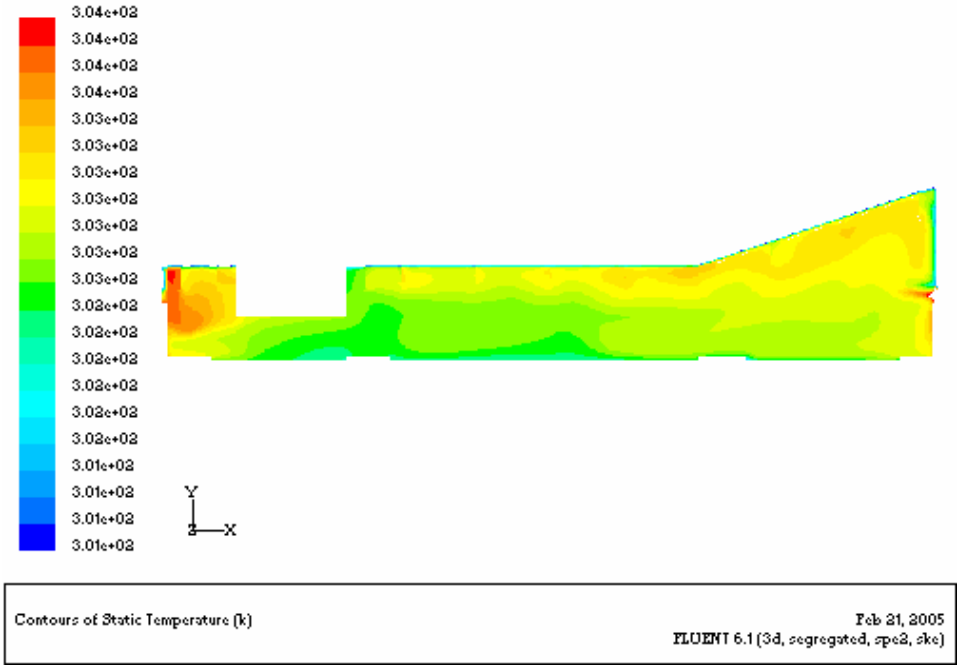

Figure 7.14: Temperature distributions at plane Z = 11.25 m.

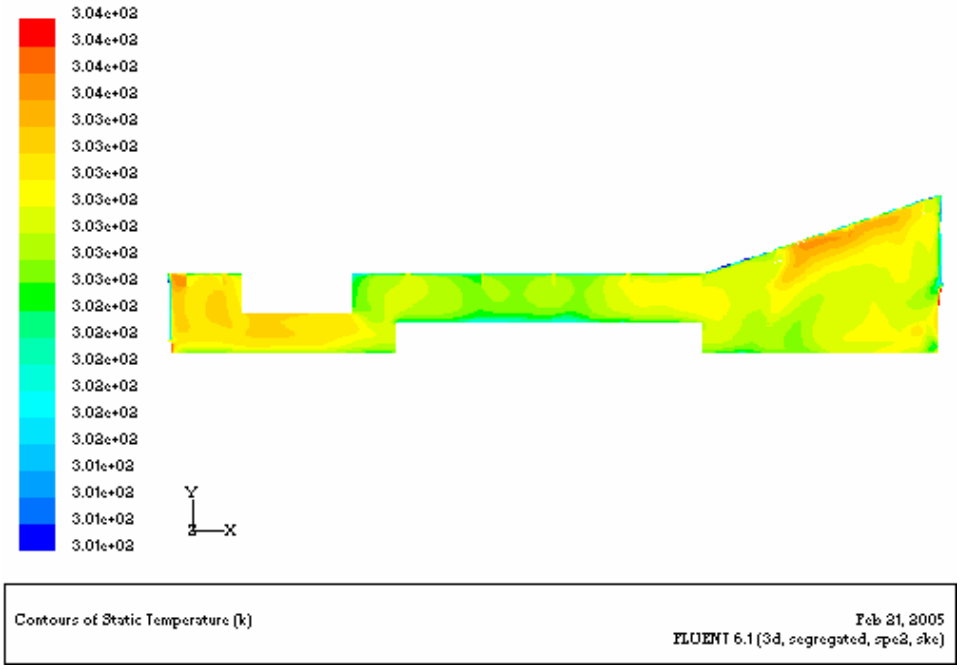

Figure 7.15: Temperature distributions at plane Z = 21.5 m.

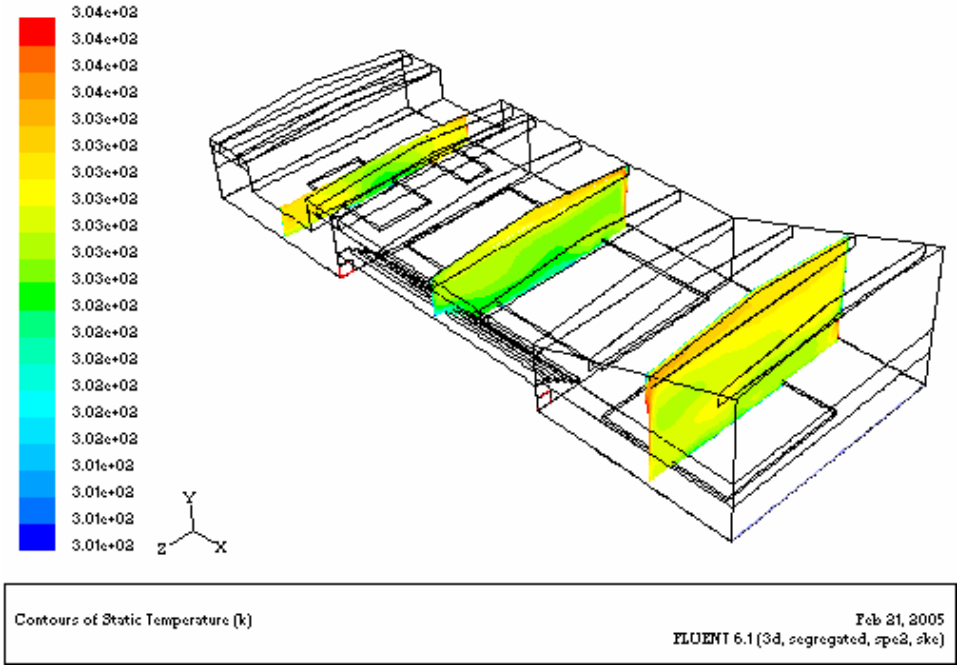

Figure 7.16: Temperature distributions at plane X = 10 m, X = 31.5 m and X = 55 m.

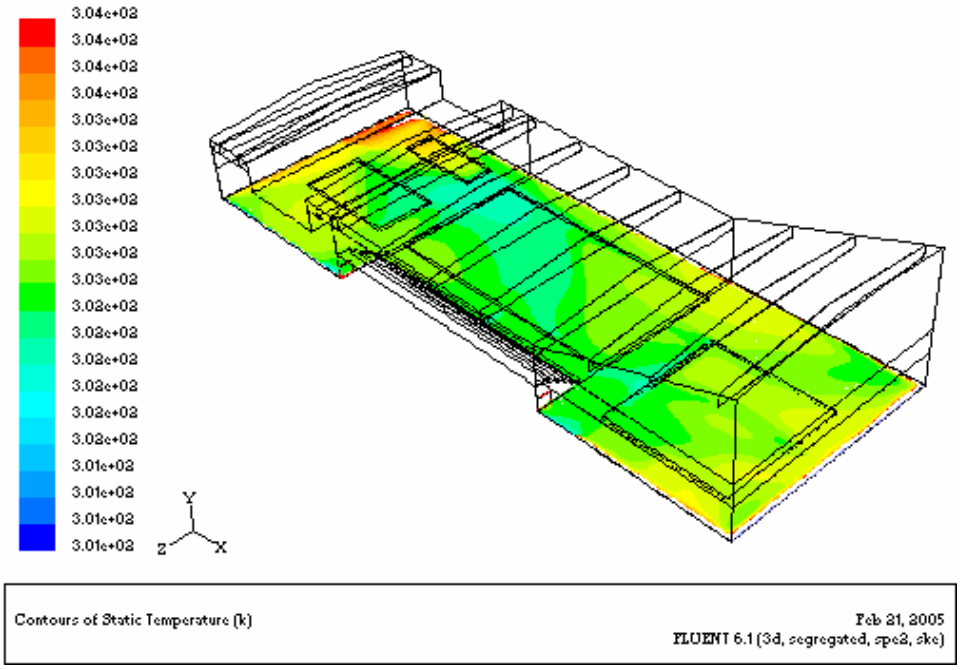

Figure 7.17: Temperature distributions at plane Y = 0.1 m.

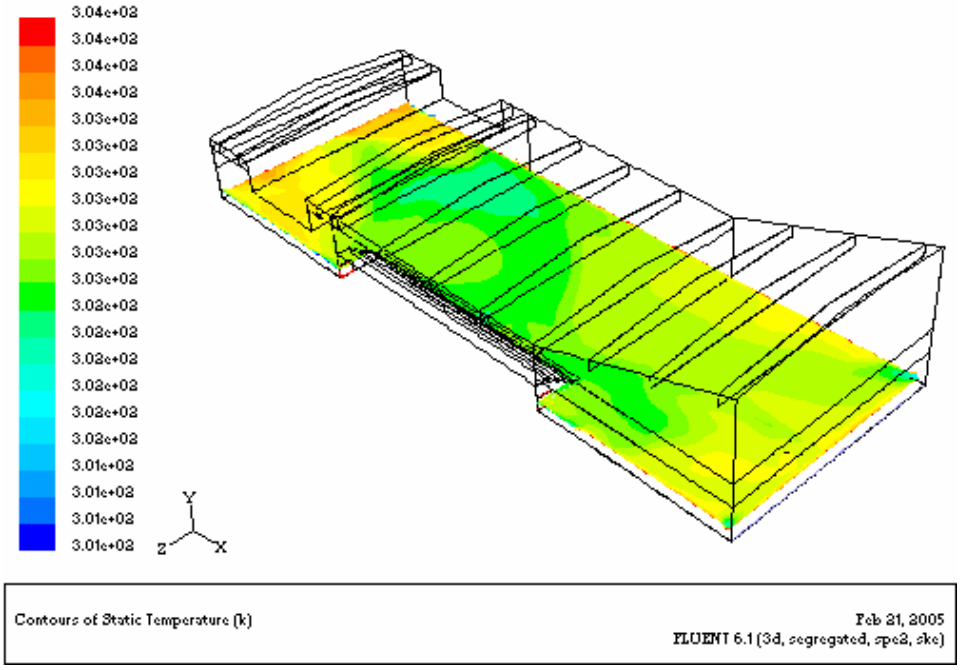

Figure 7.18: Temperature distributions at plane Y = 0.77 m.

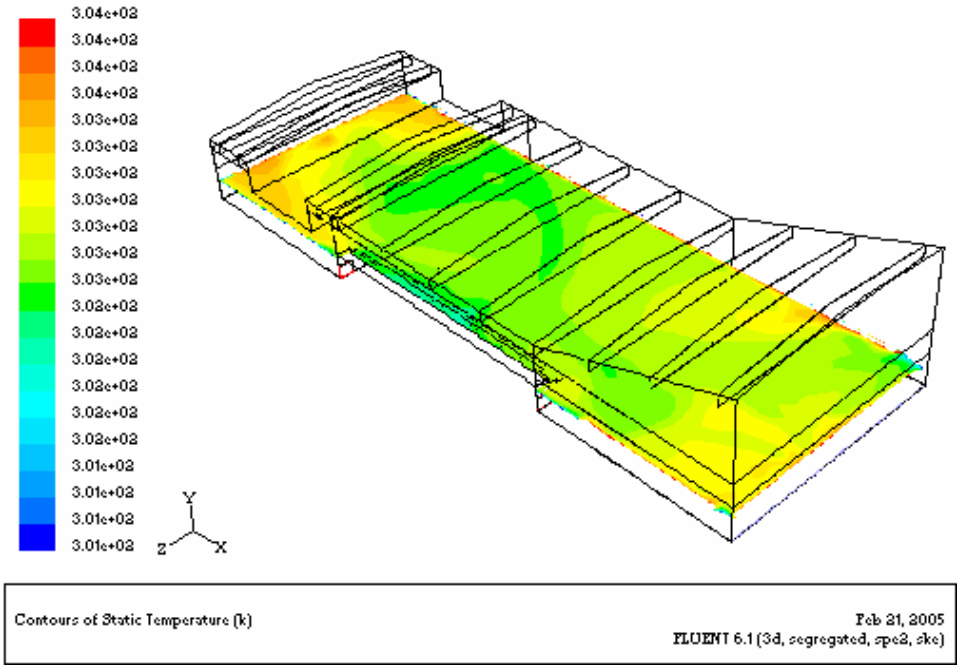

Figure 7.19: Temperature distributions at plane Y = 2 m.

7.2.1.3 Relative humidity distribution

Figure 7.20 – Figure 7.27 show the relative humidity distributions for different planes in the swimming hall. It is clear to see that the relative humidity varies greatly inside

the building and the relative humidity is higher than it of the 100% supply air rate case because of the higher water evaporation rate. The relative humidity is lower in the spring bath part of the building because of the higher ventilation rate, and the relative humidity is higher in the small child bath part because of the higher water temperature and higher water evaporation rate. The relative humidity is very higher close to the water surface because the water vapour evaporates.

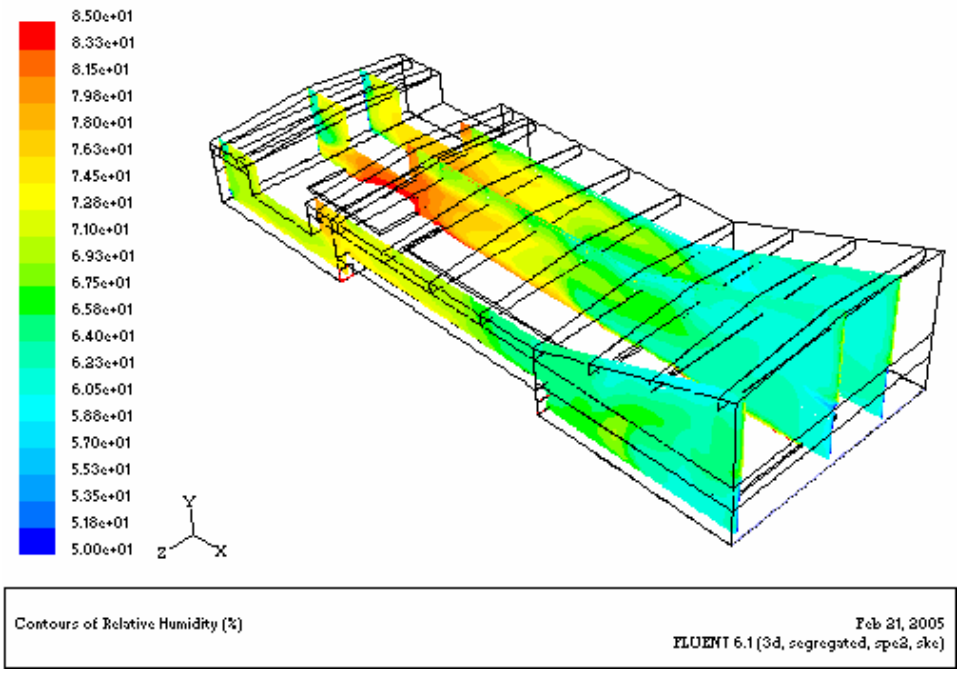

Figure 7.20: Relative humidity distributions at plane Z = 5 m, Z = 11.25 m and Z = 21.5 m.

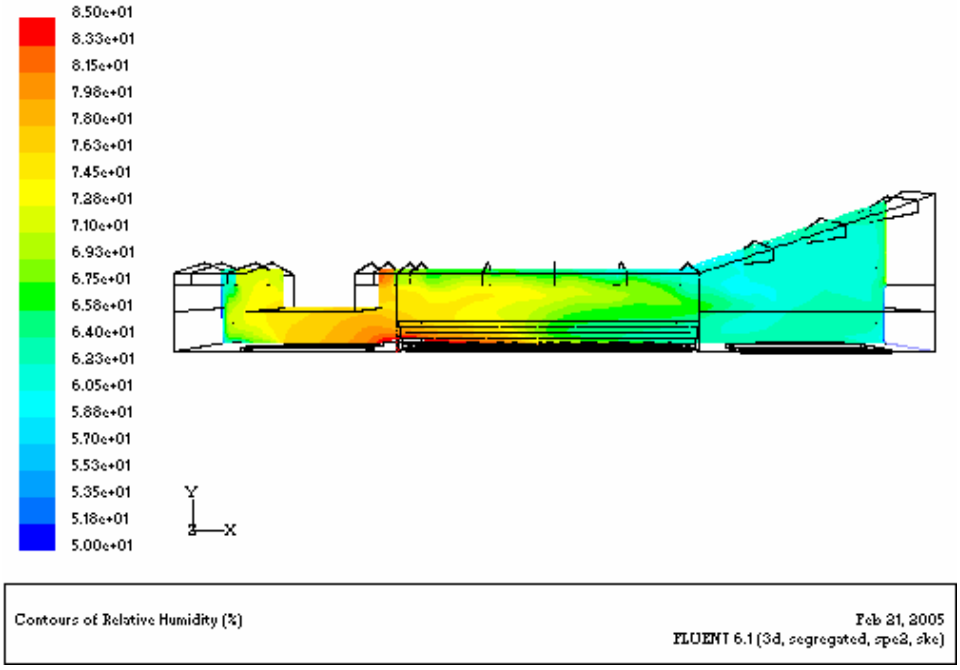

Figure 7.21: Relative humidity distributions at plane Z = 5 m.

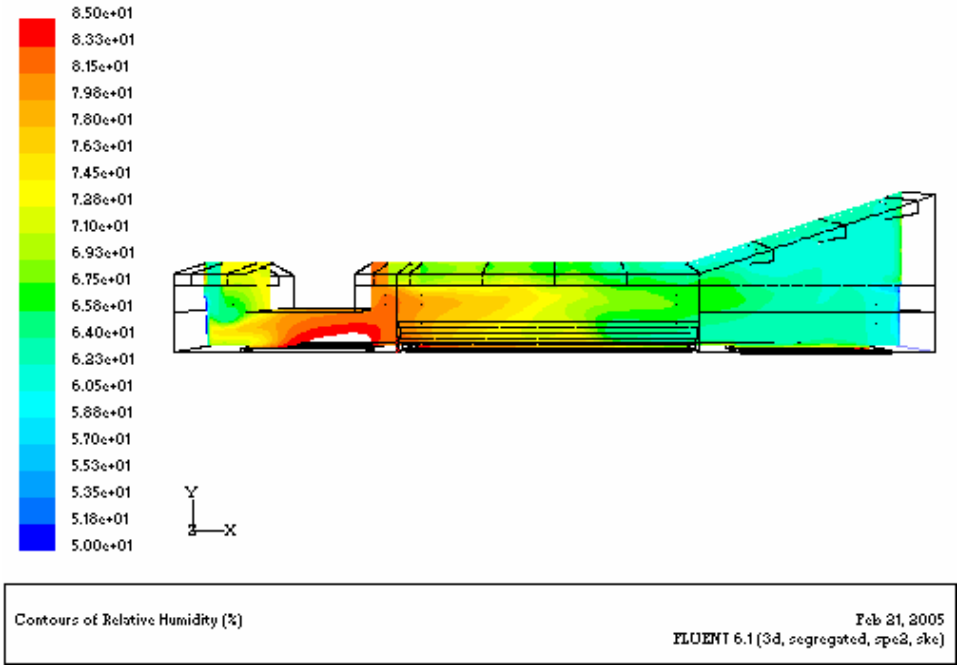

Figure 7.22: Relative humidity distributions at plane Z = 11.25 m.

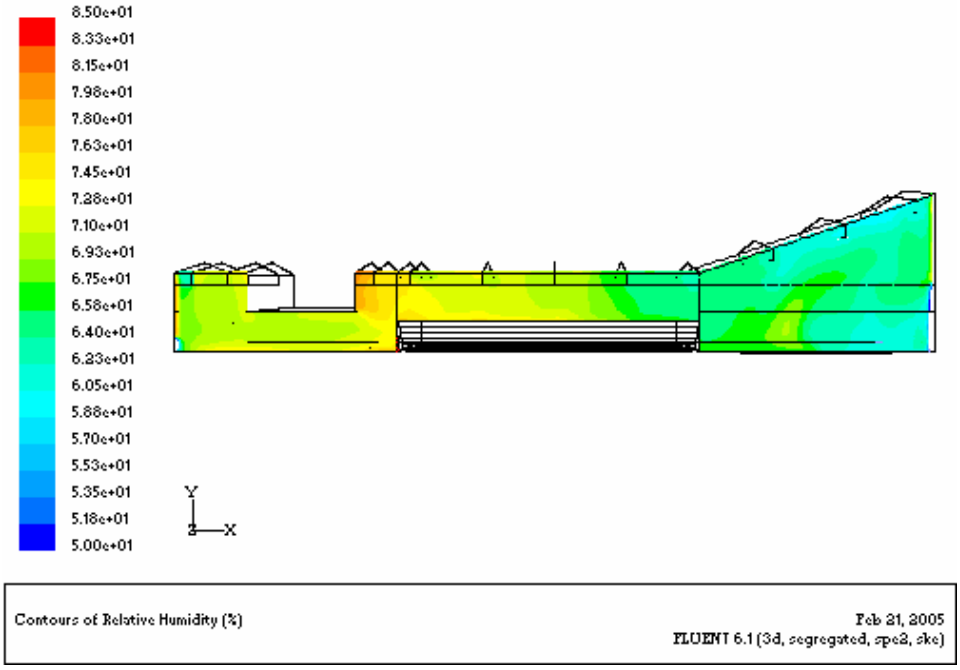

Figure 7.23: Relative humidity distributions at plane Z = 21.5 m.

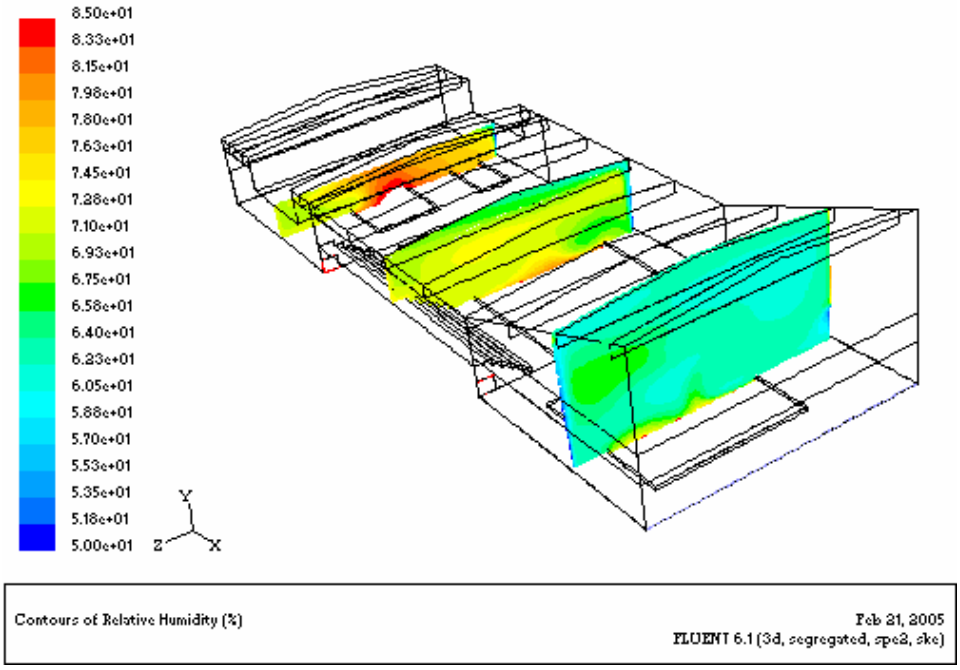

Figure 7.24: Relative humidity distributions at plane X = 10 m, X = 31.5 m and X = 55 m.

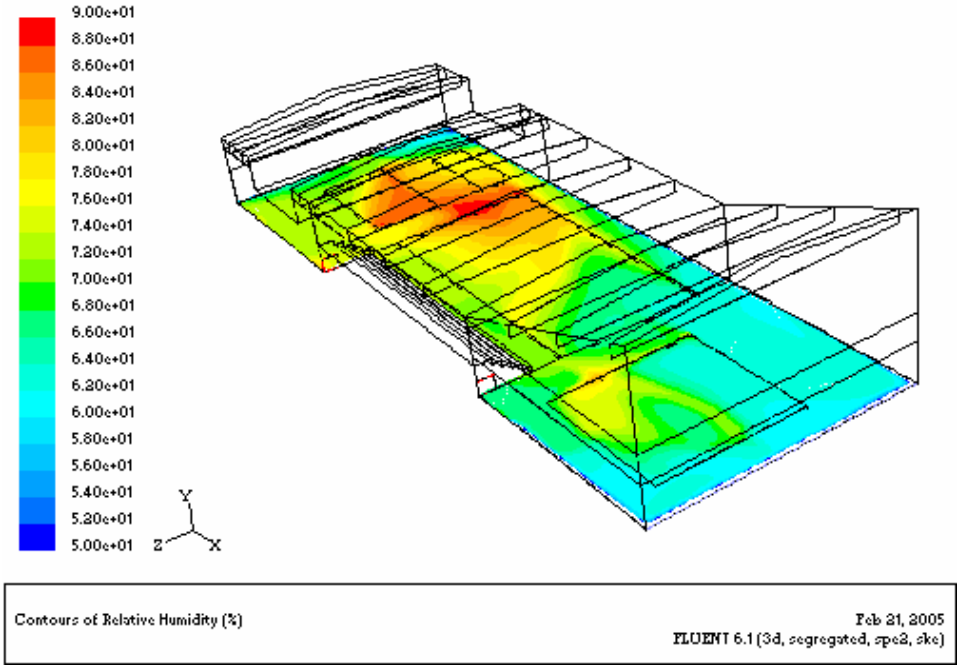

Figure 7.25: Relative humidity distributions at plane Y = 0.1 m.

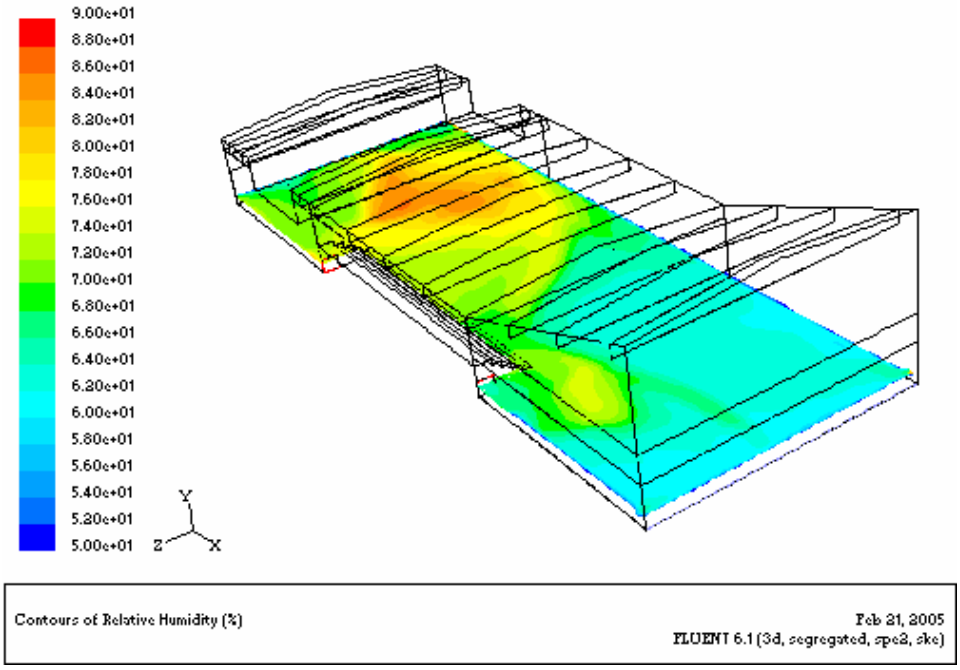

Figure 7.26: Relative humidity distributions at plane Y = 0.77 m.

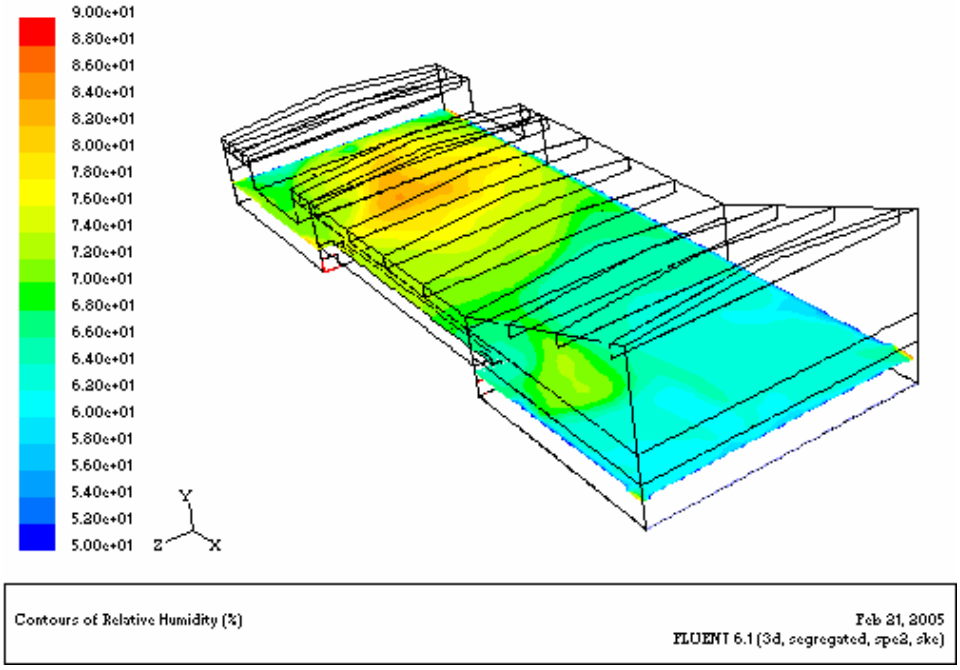

Figure 7.27: Relative humidity distributions at plane Y = 2 m.

7.2.1.4 Profiles

The air velocity, air temperature and air relative humidity at different lines in the middle plane are shown in Figure 7.28 – Figure 7.30.

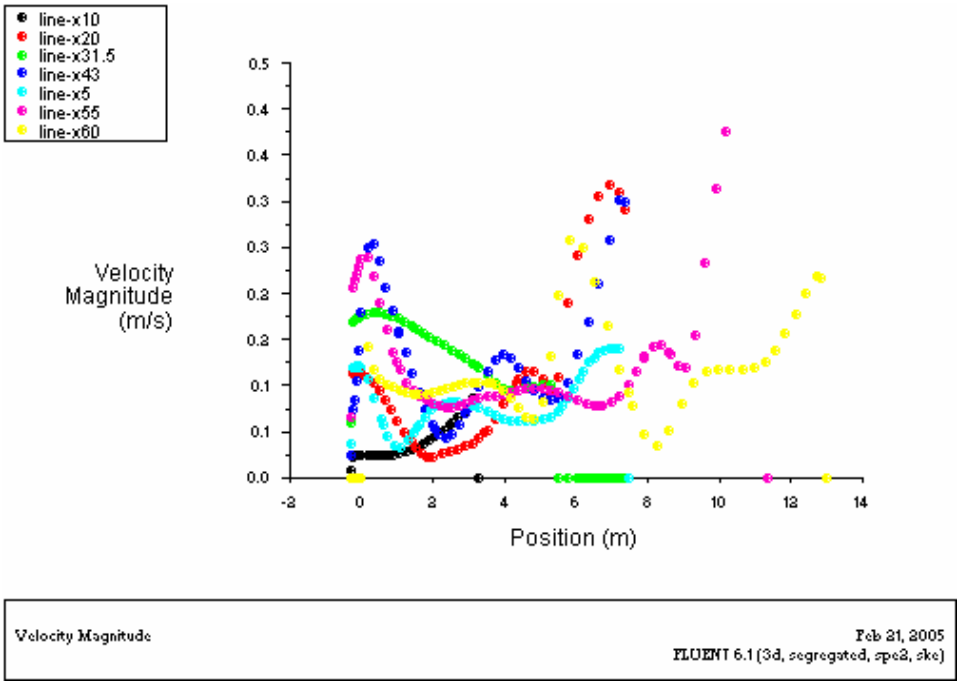

Figure 7.28: Velocity magnitude profile at line X = 5 m, 10 m, 20 m, 31.5 m, 43 m, 55 m and 60 m of the middle plane Z = 11.25m.

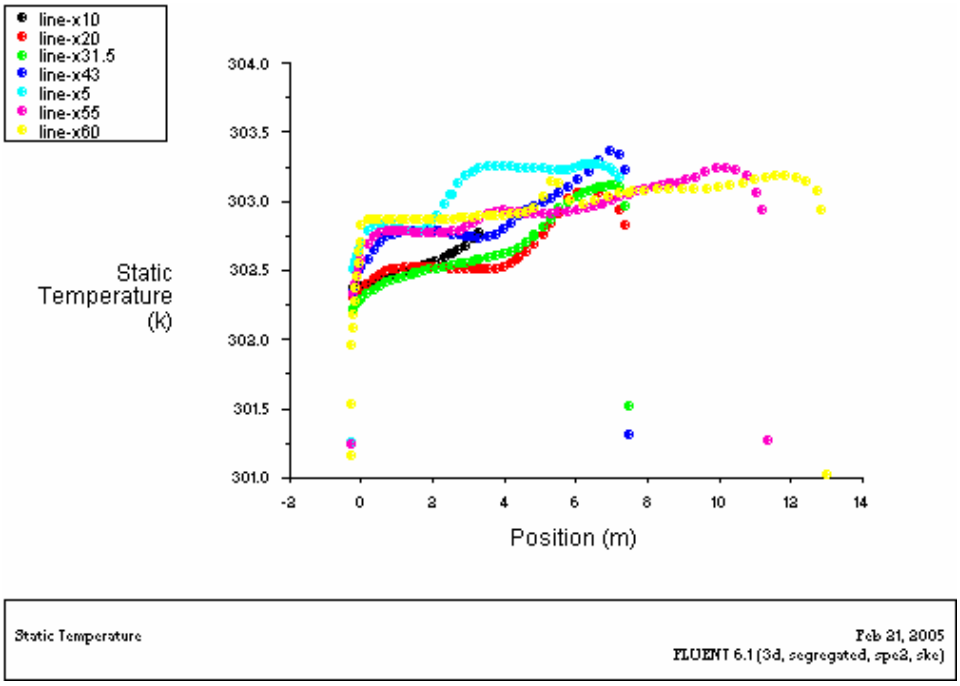

Figure 7.29: Temperature profile at line X = 5 m, 10 m, 20 m, 31.5 m, 43 m, 55 m and 60 m of the middle plane Z = 11.25m.

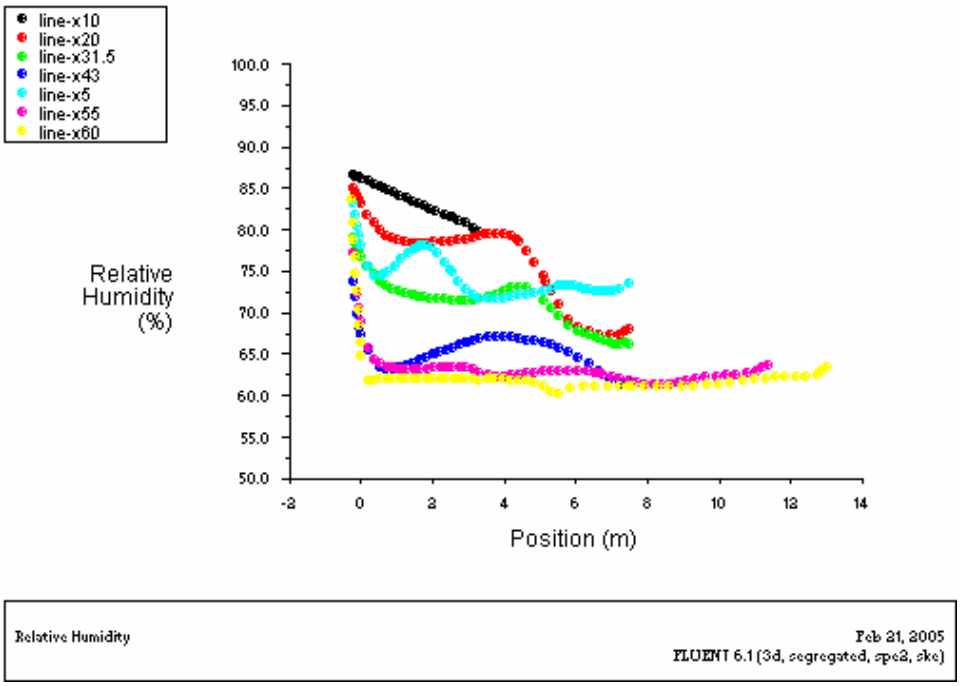

Figure 7.30: Relative humidity profile at line X = 5 m, 10 m, 20 m, 31.5 m, 43 m, 55 m and 60 m of the middle plane Z = 11.25m.

7.2.2 Results of occupied Shah empirical correlation new case2

7.2.2.1 Velocity distribution

Figure 7.31 – Figure 7.41 show the velocity vector distributions for different planes in the occupied swimming hall.

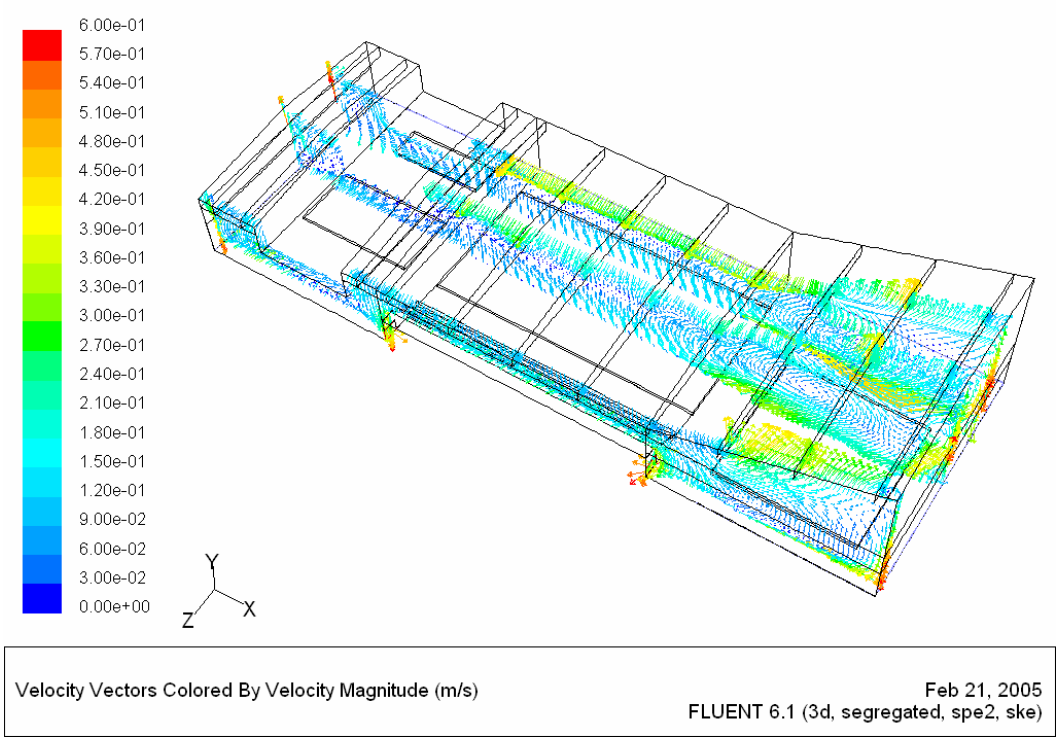

Figure 7.31: Velocity distributions at plane Z = 5 m, Z = 11.25 m and Z = 21.5 m.

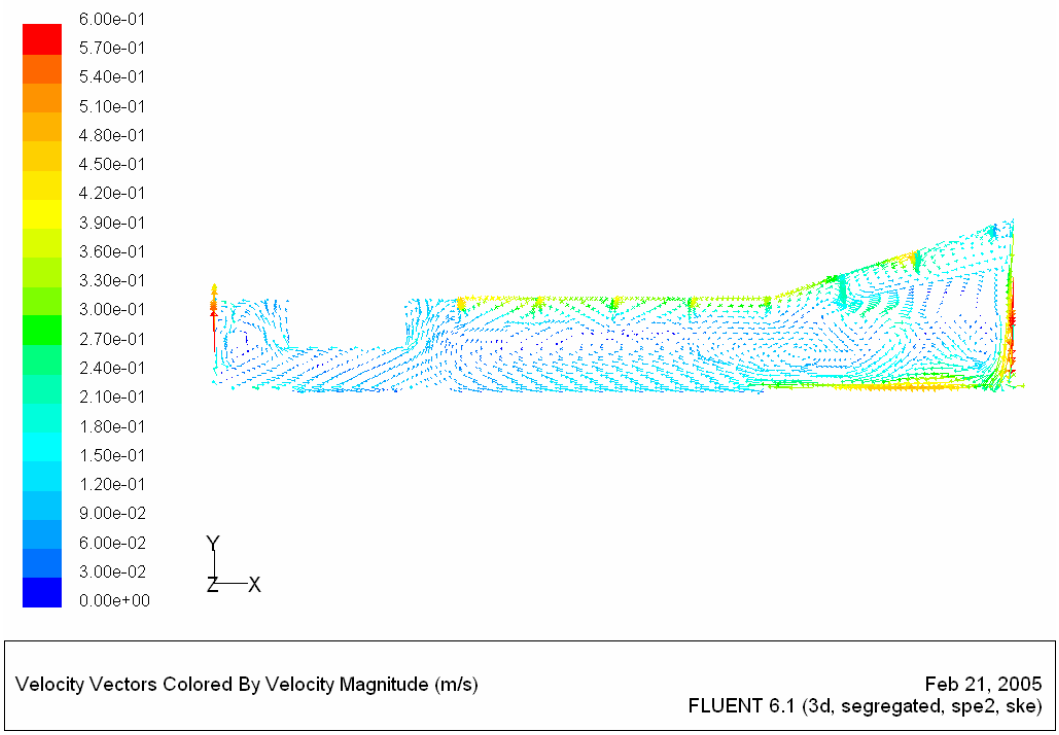

Figure 7.32: Velocity distributions at plane Z = 5 m.

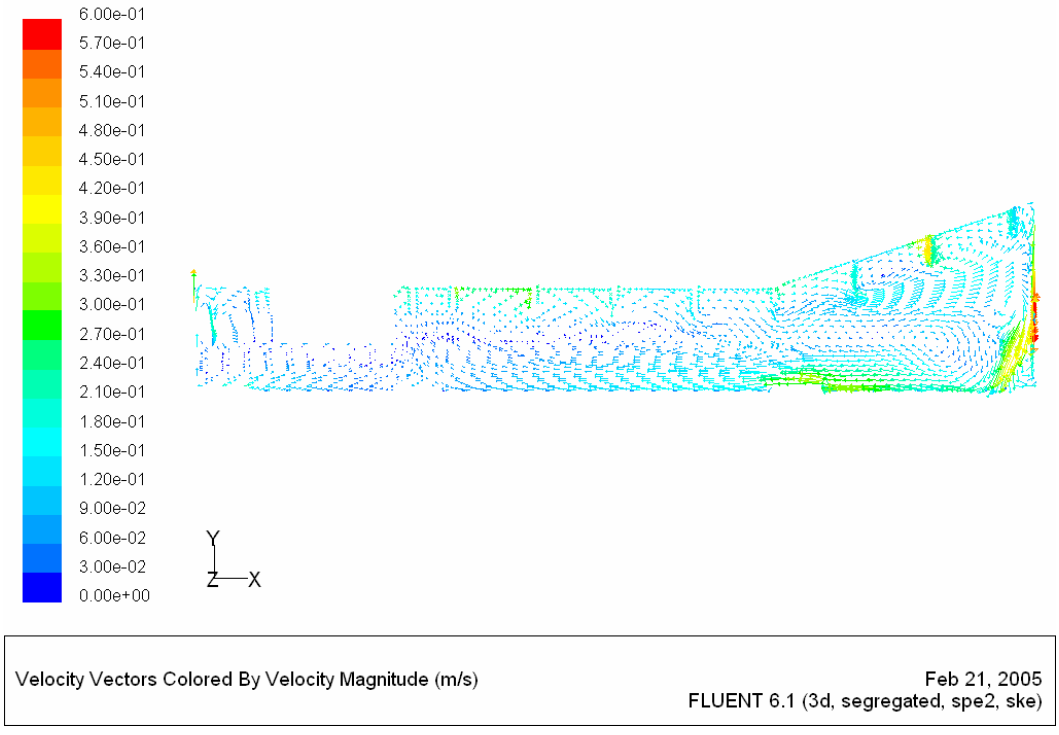

Figure 7.33: Velocity distributions at plane Z = 11.25 m.

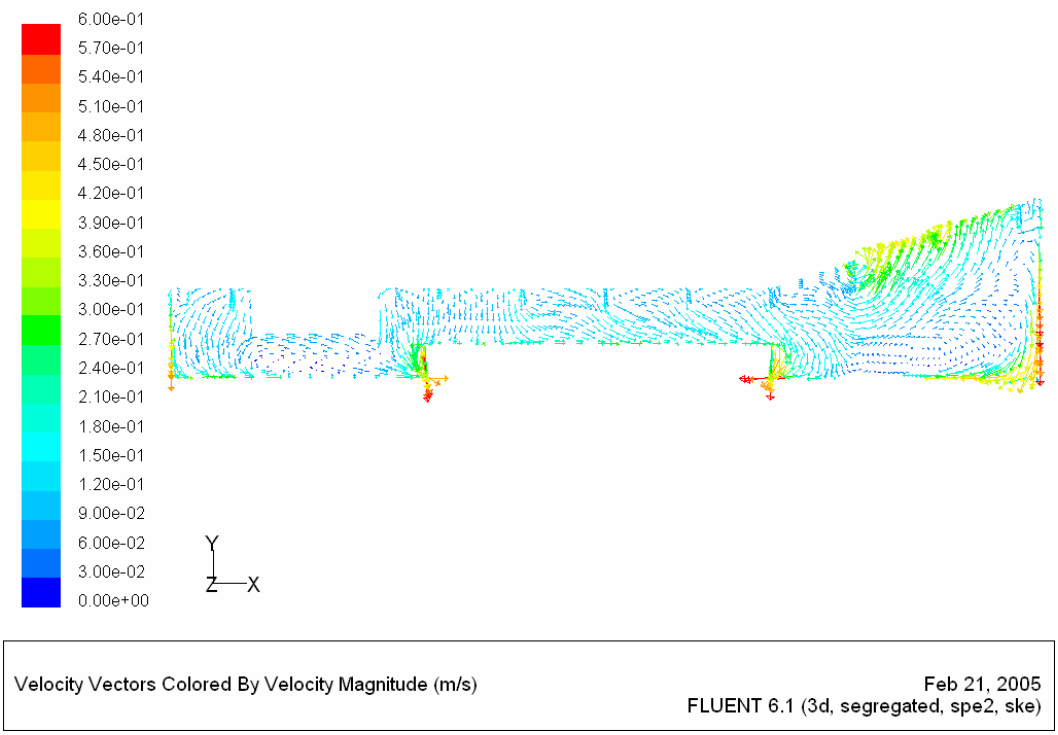

Figure 7.34: Velocity distributions at plane Z = 21.5 m.

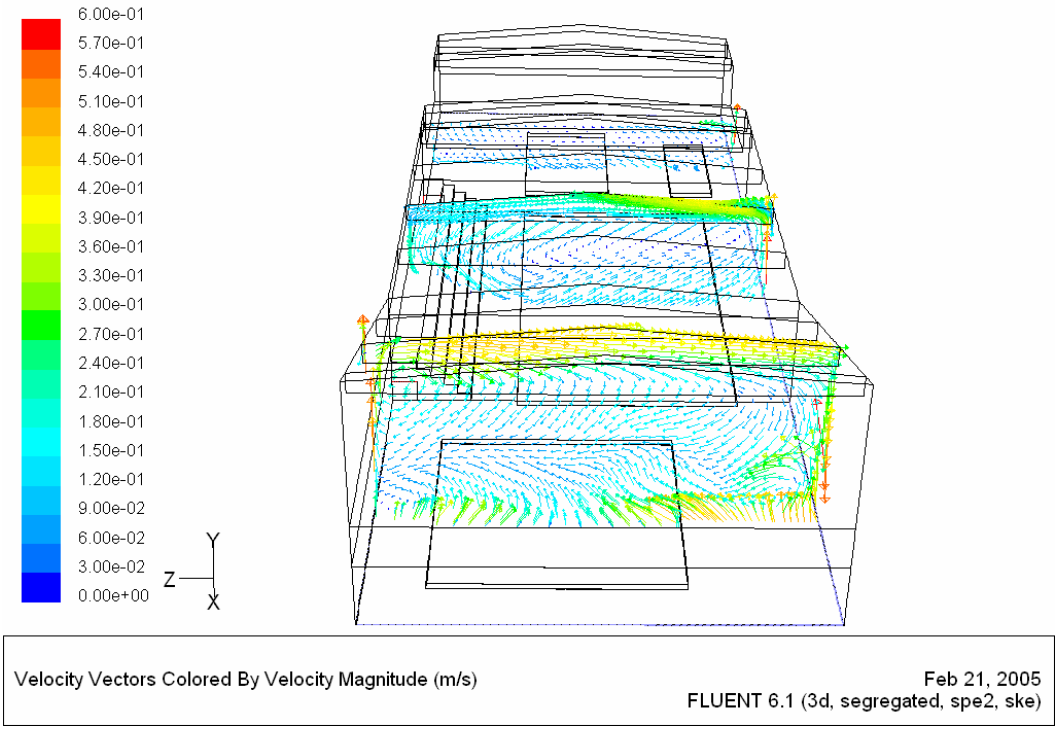

Figure 7.35: Velocity distributions at plane X = 10 m, X = 31.5 m and X = 55m.

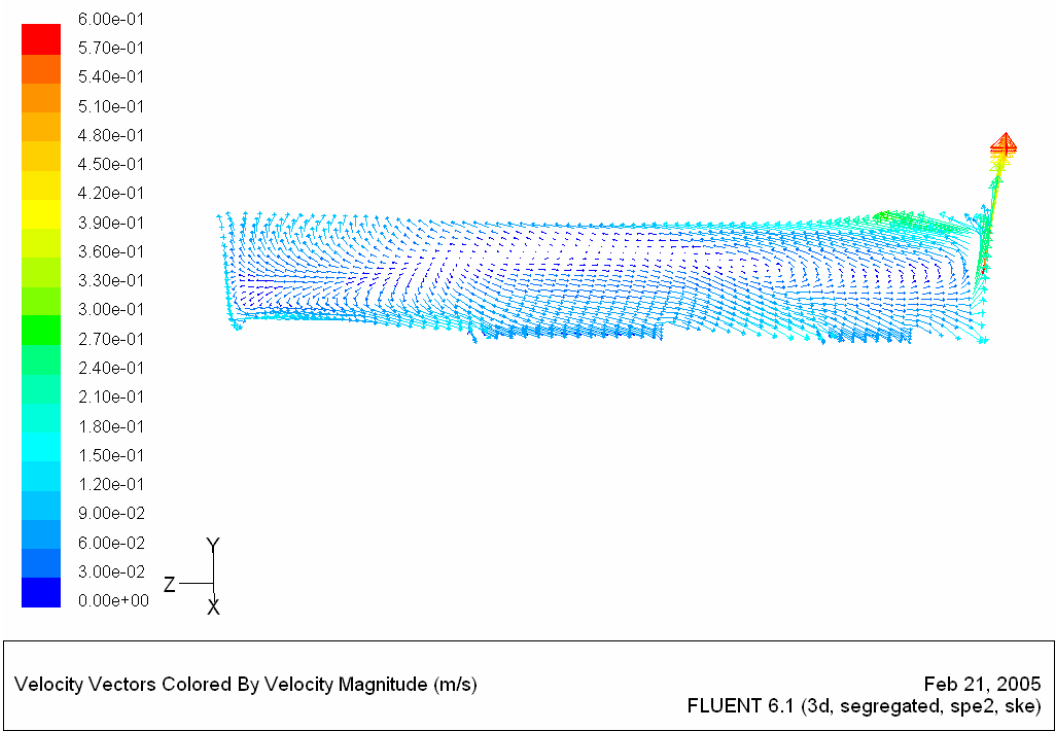

Figure 7.36: Velocity distributions at plane X = 10 m.

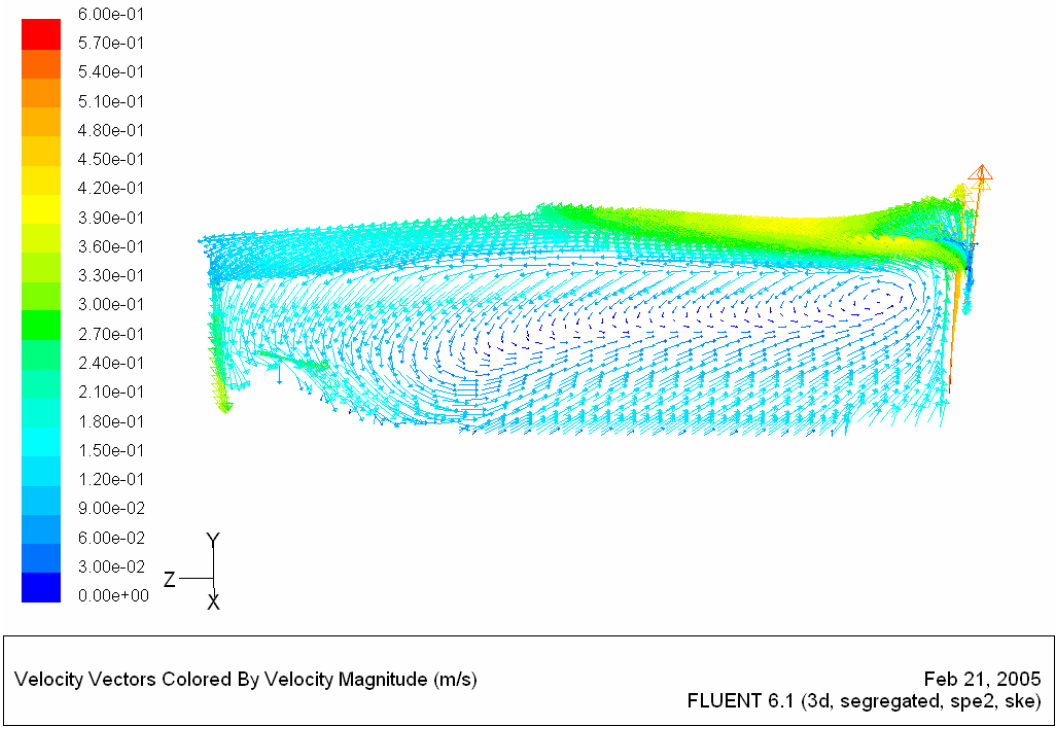

Figure 7.37: Velocity distributions at plane X = 31.5 m.

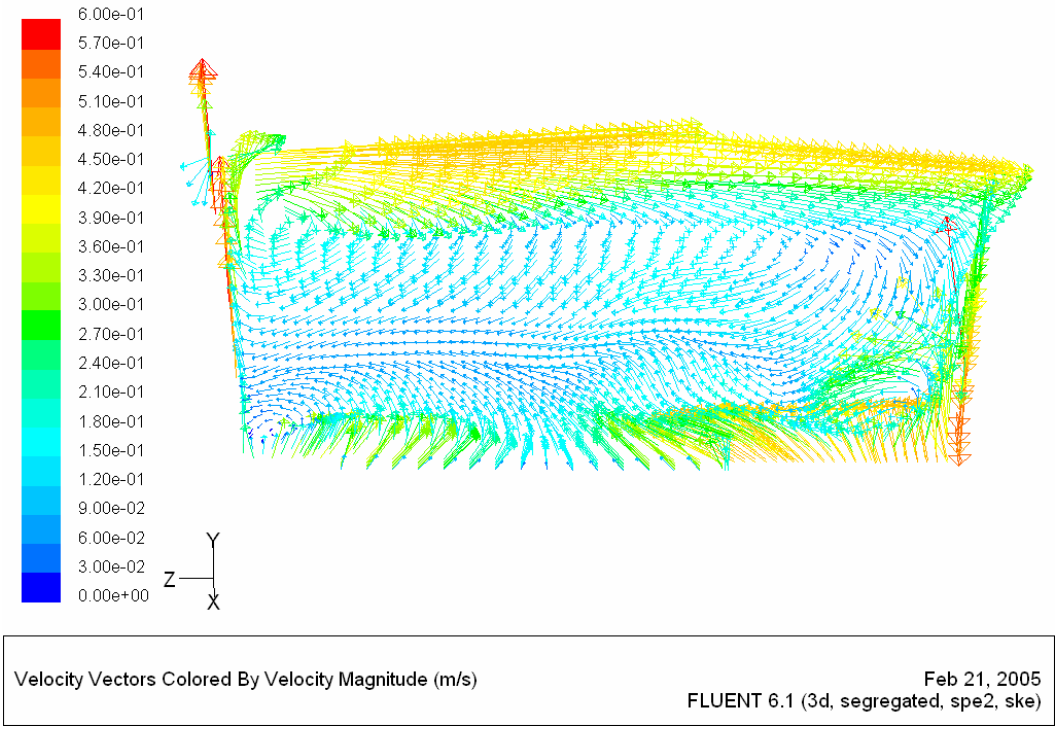

Figure 7.38: Velocity distributions at plane X = 55m.

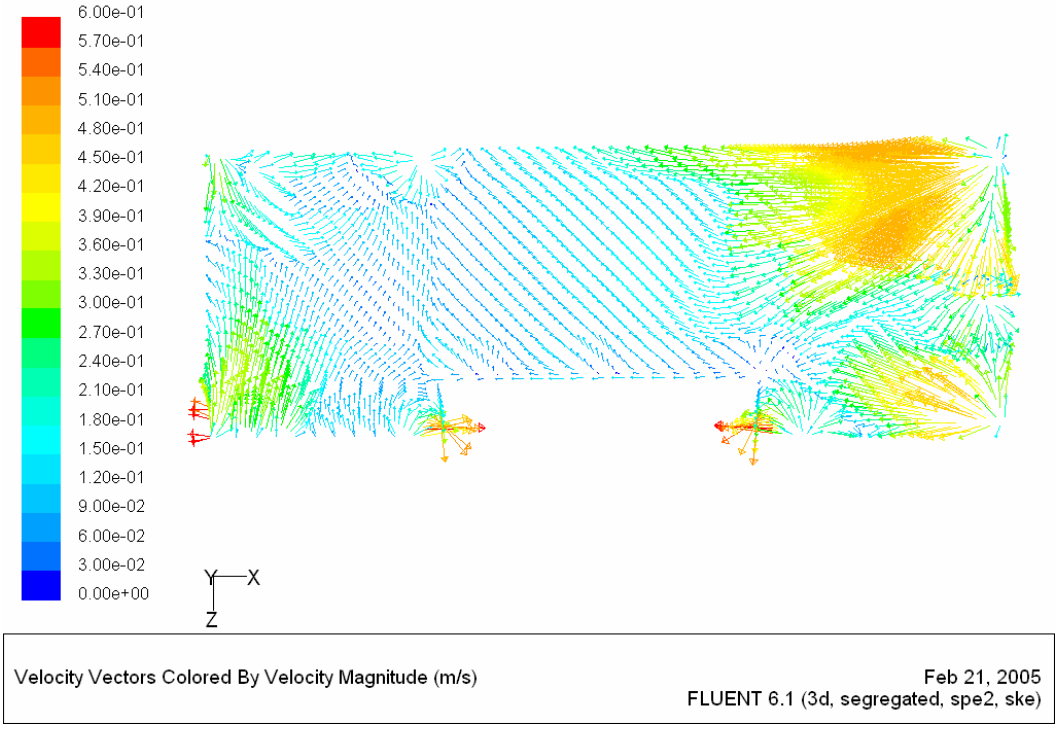

Figure 7.39: Velocity distributions at plane Y = 0.1 m.

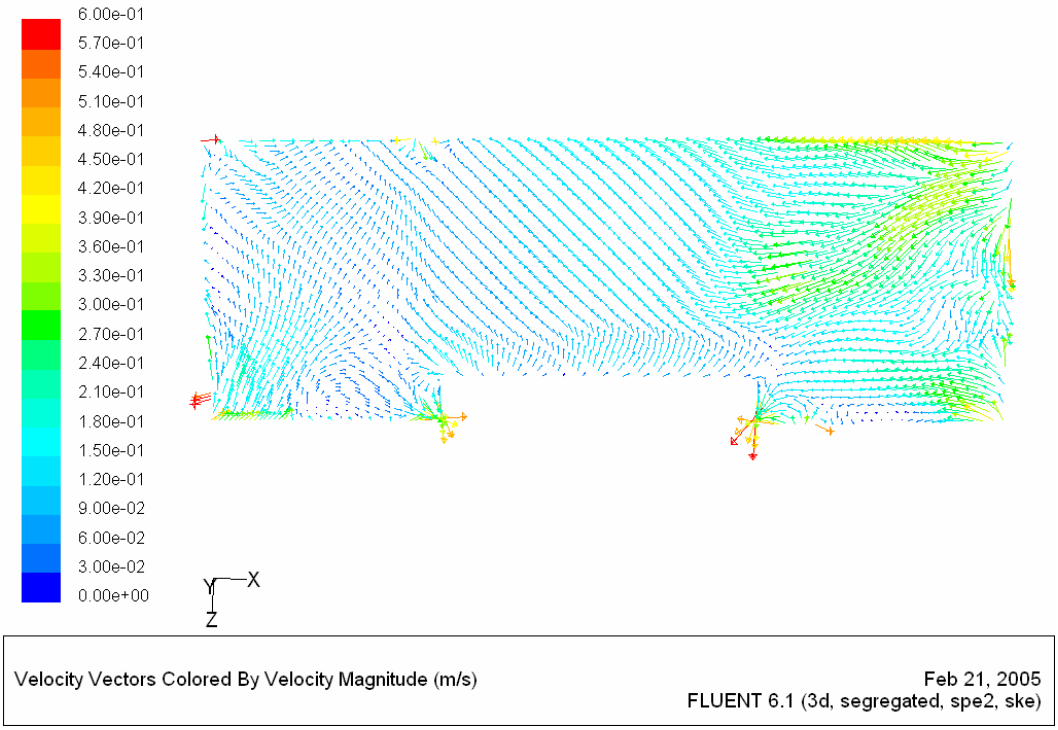

Figure 7.40: Velocity distributions at plane Y = 0.77 m.

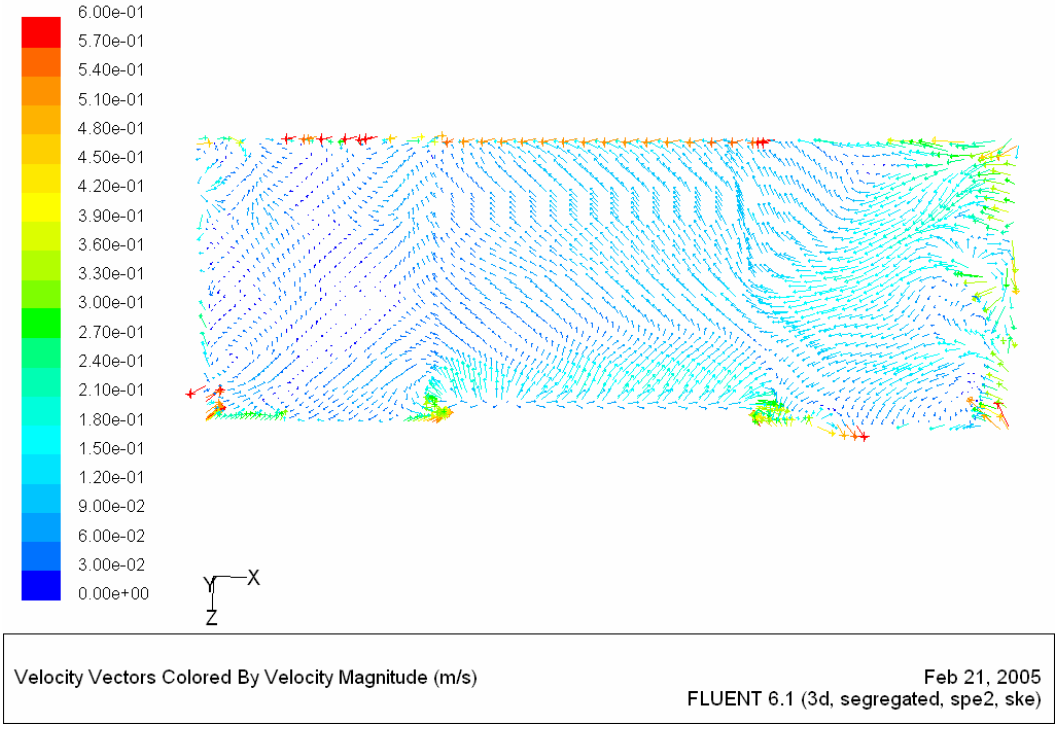

Figure 7.41: Velocity distributions at plane Y = 2 m.

7.2.2.2 Temperature distribution

Figure 7.42 – Figure 7.49 show the air temperature distributions for different planes in the occupied swimming hall.

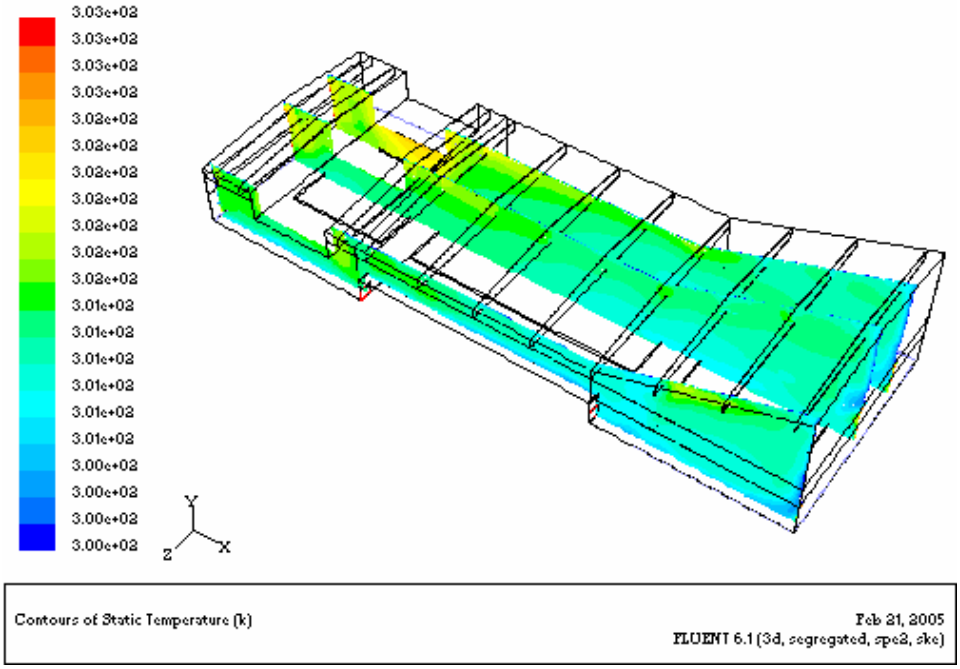

Figure 7.42: Temperature distributions at plane Z = 5 m, Z = 11.25 m and Z = 21.5 m.

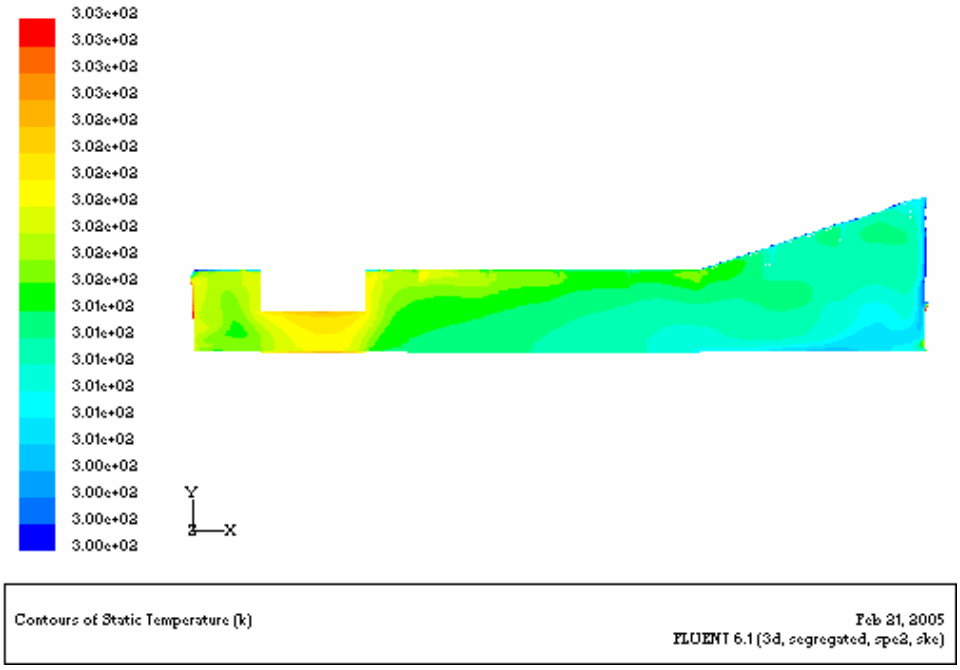

Figure 7.43: Temperature distributions at plane Z = 5 m.

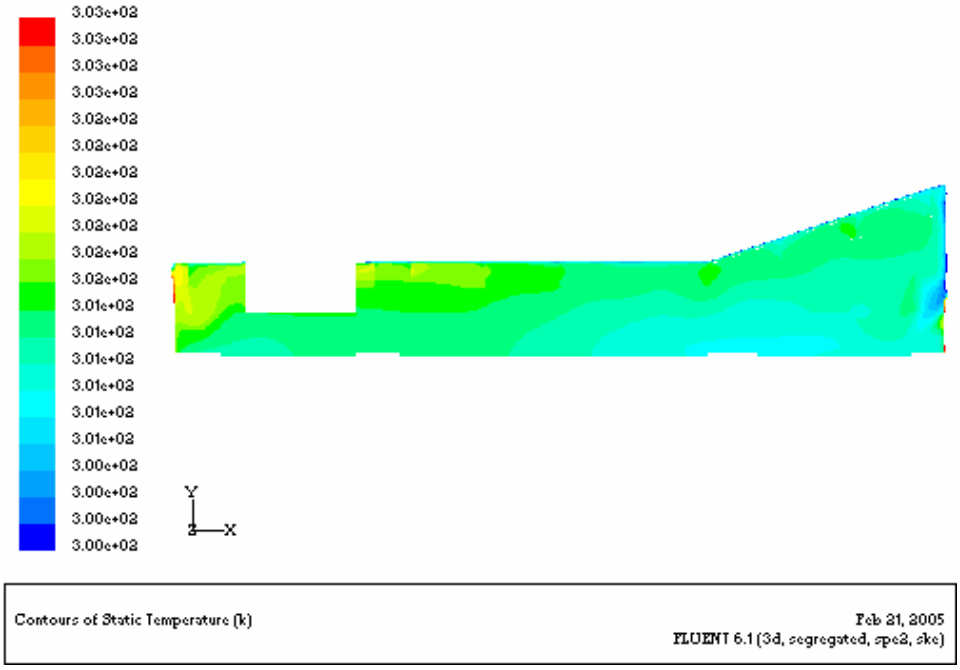

Figure 7.44: Temperature distributions at plane Z = 11.25 m.

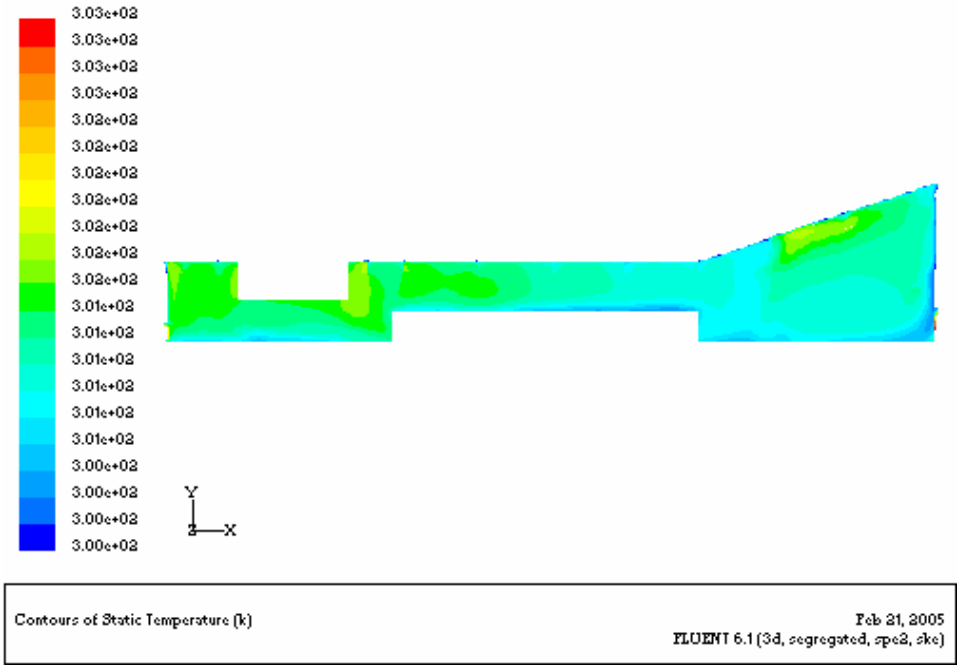

Figure 7.45: Temperature distributions at plane Z = 21.5 m.

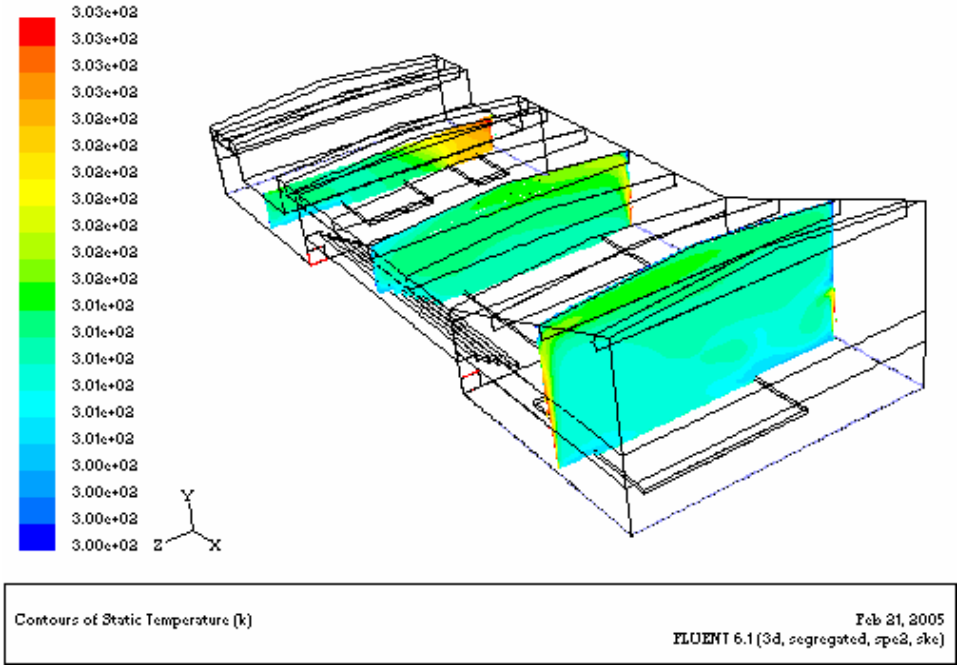

Figure 7.46: Temperature distributions at plane X = 10 m, X = 31.5 m and X = 55 m.

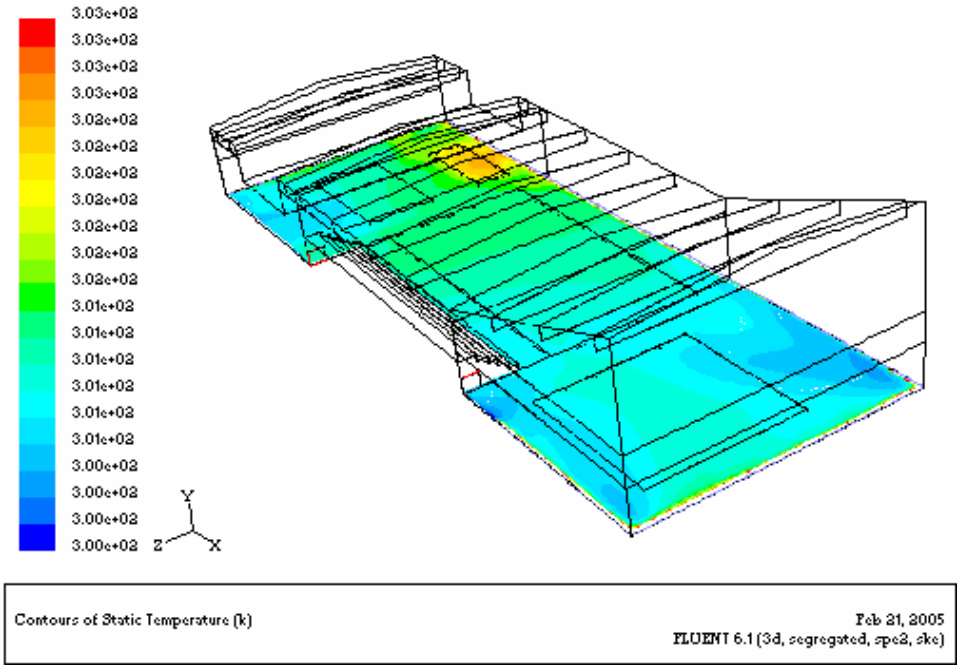

Figure 7.47: Temperature distributions at plane Y = 0.1 m.

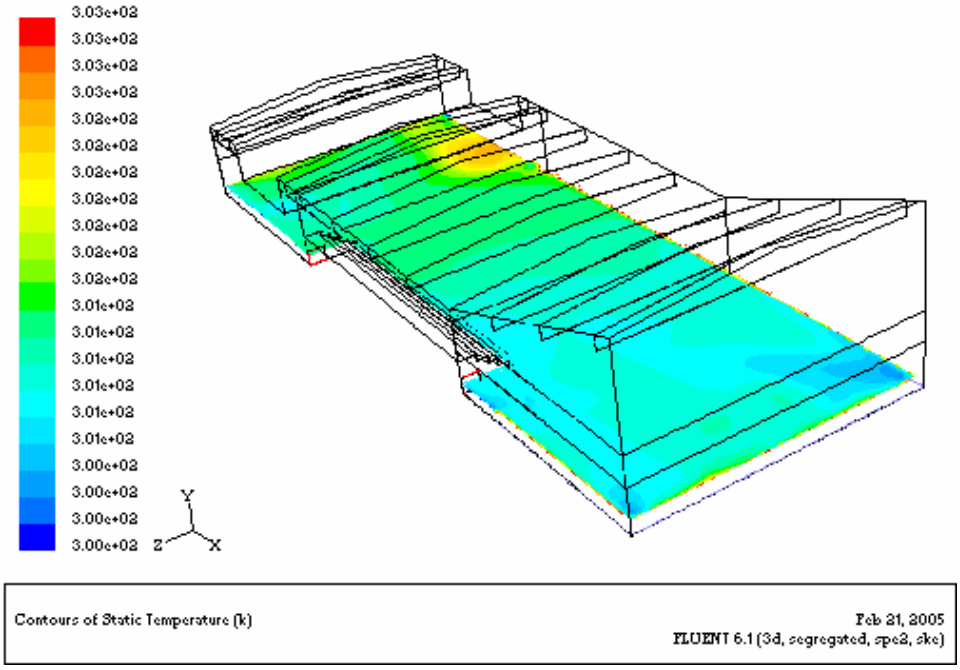

Figure 7.48: Temperature distributions at plane Y = 0.77 m.

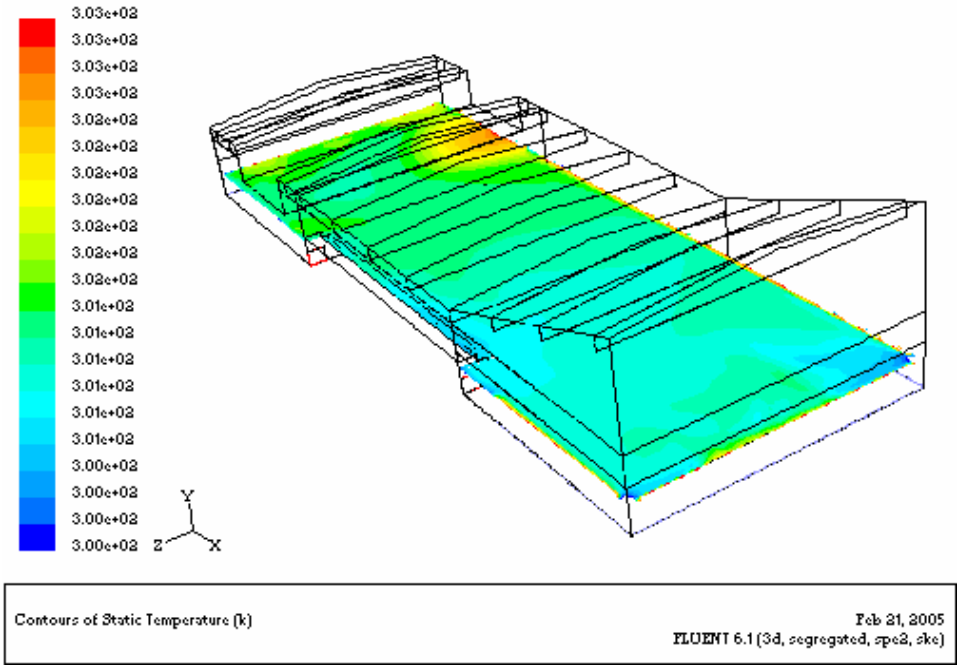

Figure 7.49: Temperature distributions at plane Y = 2 m.

7.2.2.3 Relative humidity distribution

Figure 7.50 – Figure 7.57 show the relative humidity distributions for different planes in the swimming hall. It is clear to see that the relative humidity varies greatly inside the building and the relative humidity is higher than it of the indoor temperature 30 °C

case because of the higher water evaporation rate. The relative humidity is lower in the spring bath part of the building because of the higher ventilation rate, and the relative humidity is higher in the small child bath part because of the higher water temperature and higher water evaporation rate. The relative humidity is very higher close to the water surface because the water vapor evaporates.

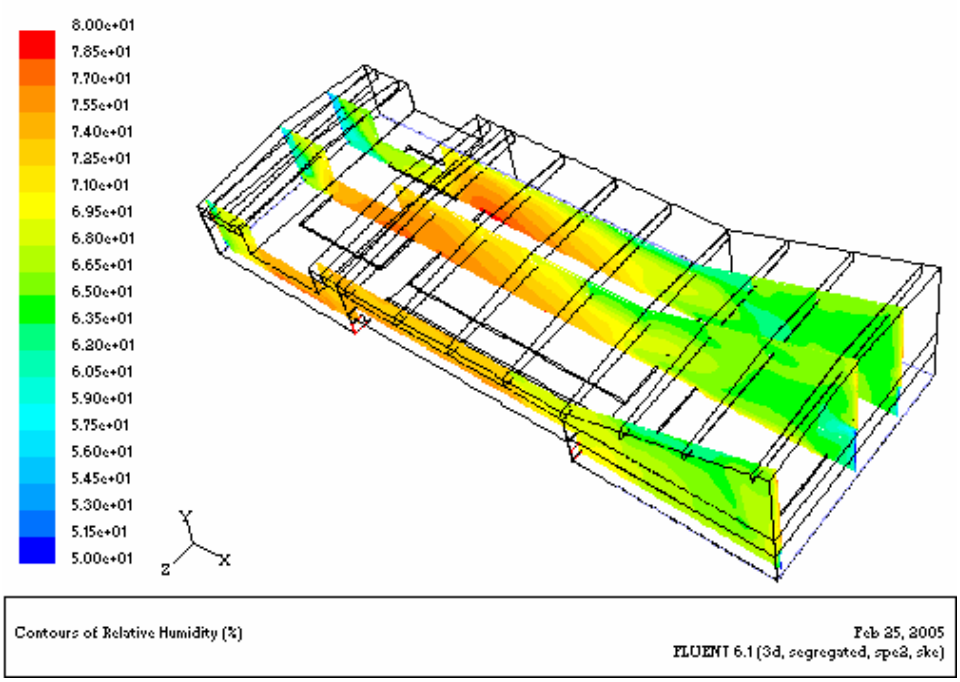

Figure 7.50: Relative humidity distributions at plane Z = 5 m, Z = 11.25 m and Z = 21.5 m.

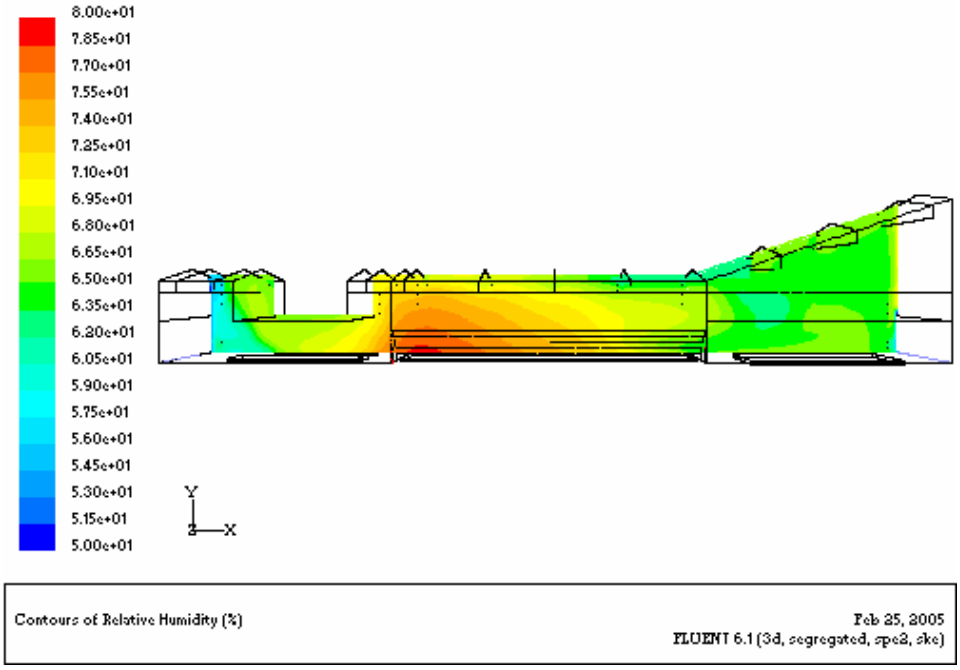

Figure 7.51: Relative humidity distributions at plane Z = 5 m.

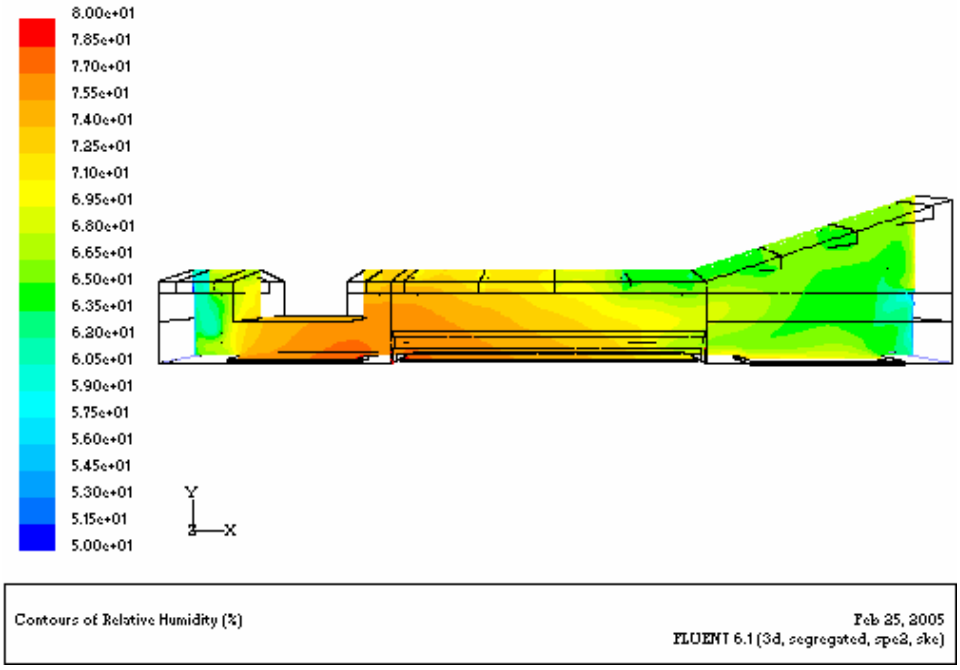

Figure 7.52: Relative humidity distributions at plane Z = 11.25 m.

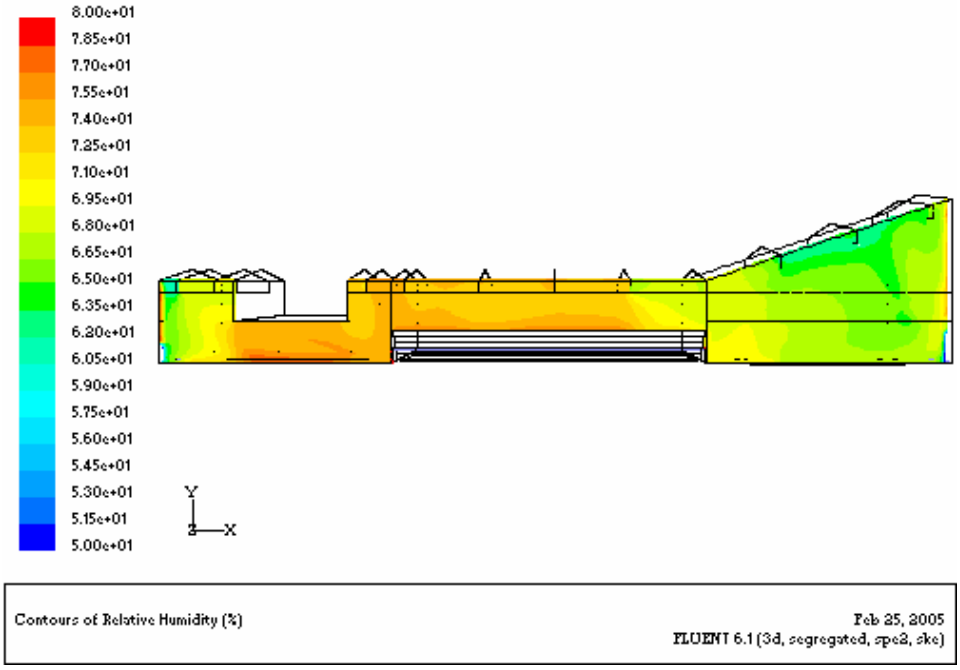

Figure 7.53: Relative humidity distributions at plane Z = 21.5 m.

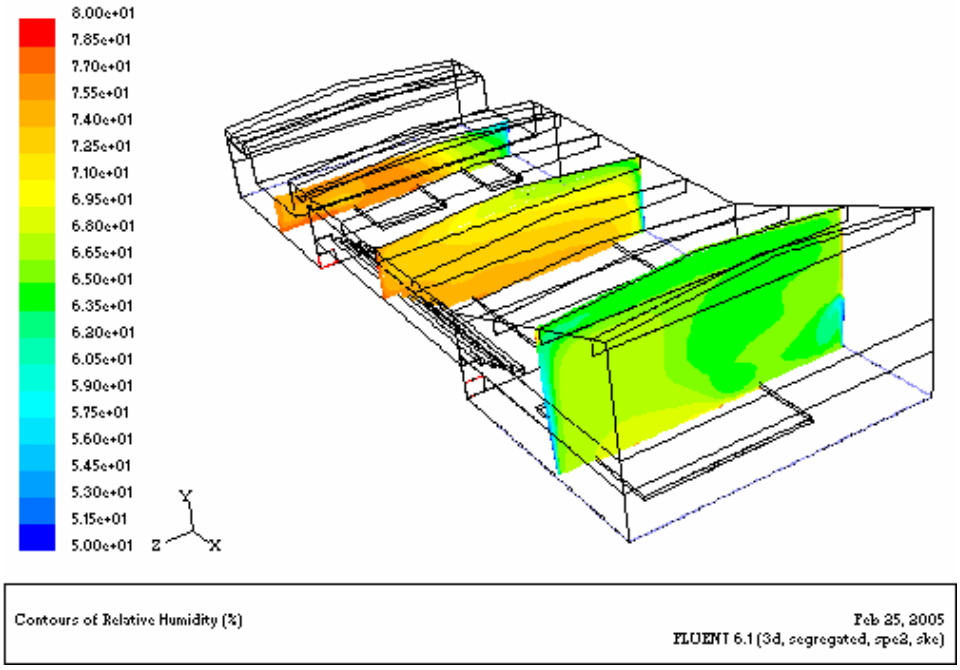

Figure 7.54: Relative humidity distributions at plane X = 10 m, X = 31.5 m and X = 55 m.

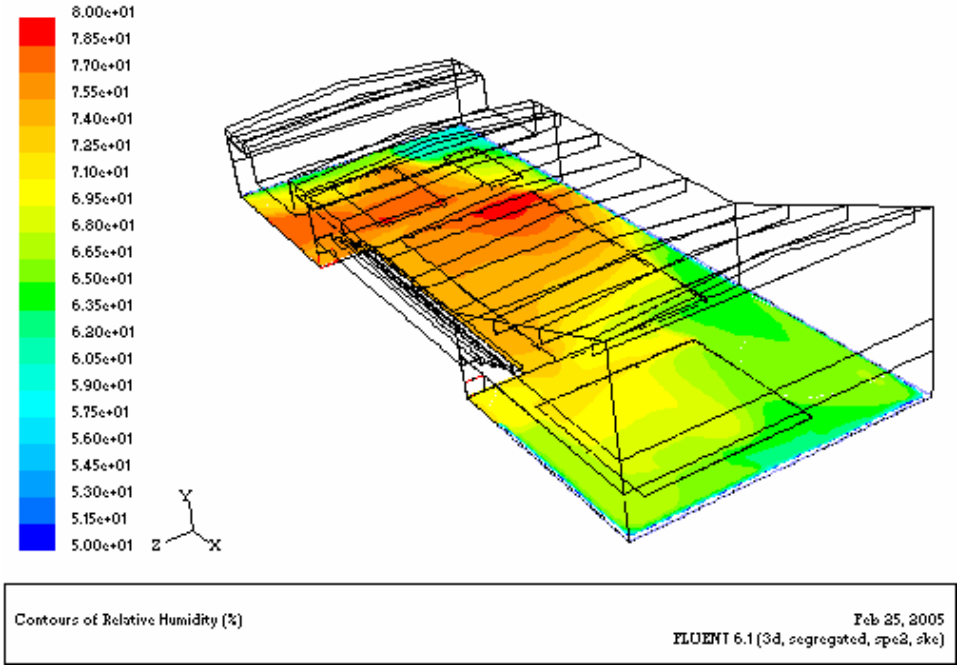

Figure 7.55: Relative humidity distributions at plane Y = 0.1 m.

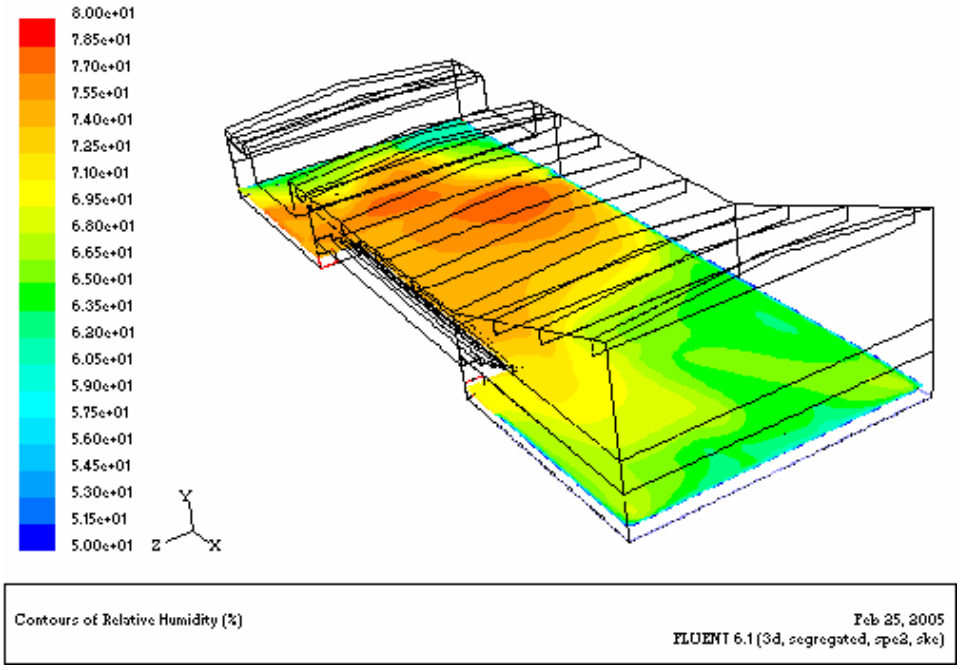

Figure 7.56: Relative humidity distributions at plane Y = 0.77 m.

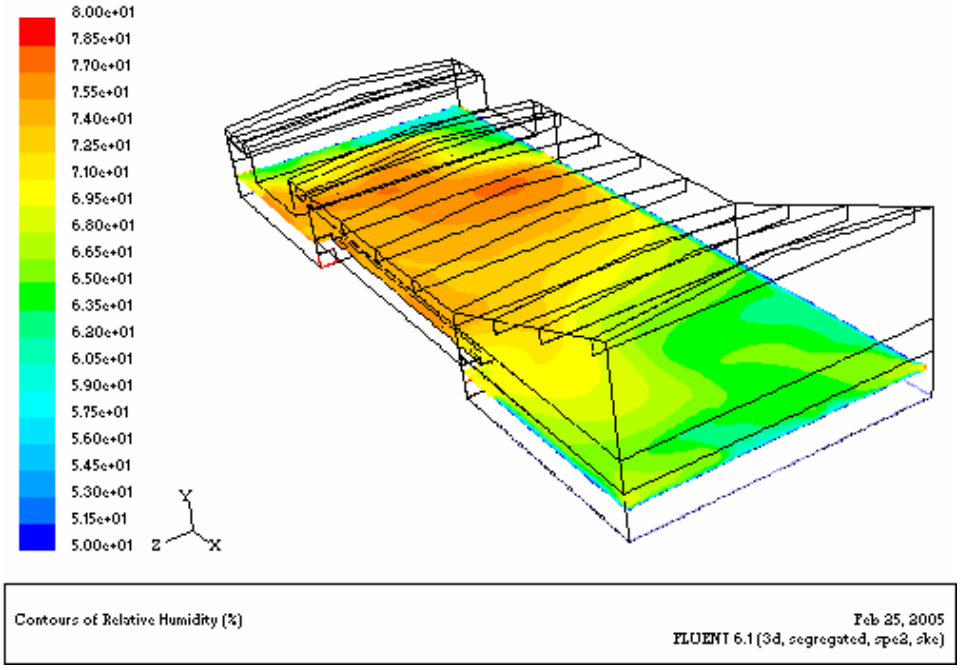

Figure 7.57: Relative humidity distributions at plane Y = 2 m.

7.2.2.4 Profiles

The air velocity, air temperature and air relative humidity at different lines in the middle plane are shown in Figure 7.58 – Figure 7.60.

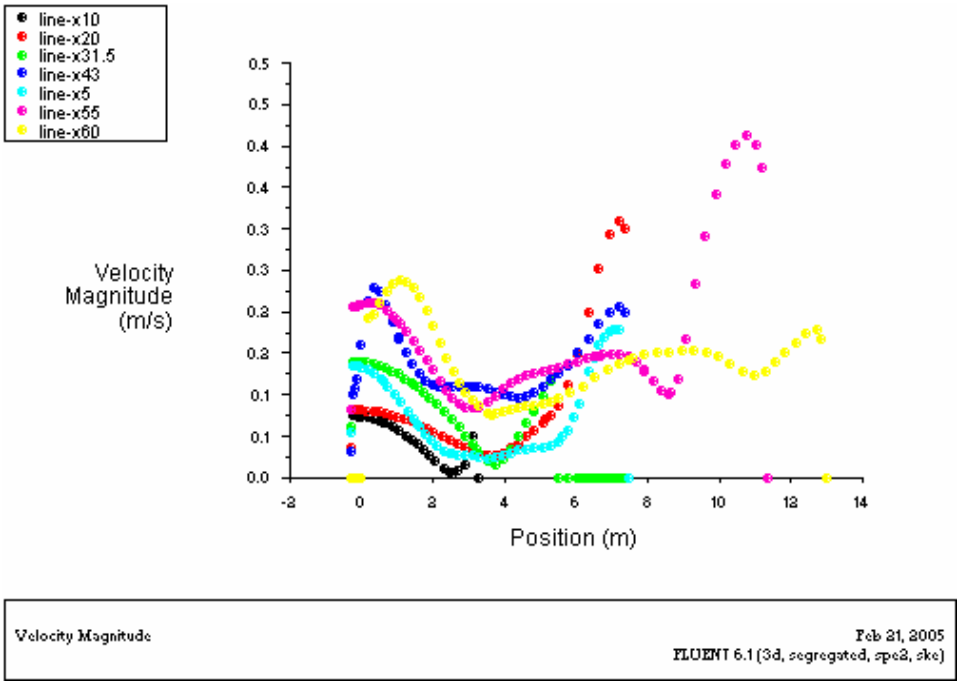

Figure 7.58: Velocity magnitude profile at line X = 5 m, 10 m, 20 m, 31.5 m, 43 m, 55 m and 60 m of the middle plane Z = 11.25m.

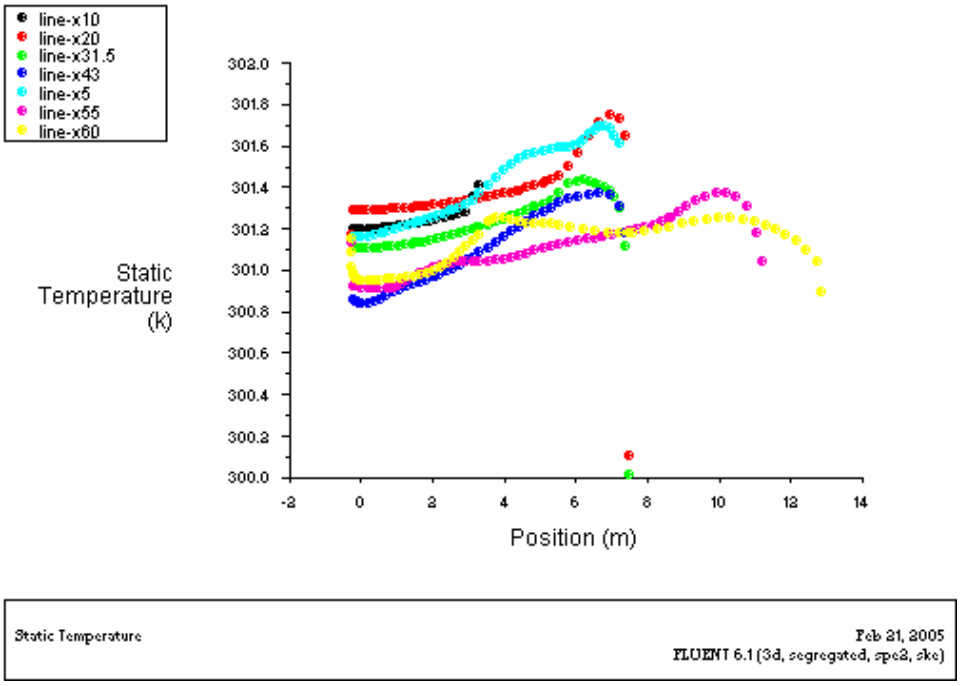

Figure 7.59: Temperature profile at line X = 5 m, 10 m, 20 m, 31.5 m, 43 m, 55 m and 60 m of the middle plane Z = 11.25m.

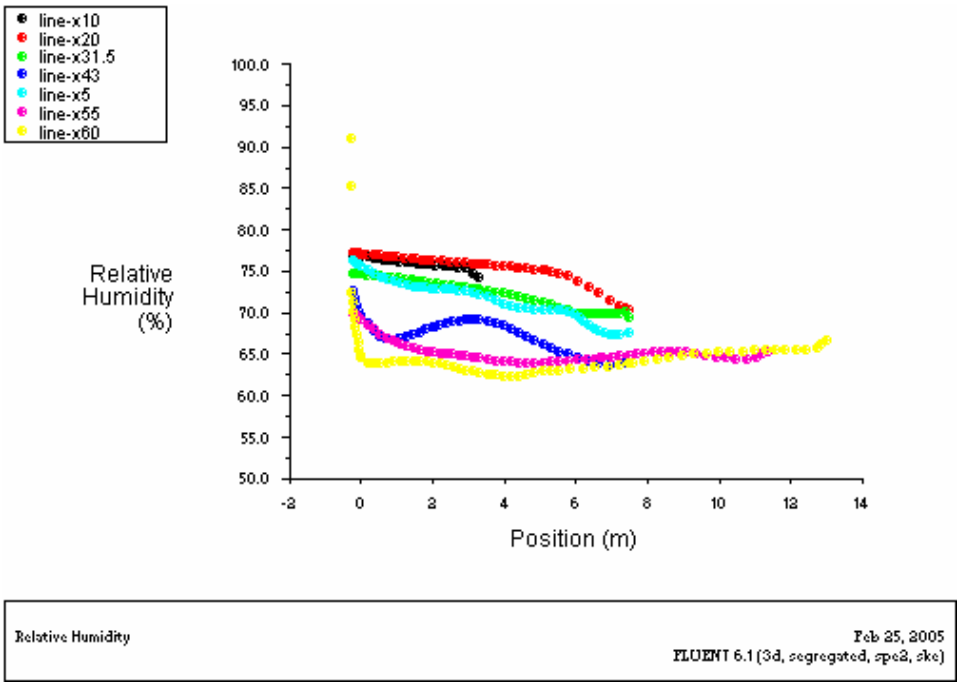

Figure 7.60: Relative humidity profile at line X = 5 m, 10 m, 20 m, 31.5 m, 43 m, 55 m and 60 m of the middle plane Z = 11.25m.

7.2.2.5 Relative humidity comparison

Relative humidity					
Case	Pool type	Simulation set value	3D simulation results value		
		for the other three baths	outlet-left close to teaching bath zone	outlet-right close to spring bath zone	room average value
New case1	Occupied	68%	74.9%	66.3%	68.2%
New case2	Occupied	69%	75.0%	70.3%	68.8%

Table 7.7: Relative humidity comparison.

Table 7.7 shows the relative humidity simulation results compared with the simulation set values. The CFD simulation results are quite good agreement with the simulation set values.

8 Conclusion

This project report describes the investigation of the relation between water evaporation and air movement by means of different water evaporation models comparison and CFD simulations. The two-dimensional and three-dimensional steady state CFD simulations are carried out based on water evaporation and moist air flow in the Korsør Svømmehal.

Through the comparisons of the different evaporation models in the unoccupied pool and occupied pool, it can be found out that the different evaporation models will give rise to quite different evaporation rates. The comparison results show that the Shah correlation is quite good to calculate the water evaporation rate in unoccupied pool and the Shah empirical correlation is quite good to calculate the water evaporation rate in occupied pool.

It also can be found out from this comparison that the higher temperature difference between air and water will cause the lower evaporation rate from the baths. In order to minimize evaporation rate the air temperature should always be higher than the water temperature. However, in order to maintain a reasonable operating economy, the difference should not be bigger than 2-3°C.

2D and 3D CFD simulations are carried out in steady state conditions for the Korsør Svømmehal. The boundary conditions are collected from the measurement results including air temperature, water temperature, humidity, ventilation flow rate and so forth. The CFD results give detailed information of air flow and humidity distribution in the swimming hall due to different water evaporation models. The simulation results show that the two water evaporation models - Shah correlation for unoccupied pool and Shah empirical correlation for occupied pool – are quite good and reasonable to calculate the water evaporation rate from baths.

Summarily, these two models are valid to calculate the water evaporation from baths and can be used to develop a simplified model in BSIM2002.